Philipps Universität Marburg

Identification of transcriptional regulators for the *Ustilago maydis mig* genes

Dissertation

zur Erlangung des Doktorgrades

der Naturwissenschaften

(Dr. rer. nat.)

dem
Fachbereich Biologie
der Philipps-Universität Marburg
vorgelegt von
Yan Zheng
aus Changchun, China
Marburg / Lahn, November 2007

The work in my thesis was carried out from May 2004 until August 2007 at the Max-Planck-Institute for Terrestrial Microbiology, Marburg, Germany, under supervision of Dr. Christoph Basse.

By the Biology department of the Philipps University, Marburg as doctoral thesis accepted on:

Date of oral examination: 18. 12. 2007

First reviewer: Prof. Dr. Regine Kahmann

Second reviewer: Prof. Dr. Hans-Ulrich Mösch

The following paper was in preparation by the date of submission of the present thesis:

Yan Zheng, Jan Kief, Kathrin Auffarth, Jan Farfsing, and Christoph W. Basse. 2007. The *Ustilago maydis* Cys_2His_2-type zinc finger transcription factor Mzr1 regulates fungal gene expression during the biotrophic growth stage.

Pledge

I certify that my thesis entitled "Identification of transcriptional regulators for the *Ustilago maydis mig* genes" was carried out without any unlawful devices. I did not use any other than the described literatures or technical devices.

This thesis has never been submitted before to any other university and has not been used before any examination.

Marburg, 05.11. 2007

Yan Zheng

Summary

The basidiomycete fungus *Ustilago maydis* is a plant pathogen. It can infect maize plants specifically and depends on the plant host for pathogenic development. This fungus has become an interesting research model for plant-fungus interactions.

A maize induced gene family, the *mig* genes, has been identified in *U. maydis*. This gene family contains *mig1*, the *mig2-1* to *mig2-5* gene cluster, and *mig2-6*. All *mig* genes showed strongly plant induced expression patterns and were predicted to be involved in the plant-fungus interactions. Detailed analysis of the *mig2-5* promoter has uncovered a consensus motif (5'-CCAC/AC/A-3'), which is present in multiple copies in all *mig2* promoters and whose activity specifically depends on the sequence triplet 5'-CCA-3' (5'-TGG-3'). On this basis, I considered C2H2 zinc finger and Myb proteins in *U. maydis* as potential regulators for *mig* genes. Candidate genes were analyzed by a PCR-based deletion approach.

I could show that deletion of *mzr1*, which encodes a C2H2 zinc finger protein, strongly decreases the expression level of *mig2-5* after plant inoculation. In addition, another C2H2 zinc finger protein called Biz1 has been found to be involved in the transcriptional activation of *mig* genes (M. Vranes and J. Kämper, unpublished). Conditional overexpression of both *mzr1* and *biz1* is sufficient to induce transcription of several *mig* genes under culture conditions. Furthermore, I could show that the truncated Mzr1 protein expressed in *E. coli* could specifically bind to the *mig2-5* promoter *in vitro*. Apart from this, another C2H2 zinc finger protein, named Znf23, was found to be involved in *mig* gene regulations. I could show that the expression of *mig* genes in the *znf23* deletion strain was stronger than in the wild type strain after plant infection.

These results suggest that Mzr1 is a direct positive regulator to *mig2-5*, while Znf23 appears to negatively influence *mig* gene expression. The implications of these results are discussed.

Zusammenfassung

Ustilago maydis ist ein pflanzenpathogener Basidiomycet. Er infiziert spezifisch Maispflanzen und ist in der Vollendung seines Lebenszyklus auf diesen Wirt angewiesen. Der Organismus wurde zu einem interessanten Forschungsmodell für Interaktionen zwischen Pflanze und Pilz.

Mit den *mig*-Genen wurde in *U. maydis* eine Genfamilie entdeckt, deren Expression in Anwesenheit der Pflanze induziert wird. Diese Familie enthält das Gen *mig1,* das Gencluster *mig2-1* bis *mig2-5* und das Gen *mig2-6*. Alle *mig*-Gene zeigen ein stark pflanzeninduziertes Expressionsmuster. Daraus wurde gefolgert, dass sie eine Rolle in der Interaktion zwischen Pilz und Pflanze spielen. Eine detaillierte Analyse des *mig2-5* Promotors führte zur Entdeckung des Konsensusmotivs (5'-CCAC/AC/A-3'), das in allen *mig2*-Promotoren in mehreren Kopien vorkommt und dessen Aktivität von der Anwesenheit des Sequenztripletts 5'-CCA-3' (5'-TGG-3') abhängig ist. Diese Tatsachen führten zu der Hypothese, dass C2H2-Zinkfingerproteine und Myb-Proteine mögliche Regulatoren der *mig*-Gene sind. In dieser Arbeit wurden Kandidatengene über PCR-basierte Gendeletion analysiert.

Dabei konnte gezeigt werden, dass die Deletion von *mzr1*, einem Gen, das für ein Zinkfingerprotein codiert, zu einer drastischen Reduktion des Expressionslevels von *mig2-5* nach der Pflanzeninfektion führt. Unabhängig wurde mit Biz1 ein weiteres Zinkfingerprotein identifiziert, welches ebenfalls an der transkritionellen Aktivierung der *mig* Gene beteiligt ist (M. Vranes und J. Kämper, nicht veröffentlicht). Die konditionale Überexpression von *mzr1* und *biz1* ist hinreichend, um unter Kulturbedingungen die Transkription mehrerer *mig* Gene zu induzieren. Es konnte ausserdem gezeigt werden, dass ein in *E. coli* exprimiertes verkürztes Mzr1-Protein *in vitro* spezifisch an den *mig2-5* Promotor bindet. Weiterhin wurde ein drittes C2H2 Zinkfingerprotein namens Znf23 identifiziert,

das an der Regulation der *mig* Gene beteiligt ist. In Abwesenheit von *znf23* fällt die Expression der *mig* Gene nach der Pflanzeninfektion deutlich stärker aus als in der wildtyp-Situation.

Aus diesen Ergebnissen lässt sich folgern, dass Mzr1 ein positiver Regulator von *mig2-5* ist, während Znf23 die Expression der *mig* Gene negativ beeinflusst. Die Schlussfolgerungen aus diesen Ergebnissen werden diskutiert.

List of abbreviations

Amp   ampicillin

BSA   Bovine serumalbumine

bp   base pair

Cbx   Carboxin

CM   complete medium

cDNA   complementary DNA

DIC   differential interference contrast

DMSO   dimethylsulfoxide

ddH$_2$O   doubled distilled water

DNA   deoxyribonucleic acid

dNTP   deoxyribonucleotide

EDTA   Ethylenediamin-N, N', N', N' tetra acetic acid

eGFP   enhanced green fluorescent protein

EMSA   electrophoretic mobility shift assay

GFP   green fluorescent protein

Hyg   Hygromycin

kDa   kilo dalton

Kb   kilo base pair

MOPS   3-(N-Morpholino)- propanesulfonic acid

ml   milliliter

mM   millimolar

Nat   Nourseothricin

OD   optical density

ORF   open reading frame

PCR   polymerase chain reaction

RT   room temperature

RNA	ribonucleic acid
RT-PCR	reverse transcription PCR
SDS	sodium dodecyl sulfate
TBE	Tris-borate +Na_2-EDTA
TE	Tris-Cl + Na_2-EDTA
wt	wild type
U. maydis	*Ustilago maydis*
%	percent
μg	microgram
μl	microliter
°C	degree celsius

Table of contents

Curriculum vitae

Acknowledgement

1   Introduction

1.1 Plant-fungus interactions

It is estimated that there are about 1.5 million species of fungi in nature (Grayer *et al.*, 2001). Like all other organisms that cannot obtain nutrition by photosynthesis, fungi depend on plants for their carbon and energy source. The majority of fungi lives on dead plant tissue and recycles the nutrients for plant reuse. Thus, fungi play a key role during the nutrient cycle in nature.

After a long time of evolution, nutrient sources of some fungi have been changed from dead plant tissue to living plants. In fact, most of the fungi, which interact with living plants are advantageous to host plants. Furthermore, among them some fungal species evolved that acquired the ability to break the balance with the host and thus became pathogens. Interestingly, in most plant populations, there are individuals that can resist fungal infection.

In 1898, W. Farrer discovered that resistance to rust in wheat is inherited (Farrer, 1898). Then R. H. Biffen' s discovery in 1905 about resistance to yellow rust in wheat caused a breakthrough in breeding for disease resistance (Biffen, 1905). But only a decade later, research about resistance in wheat to wheat stem rust showed that host resistance had been overcome by variants of the pathogen (Stakman, 1917; Stakman *et al.*, 1918). The battle between resistant plant cultivars and their pathogens has been described as the 'boom and bust' cycle (Crute, 1985). H. H. Flor's studies demonstrated that flax is resistant to a particular physiologic race of *Melampsora lini* only when the cultivar carries a dominant resistance gene corresponding to a dominant avirulence gene of the pathogen (Flor, 1942, 1946, 1971; reviewed in De Wit, 1992). This is the basis for gene-for-gene relationships of plant-fungus interactions (Barrett, 1985; Crute, 1985; Day, 1974; Islam *et al.*, 1991; Keen, 1982; Michelmore *et al.*, 1988; Parlevliet, 1983; Thomas, 1991). During the past few years, many models, mainly involving bacterial pathogens,

have been postulated to explain this gene-for-gene relationships. The tobacco (*Nicotiana tabacum*) *N* gene was isolated from *N. glutinosa* and confers resistance to most strain of tobacco mosaic virus (Whitham *et al*., 1994). *Xa21* confers resistance to over 30 distinct strains of the bacterium *Xanthomonas oryzae* pv. *Oryzae*, which causes leaf blight in rice (Song *et al*., 1995). The tomato *Pto* gene, which was the first race-specific disease resistance gene to be isolated, confers resistance to races of *Pseudomonas syringae* pv. *tomato* that carry the *avrPto* gene (Martin *et al*., 1993). Because of the larger genomes and the fact that transformation protocols do not exist for many phytopathogenic fungal species, in particular for most obligate biotrophs, avirulence genes have only been cloned from a few fungal species (Knogge, 1996). The first disease resistance gene to be isolated was *Hm1* from maize, which confers resistance to the leaf spot fungus *Cochliobolus carbonum* (Hammond-Kosack *et al*., 1997; Johal *et al*., 1992; Walton, 1984).

1.2 *Ustilago maydis*

Maize smut is distributed throughout the world (Davis, 1936). Common smut of maize has been of interest to biologists for more than 250 years. Some reports that discuss maize smut with some precision appeared in 1760 (Anon *et al*., 1891; Christensen *et al*., 1963). The cause of common smut, the basidiomycete fungus *Ustilago maydis* (which was carried to Europe by the early Spanish explorers), was described first by O. Brefeld in 1883 (Brefeld, 1883). He proved that the young meristematic tissues above ground were subject to infection. Brefeld also recognized that *U. maydis* undergoes multiple morphological transitions during pathogenic growth. The complete life cycle of the fungus was still unknown until 1927 when the sexual stage was discovered. The initiation of pathogenic development is characterized by the morphological switch from yeast-like budding cells to tip-growing hyphae (Christensen *et al*., 1963; reviewed in Kahmann *et al*., 2000). Haploid *U. maydis* cells arrest in the G2 phase after

recognition of compatible mating partners (Garcia-Muse *et al*., 2003; Snetselaar *et al*., 1996) and form a conjugation tube. This directed tip growth towards the pheromone source (Snetselaar *et al*., 1993, 1996) leads to cell fusion and the formation of dikaryotic hyphae. Dikaryotization occurs after hyphal fusion of opposite mating types (Christensen *et al*., 1963; Hanna *et al*., 1929). After mating, the filamentous dikaryon depends on the maize host for further pathogenic development. Dikaryotic hyphae grow in the meristematic region of the plant and cause galls in early stages of proliferation of tissue (reviewed in Paredes-Lopez *et al*., 1995). During this stage, the fast growing, branching hyphae invade plant tissue by intra- and intercellular growth (Snetselaar *et al*., 1994). Massive fungal proliferation causes the tumour formation. Finally nuclear fusion and fragmentation of hyphae lead to the formation of the diploid teliospore (Ehrlich *et al*., 1958; reviewed in Basse and Steinberg, 2004). Before germination, these cells reside in the soil until the spore wall cracks. Meiosis takes place and promycelium is forms, which contains the meiotic products that are able to restart the sexual life cycle (Christensen, 1963; Kahmann *et al*., 2000).

It has been confirmed that haploid sporidia of *U. maydis* contain the mating-type loci *a* and *b* (reviewed in Kahmann *et al*., 2000; Kronstad *et al*., 1997). The *a* locus consists of two alleles called *a1* and *a2*. It encodes a pheromone/receptor system that enables mating in response to pheromone recognition by the receptor of the opposite mating type (Bölker *et al*., 1992). The *b* locus encodes a pair of homeodomain proteins *bE* and *bW* that in nonallelic combinations dimerize to an active transcription factor required for filamentous growth and pathogenic development (Kronstad *et al*., 1990; Romeis *et al*., 2000; Gillissen *et al*., 1992; Kämper *et al*., 1995; Brachmann *et al*., 2001).

U. maydis has become an interesting molecular model to investigate the plant-fungus interaction based on its tight dependency on the plant host. The complete genome of strain UM521 has been sequenced and released by the Broad Fungal Genome Initiative (http://www.broad.mit.edu), which made it possible to investigate gene functions in more detail. An efficient PCR-based system for gene

replacement has been developed (Kämper, 2004), which makes it easier to investigate the function of specific gene(s) by single or multiple gene deletions.

1.3 *mig* genes in *Ustilago maydis*

U. maydis depends on the host plant to complete its pathogenic development. Presumably, a lot of *U. maydis* genes and specific plant compounds are involved in the plant-fungus interaction process. Identification of such stage specific genes in *U. maydis* may offer insight into the mechanisms for plant-fungus interaction. Many stage specifically expressed genes have been identified in *U. maydis* (Basse *et al*., 2006; Bohlmann 1996; Brachmann *et al*., 2001, 2003; Romeis *et al*., 2000; Schauwecker *et al*., 1995; Urban *et al*., 1996; Wösten *et al*., 1996). A maize induced *mig* gene family has been detected (Basse *et al*., 2000, 2002). This gene family consists of *mig1*, the highly homologous *mig2-1* to *mig2-5* cluster genes and *mig2-6*. The five *mig2* genes, *mig2-1* to *mig2-5,* are arranged as direct repeats within a 7.1 kb DNA region and reside on chromosome XXII of *U. maydis* strain 521 (**Fig.1**). The *mig2-6* resides on chromosome XXI. The C-terminal 81 amino acids of Mig2-6 are 58% identical to its closest homologue, Mig2-4 (Farfsing *et al*., 2005).
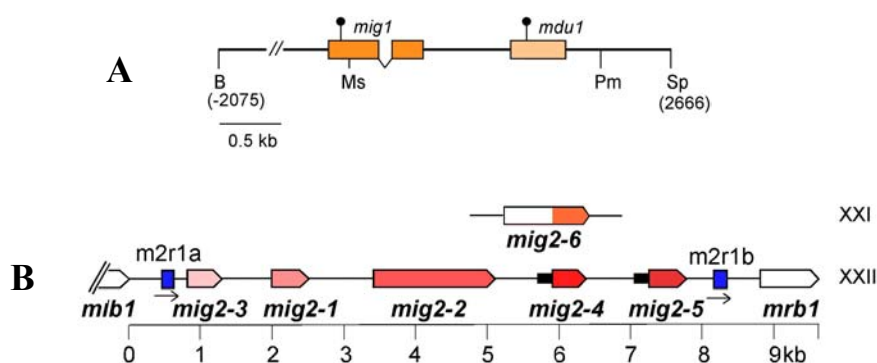
Figure 1. The *mig* locus.
A. *mig1* lous (cited from Basse *et al*., 2000). **B.** *mig2* locus (cited from Basse *et al*., 2002).
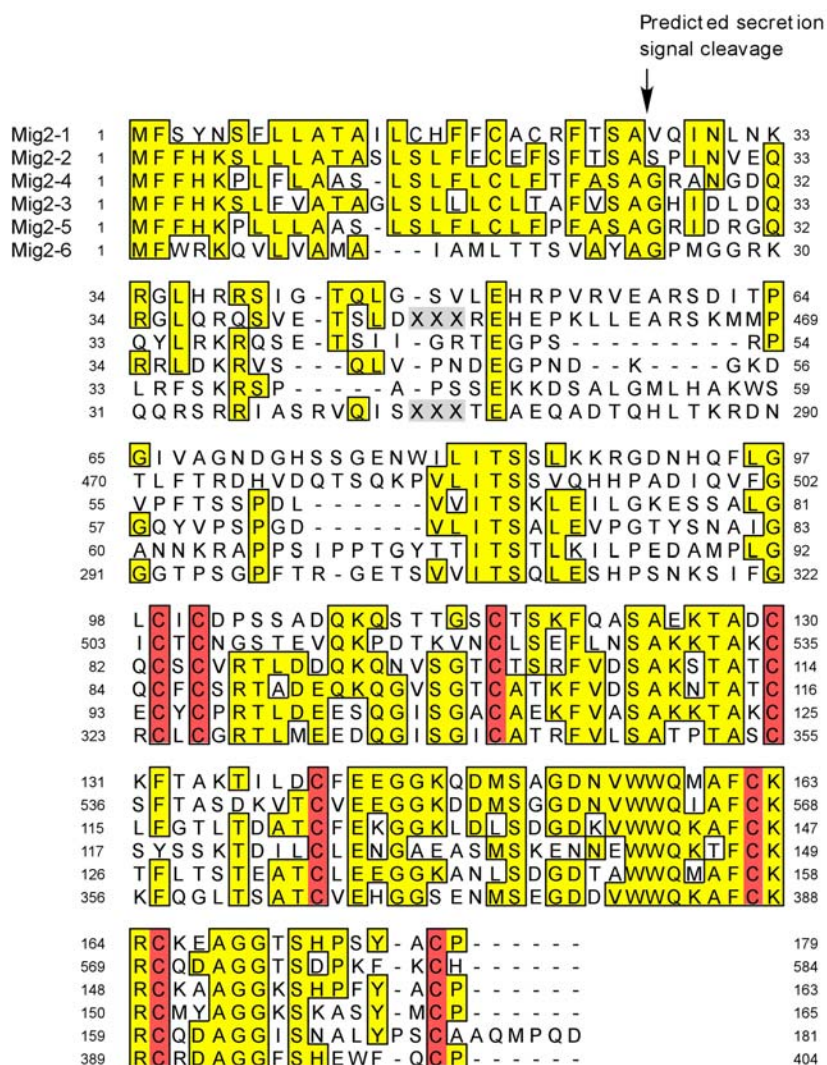
Figure 2. Amino acid alignment of *mig2* genes.
Amino acid alignment of the six *mig2* genes (cited from Christoph Basse). Conserved Cys residues are marked in red.

All *mig* genes encode small, secreted, cysteine-containing proteins (**Fig.2**) and lack homology in the NCBI database. They show very similar expression profiles during fungal growth: as assessed from Northern blot analysis and microscopy of reporter strains carrying *eGFP* under various *mig* promoters, all genes exhibit strongly upregulated transcription levels after plant penetration and maintain a high expression level until the formation of teliospores, whereas expression is absent or only faintly detectable during axenic growth (**Fig.3**). Transcripts of

mig2-1, mig2-4 and *mig2-5* were detectable 2 days after plant infection and peaked 2 days later, whereas transcripts of *mig2-2* and *mig2-3* were undetectable until 4 days after plant inoculation and then declined. Among them, *mig2-5* showed highest expression levels, followed by *mig2-4, mig2-2, mig2-1,* and *mig2-3* (Basse *et al*., 2002). Neither starvation conditions, which have been reported to mimic fungal gene expression *in planta* (Coleman *et al*., 1997; Pieterse *et al*., 1994; Van den Ackerveken *et al*., 1994), nor growth in the presence of tumor extracts could induce *mig1* or *mig2-1* expression under culture conditions (Farfsing *et al*., 2005). After deletion of *mig1* or the entire *mig2* cluster, no significant influence could be detected on pathogenic development. Based on their extracellular localization and plant-specific expression profile, Mig proteins were predicted to be involved in plant-fungal interaction (Basse *et al*., 2000, 2002).

Figure 3. Expression profile of *mig* genes.
A. Expression profile of *mig1* (cited from Basse *et al*., 2000), the constitutive expression of the *cbx* gene reflects the amount of *U. maydis* RNA loaded. **B**. Expression profile of *mig2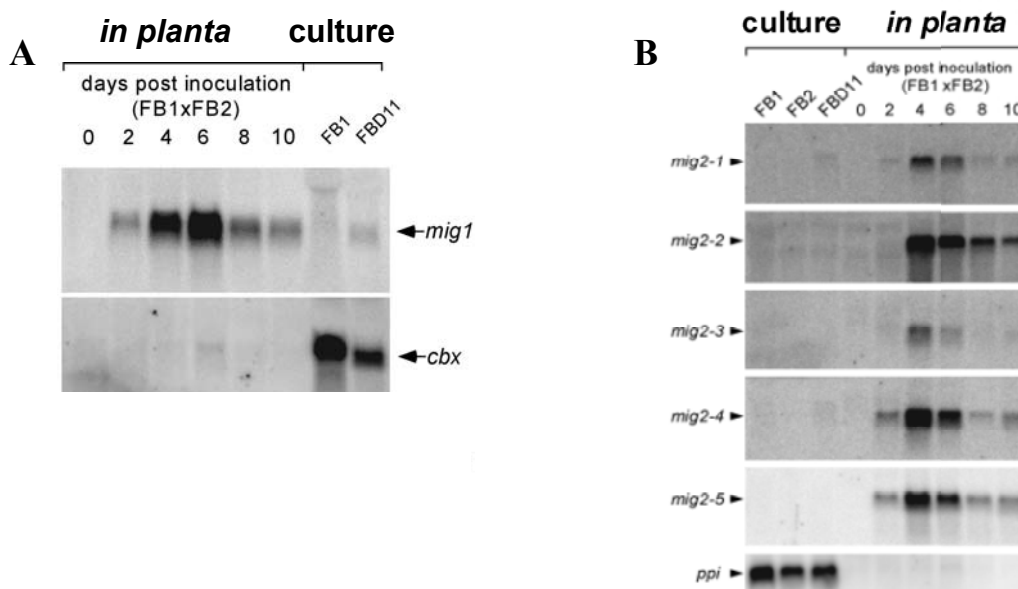* (cited from Basse *et al*., 2002), the constitutive expression of the *ppi* gene reflects the amount of *U. maydis* RNA loaded.

Jan Farfsing had analysed the transcriptional start position and promoter sequences of *mig2* genes. His results showed that the sequence context of all determined transcriptional start sites was CCACA$^T/_A$C. A putative TATA-like element (TLE) was found in the promoters of all *mig2* genes. Furthermore, the TLE appeared to be specifically required for *mig2-5* promoter activity *in planta*, which suggested that inducible *mig2-5* promoter activity relies on cooperation with a putative TATA box-binding protein. To investigate the *mig2-5* promoter in more detail, the JF1 strain was constructed, in which the 870 bp intergenic region between *mig2-4* and *mig2-5* was fused to the *eGFP* (enhanced green fluorescent protein) gene at the transcriptional start ATG and the construct was ectopically integrated in single copy into the *ip* locus of the solopathogenic *U. maydis* strain SG200 (*a1mfa2bE1bW2*). The GFP signal was strongly expressed in strain JF1 after plant penetration. By promoter deletion analysis, it was shown that elements required for inducible expression were located between position –234 and –161 relative to the start ATG, while adjacent regions on either side contributed to promoter activity. Based on the JF1 strain, a series of promoter mutation experiments were performed. In these experiments the GFP fluorescence was no longer detectable *in planta* when six 5'-CCA-3' motifs within positions –215 to –169 in the *mig2-5* promoter were substituted by the sequence 5'-GTC-3' (*U. maydis* strain JS12). This suggested the strong requirement for several 5'-CCA-3'containing motifs in this short stretch of the *mig2-5* promoter to confer inducible promoter activity (Farfsing *et al*., 2005).

1.4 Myb and C2H2 zinc finger regulators

There are a number of different families of zinc finger proteins that contain multiple cysteine and/or histidine residues and use zinc coordination to stabilize their folds (Berg *et al*., 1996,1997; Coleman, 1992; Klug *et al*., 1995; Wolfe *et al*., 1999). Cys$_2$His$_2$ zinc finger proteins were the founding members of the zinc finger

superfamily and were first noted as repeating domains in the TFIIIA sequence (Brown *et al.*, 1985; Engelke *et al.*, 1980; Hanas *et al.*, 1983; Miller *et al.*, 1985). The DNA-binding activity of these domains has been the major focus of investigation (Choo *et al.*, 1997). A number of studies were done to determine the principles of zinc finger-DNA recognition (Desjarlais *et al.*, 1992; Kim *et al.*, 1995; Nardelli *et al.*, 1991, 1992; Thukral *et al.*, 1992). It has been clear that these fingers possess the consensus sequence (F/Y)-X-C-X_{2-5}-C-X_3-(F/Y)-X_5- ψ -X_2-H-X_{3-5}-H, where X represents any amino acid and ψ is a hydrophobic residue (Wolfe *et al.*, 1999).

Sp1 (named according to the original purification scheme that included Sephacryl and phosphocellulose columns) was one of the first transcription factors to be purified and cloned from mammalian cells (Dynan *et al.*, 1983; Kadonaga *et al.*, 1987). It was shown to recognize and specifically bind to GC-rich sites within the simian virus 40 promoter via three Cys_2His_2 zinc-finger motifs. A similar DNA-binding domain has been found in many developmental regulators, including the *Drosophila* embryonic pattern regulator Krüppel (Kadonaga *et al.*, 1987). Subsequently, some transcription factors were identified that had zinc-finger motifs highly similar to those of Sp1, thereby defining a novel class of Sp1-like proteins or Krüppel-like factors (KLF, Turner *et al.*, 1999; Black *et al.*, 2001; Dang *et al.*, 2000; Suske, 1999). Like Sp1, factors of the Sp1-like/KLF family can bind various GC-rich DNA elements and regulate transcription. All these C2H2 zinc finger proteins share the same structure: a short peptide loop with a small β-hairpin, followed by an α-helix held in place by a zinc ion. In the folded state, the α-helix contacts directly the major groove of the DNA (Choo *et al.*, 1997).

The Myb protein family is a group of functionally diverse proteins found in plants and animals. Members of this family share a similar domain organization. The most conserved region is the DNA-binding domain located in the N terminus, which is composed of three imperfect repeats of 51-52 amino acids that recognize

the canonical Myb-binding site C/TAACNG (Biedenkapp *et al*., 1988; Howe *et al*., 1991). After binding, Myb proteins function to facilitate transcriptional activation (Goff *et al*., 1992).

In my work, zinc finger and Myb proteins in *U. maydis* were selected as candidates for the identification of possible *mig* regulators.

1.5 Aim of work

The aim of my work was the identification of possible *mig* regulators to get insight into the regulatory network, by which *U. maydis* is able to recognize and to invade into maize plants. In my work, the *mig2-5* promoter was used as major target for the *mig* regulator identification. It was planed to show the influence of regulator(s) to the *mig2-5* promoter both in culture and *in planta*. To confirm the function of the identified regulators, it was planed to verify the direct interaction between the promoter(s) and the *mig2-5* promoter both *in vitro* and *in vivo*. On another hand, I want to show the influence of the identified *mig2-5* regulator(s) to the other *mig* genes. Based on these experiments, I want to characterize the role of *mig* regulator(s) during pathogenic development of *U. maydis*.

2   Results

2.1 Myb and zinc finger proteins in *Ustilago maydis*

Based on the results of the *mig2-5* promoter mutation experiments, a promoter region has been uncovered in more detail (Farfsing *et al*., 2005). Inspection of the sequence context of the *mig2* genes led to the consensus sequence 5'-CCA-3'. This underlined the importance of CCA-containing motifs for inducible *mig2-5* promoter activity.

The zinc finger and Myb proteins are usual DNA-binding proteins found in eukaryotes. Many zinc finger proteins that have been identified can bind to various GC-rich DNA elements and regulate transcription. On this basis, Myb and Znf (zinc finger) proteins in *U. maydis* (**Table 1**) were selected as candidates for possible *mig2* regulators.

Table 1. Myb and Zinc-finger proteins in *U. maydis*

Proteins	MUMB um number	MUMDB Homology	Myb/Znf domain
Myb1	UM00808.1	Basal TF SNAPc large chain SNAP190 human	3
Myb2	UM04101.1	Related to Myb proto-oncogene protein	3
Myb3	UM04411.1	Related to CEF1	2
Myb4	UM05246.1	Predicted protein	3
Myb5	UM00808.1	Related to BDP1- TFIIIB subunit	1
Myb6	UM00983.1	Related to nuclear receptor co-repressor 1	2
Myb7	UM01400.1	Predicted protein	1
Myb8	UM02326.1	DNA- binding protein PCMYB1	2
Myb9	UM03856.1	Related to RSC8- subunit of the RSC	1
Myb10	UM05213.1	Related to ADA2	1
Znf1	UM00136.1	Transcription factor IIIA	9
Znf2	UM00264.1	Probable ZAP1- metalloregulatory protein	7
Znf3	UM00551.1	Oocyte Zinc finger protein XLCOF7.1	2
Znf4	UM00946.1	DNA-binding protein CREA	2
Znf5	UM01667.1	Hypothetical 76.3kDa Zinc finger protein in KTR5-UME3 intergenic region	2
Znf6	UM02038.1	Related to RGM1-transcriptional repressor protein	2
Znf7	UM02301.1	Transcription factor FST12	2
Znf8	UM02549.1	Zinc finger protein	2
Znf9	UM02857.1	Similar to RIKEN cDNA 6030404E16 gene	2
Znf10	UM03167.1	Zinc finger protein 211	4
Znf11	UM03172.1	Related to Zinc finger protein Zfp-38	4
Znf12	UM03403.1	Predicted protein	2
Znf13	UM03536.1	Zinc finger prottein SFP1	2
Znf14	UM03570.1	Zinc finger prottein FEZ	3
Znf15	UM03698.1	Zinc finger protein GLI3	3
Znf16	UM04274.1	Transcription factor PACC	3
Znf17	UM04774.1	Early growth response protein 1(EGR-1)	3
Znf18	UM04875.1	Zinc finger protein 1	2
Znf19	UM04909.1	DNA-binding protein CREA	2
Znf20	UM05144.1	PPG3	3
Znf21	UM05801.1	Predicted protein	2
Znf22	UM05804.1	Predicted protein	2
Znf23	UM05937.1	Transcription factor STEA	2
Znf25	UM01644.1	Predicted protein	2

The um number represents the original gene name obtained from MUMDB (http://mips.gsf.de/genre/proj/ustilago). Myb and Znf represent Myb and Zinc-finger proteins.

2.1.1 Expression analysis of zinc finger and *myb* genes in *Ustilago maydis*

Based on the expression profiles of *mig* genes, I presumed that the putative positive *mig* regulators should possess the same expression patterns. To examine expression patterns of *myb* and zinc finger genes in *U. maydis* during different pathogenic development stages, reverse transcription PCR (RT-PCR) quantification was done. RNA was isolated from three different stages: the haploid stage of strain FB1, the dikaryotic stage of strains FB1xFB2 grown on solid CM charcoal medium, and the stage *in planta* five days after inoculation. After reverse transcription, the cDNA samples were used as templates for quantification by PCR. Gene specific primers for the six *myb* and 20 *znf* genes, together with the primers for the *mig2-5* and *ip* (*cbx*) genes (controls), were used to quantify the transcription profiles for these genes during the three different development stages. The *ip* gene is constitutively expressed in all developmental stages (Broomfield *et al*., 1992), whereas the *mig2-5* gene is strongly upregulated *in planta*.

First, the PCR cycle number was tested and 34 cycles were found to be suitable to allow detection and quantification of all probes. Primers used for each gene are described in **Table 2**.

Table 2. Primers used for RT-PCR quantification

Gene	Primers*	Gene	Primers*	Gene	Primers*
myb5	JF219/JF220	*znf11*	JF280/JF281	*znf25*	JF282/JF283
myb6	JF221/JF222	*znf12*	JF241/JF242	*znf27*	JF261/JF262
myb7	JF223/JF224	*znf13*	JF243/JF244	*znf29*	JF263/JF264
myb8	JF225/JF226	*znf14*	JF245/JF246	*znf31*	JF265/JF266
myb9	JF227/JF228	*znf15*	JF247/JF248	*znf36*	JF267/JF268
myb10	JF229/JF230	*znf16*	JF249/JF250	*znf40*	JF269/JF270
znf5	JF231/JF232	*znf18*	JF251/JF252	*mig2-5*	m25gsa/m25gsb
znf6	JF233/JF234	*znf21*	JF253/JF254	*ip*	CBS1/CBS2
znf8	JF235/JF236	*znf22*	JF255/JF256		
znf9	JF237/JF238	*znf23*	JF257/JF258		

The length of these primers is 20 bp (average); the length of the PCR products for each gene is approximately 800 bp. *See Table 8 for sequence and details.

Quantification of the PCR products upon gel electrophoresis showed that the *znf21*, *znf22*, *znf23* and *znf25* exhibited similar expression profiles to *mig2-5* during the three stages tested (**Fig.4**): they were strongly upregulated during the five day-tumor stage, whereas expression was absent or only faintly detectable during axenic growth (FB1 and FB1xFB2). This result made these genes prime candidates for corresponding regulators *in planta*.
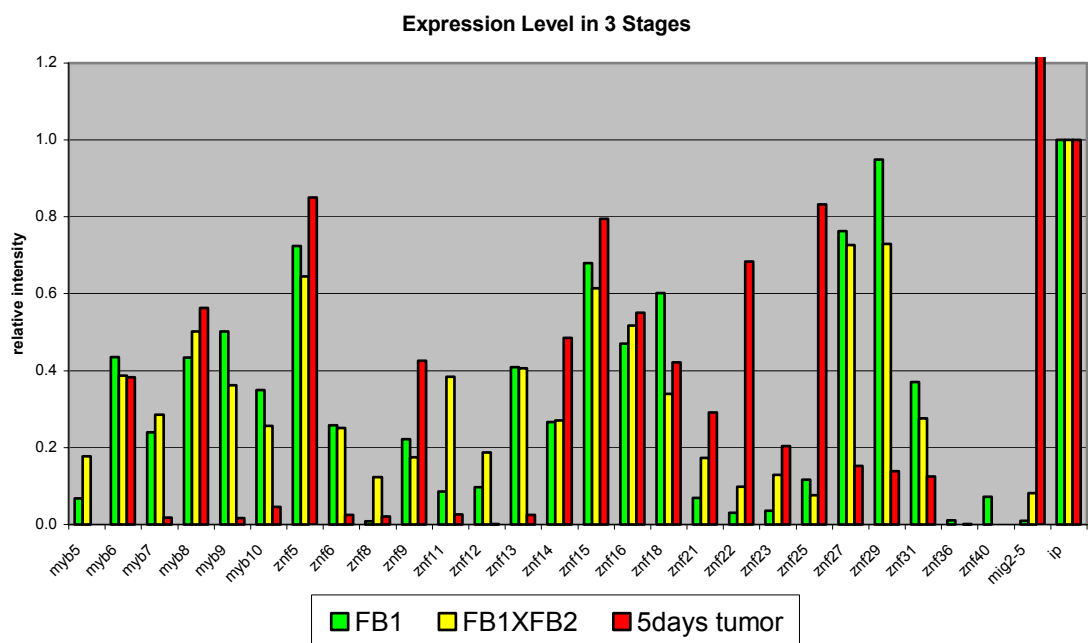
Figure 4. RT-PCR quantification of *myb* and zinc finger genes (abbreviated with *znf*) in *U. maydis* during different stages.

Signal intensities were obtained from RT-PCR analysis. RNA was isolated from three development stages: FB1, FB1xFB2, and infected plant tissue five days after inoculation. After reverse transcription, the cDNA templates were used for PCR (34 cycles). The green columns represent gene expression levels in the haploid stage, the yellow columns represent gene expression levels during the dikaryotic stage in culture, and the red columns represent gene expression levels in plant tumors five days after inoculation.

2.2 Deletion analysis of the candidate genes

Approximately 17.4 Mb of the estimated 20.5 Mb genome of *U. maydis* strain UM521 have been sequenced by Bayer CropScience AG (Monheim, Germany). Recently, the Broad Fungal Genome Initiative has established a more complete sequence of UM521 (19.7 Mb, http://www.broad.mit.edu). The availability of the genomic sequence made it possible to analyze the function of specific gene(s) by generating defined deletion mutants.

To investigate the function of the prime candidates that were chosen from the results of the RT-PCR analysis, I constructed deletion strains of these genes. The gene deletion procedure in my work involved the generation of two homologous flanking regions of the target gene, ligation of the flanking regions to a resistance cassette, reamplification of the entire construct by PCR, and the standard transformation in *U. maydis*. For *U. maydis*, flanking sequences of about 1 kb in length had been determined to be ideal for target gene replacement constructs (Kämper, 2004).

The bacterial hygromycin phosphotransferase gene (*hph*), which confers resistance to hygromycin, is widely used as a dominant selection marker in *U. maydis* (Wang *et al.*, 1988). A hygromycin resistance cassette with a shortened *hsp70* promoter and a terminator sequence from the *Agrobacterium nos* gene was constructed to minimize the commonly used *hph* resistance cassette from 3061 to 1871 bp; it was flanked by distinct *Sfi*I restriction sites on either site in plasmid pBShhn, which was used for ligation with the two flanking regions after *Sfi*I digestion. The central five nucleotides of the *Sfi*I recognition sequence are variable, and thus allowed directed cloning of the three fragments.

The two flanking regions were amplified from genomic DNA of the wild type strain 521 by PCR using primers that introduced the respective *Sfi*I sites to the left (CACGGCC<u>TGAG</u>↓<u>T</u>GGCC) and right (GTGGGCC<u>ATCT</u>↓<u>A</u>GGCC) flanking regions. After digestion with *Sfi*I, the left and right flanking fragments were ligated to the *hph*-cassette (see above). Based on the two non-compatible *Sfi*I sites,

14

self-ligations were successfully prevented. Hence the ligation reaction gave three different products: (1) the *hph*-cassette ligated with the left flanking fragment; (2) the *hph*-cassette ligated with the right flanking fragment; (3) the *hph*-cassette ligated with both left and right flanking fragments. Subsequently, the ligation products with both flanking fragments were isolated upon agarose gel electrophoresis. The purified ligation product was cloned into the pCR4-TOPO plasmid vector and cloned in *E. coli*. After sequencing, the confirmed plasmid was used as template for a second PCR amplification using the outer primers. The amplified DNA fragment (left flank-*hph*-right flank) was transformed into the *U. maydis* strain JF1. Homologous integration was verified by PCR using outer primers of the gene ORF (see **Table 8**) and the hph-cassette specific primers hhn5 and hhn3 (**Fig.5**). In addition, gene specific primers (see **Table 2**) were used in a diagnostic PCR test to determine the absence of the target genes in the *U. maydis* genome. The absence of a PCR product could verify the deletion of the target gene.

Deletion mutants of *znf3, znf4, znf5, znf7, znf14, znf20, znf21, znf22, znf23, znf25, myb2*, and *myb8* were generated based on strain JF1. Among these genes, *znf21, znf22, znf23* and *znf25* exhibited similar expression profiles to *mig2-5* during the three stages tested (**Fig.4**); *znf3, znf4, znf5, znf7, znf14, znf20, myb2*, and *myb8* also showed stronger expression levels *in planta* than in culture. However, the construction of *myb1, myb3, znf9*, and *znf12* deletion mutants was not successful. 48 individual transformants were generated for each deletion mutant and none of them showed correct PCR results. This could be explained by the fact that these genes are crucial for *U. maydis*.
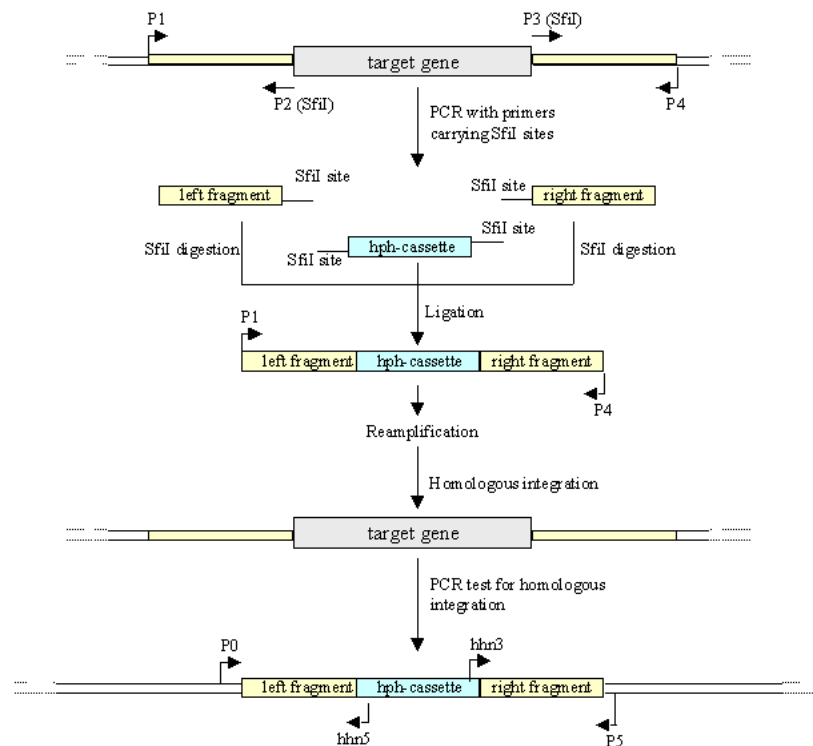
Figure 5. PCR based gene deletion procedure.

Gene deletions were generated as follows. The 5' region (left fragment) of the gene to be deleteded was amplified with PCR using the primer pair P1/P2, and the 3' region (right fragment) was amplified with the primer pair P3/P4. The PCR products were ligated to the *hph* resistance cassette (hph-cassette) after SfiI digestion. The ligation product is used as template for a second PCR using primers P1 and P4. The PCR product was used for transformation of *U. maydis*. Homologous integration was verified with PCR using primer pairs P0/hhn5 and P5/hhn3. hhn5 and hhn3 are *hph*-cassette specific primers, and P0 and P5 bind within the genomic context outside of the left and right fragments (outer primers). PCR products are obtained only if a homologous integration has taken place.

2.2.1 Plant infection with deletion mutant strains

Next, I examined whether strains deleted in candidate genes for potential *mig2-5* regulators were affected in *mig2-5* gene expression during plant infection. For this purpose, maize plants were inoculated with the individual strains and infected plant tissue was harvested three days after inoculation. The GFP fluorescence signals in these mutant strains were examined by fluorescence microscopy. Only

the *znf22* deletion mutant showed a significantly reduced GFP expression level: it emitted very weak GFP fluorescence after plant infection (**Fig.6**) and furthermore many hyphae without fluorescence were observed. This illustrated that the Znf22 protein is required for the *mig2-5* promoter activation *in planta*. For the remaining mutant strains, no significant influence on GFP expression levels could be detected after plant infections.
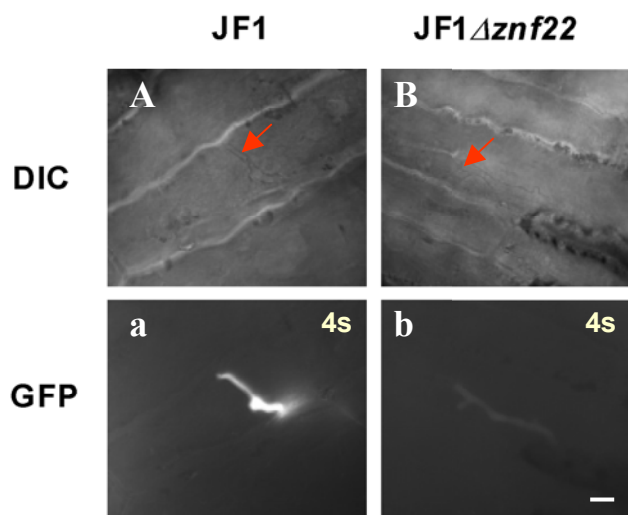
Figure 6. Comparison of GFP fluorescence in strains JF1 and JF1△*znf22*.
Infected maize tissue samples were assayed by differential interference contrast light (DIC) and epifluorescence (GFP) microscopy. Hyphae are marked by red arrows. Exposure time for fluorescence photography is indicated in the upper right corner of the pictures.
A. Maize tissue three days after infection by strain JF1 was assayed by differential interference contrast light microscopy (DIC). **B**. Maize tissue three days after infection by JF1 △*znf22* strain was assayed by DIC. **a**. Maize tissue three days after infection by JF1 strain was assayed by epifluorescence (GFP) microscopy. **b**. Maize tissue three days after infection by JF1△*znf22* strain was assayed by epifluorescence (GFP) microscopy. Bar= 10 μm for all panels.

All these deletion mutants were further examined both in culture (YEPS_L medium) and *in planta*. However, neither a morphology change nor an obvious phenotype could be detected. Also, no obvious influence on tumor formation could be found in these deletion mutants.

In addition, Northern blot analysis was performed to verify the results from fluorescence microscopy. For this purpose, RNA was isolated from five-day-old

plant tumors. The ^{32}P-labeled *eGFP, mig2-5, mig2-2* and *mig2-6* DNA fragments were used as probes for the Northern blot analysis to detect the expression levels of these genes in these mutant strains five days after plant inoculation.

Similar to the results from the fluorescence microscopy, only the *znf22* deletion mutant JF1△*znf22* showed a significant difference in the *mig2-5* promoter activity compared to the wild type strain JF1. While no *eGFP* and *mig2-5* signals could be detected for the *znf22* deletion mutant strain, *mig2-2* and *mig2-6* were still expressed. Although, expression of these genes was somewhat reduced compared to strain JF1, this appeared to be within the variation. For the remaining *znf* gene deletion strains, no drastically diminished signals could be found. Interestingly, in the *znf23* deletion strain, expression of *eGFP*, *mig2-5*, and *mig2-6* appeared stronger than in the other △*znf* mutants (**Fig.7**).

Taken together, *znf22* is required to activate the *mig2-5* promoter *in planta*. I therefore refer to Znf22 as putative positive regulator for *mig2-5* and termed it Mzr1 (*mig* zinc finger regulator). However, I could not exclude the possibility that Mzr1 was also involved in regulating the remaining *mig* genes. It is also interesting whether additional proteins are involved in *mig2-5* activation. Since *mig2-2* and *mig2-6* were still expressed in the absence of *znf22*, at least for these genes there should be other proteins to be involved in their activation after plant inoculation.
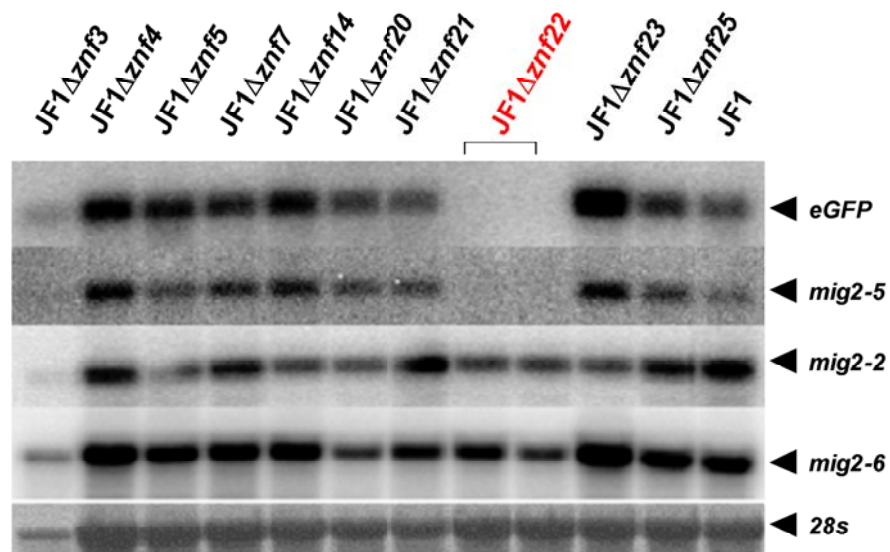
Figure 7. Expression analysis of *mig* genes in the different *U. maydis znf* deletion mutants.

RNA was prepared from infected plant tissue five days after inoculation. Each gel was loaded with comparable amounts of the same RNA preparations. The Northern blots were probed with ^{32}P-labeled gene-specific fragments of the *mig2* and *eGFP* genes. Staining with methylene blue reflects the amounts of total RNA loaded (*28s*, 8 μg).

2.3 Overexpression analysis

2.3.1 *mig2-5* promoter requirement for Mzr1 (Znf22)

Due to the identification of Mzr1 (Znf22) as an essential factor for *mig2-5* promoter activation *in planta*, two questions arise: can Mzr1 if overexpressed induce *mig2-5* promoter activation under culture conditions? Are the 5'-CCA-3' elements previously identified in the *mig2-5* promoter (Farfsing *et al.*, 2005) required for the *mig2-5* regulation by Mzr1?

To answer these two questions, the plasmid pCZ22v was generated, in which expression of the *mzr1* ORF was controlled under the carbon source-regulated *crg1* promoter (P_{crg1}; Bottin *et al.*, 1996). A nourseothricin (*nat*) resistance cassette (Müller *et al.*, 1999) was used as selectable marker for *U. maydis*. Subsequently, the linearized plasmid was ectopically integrated into the genomes of strains JF1, JT3, JS7, JS10, JS11 and JS12. These strains had been constructed on the basis of the JF1 strain (Farfsing *et al.*, 2005). In strain JT3, the 870-bp *mig2-5* promoter fragment had been shortened to 240 bp; in strain JS7, the three regions box I (-130 to −120), box II (-155 to -139), and box III (-189 to −173) were substituted; in strain JS10, three of the 5'-CCAMC-3' motifs were substituted; in strain JS11, the region between position −233 to −225 had been replaced; in strain JS12, six 5'-CCA-3' motifs within positions −215 to −169 were substituted by the sequence 5'-GTC-3'. Next, PCR was performed using primers against the *crg1* promoter and the *mzr1* (primer pair PCRG/Z22b) to confirm the integration of the *crg1* promoter-*mzr1* construct in *U. maydis* transformants. Those transformants which conferred correct PCR products were selected for further analysis.

To determine the expression levels of *mzr1,* the generated JF1/p*crg1-z22*, JT3/p*crg1-z22*, JS7/p*crg1-z22*, JS10/p*crg1-z22*, JS11/p*crg1-z22* and JS12/p*crg1-z22* strains were incubated in complete medium containing 1% arabinose (CM/Ara, for *crg1* promoter induction) for about 15 h until an OD_{600} of 0.5-0.8 was reached. RNA was prepared and hybridized with a ^{32}P labeled *mzr1*

probe to examine *mzr1* expression levels in JF1 and JF1 promoter mutant strains. In each strain, the three transformants, which showed the strongest *mzr1* expression levels were selected for further analysis to determine the *mig2-5* promoter activity. These selected transformants were incubated under the same conditions as described above. RNA was prepared and hybridized with a ^{32}P labeled *eGFP* fragment to examine *eGFP* expression in these strains after *mzr1* induction in CM/Ara. Subsequently, RT-PCR was performed to verify *mzr1* and *ip* expression levels in these strains using primer combinations.

Northern hybridization showed that *eGFP* was strongly upregulated after *mzr1* expression in strain JF1 under culture conditions. This revealed that *mzr1* expression under culture condition was sufficient to induce *mig2-5* promoter activity in strain JF1. For the JT3 strain, *mzr1* expression could still induce the expression of *eGFP*. However, the *eGFP* expression in JT3 was weaker than in the strain JF1. This confirmed previous analysis showing that the shortened 240-bp *mig2-5* promoter could still be activated by Mzr1 in culture (Farfsing *et al.*, 2005). In the JS7 strain, almost no *eGFP* signal was detectable. This showed that substitutions of the three regions box I (-130 to −120), box II (-155 to -139), and box III (-189 to −173) abolished the *mig2-5* regulation after *mzr1* expression in culture. This confirmed previous analysis showing that GFP fluorescence in planta was almost abolished in strain JS7 (Farfsing *et al.*, 2005). GFP could still be induced in strain JS10, which corresponding to previous result showing that substitution of three CCAMC motifs (positions from −205 to −202, -189 to −186, -172 to -167) only partially diminished *mig2-5* promoter activity in strain JS10 after inoculation. In contrast, no *eGFP* signal could be detected for the mutant strain JS12. This proved that the six 5'-CCA-3' motifs deleted in strain JS12, which were required for *mig2-5* promoter activity *in planta* (Farfsing *et al.*, 2005), were crucial for the *mig2-5* regulation by Mzr1. In addition, Jan Farfsing's result showed that the substitution in strain JS11 had only a limited effect on GFP fluorescence *in planta*. However, *eGFP* expression was drastically reduced in the strain JS11 after *mzr1* overexpression under culture conditions (**Fig.8**), indicating

that activities via Mzr1 require this element (box IV; Farfsing *et al*., 2005).

Taken together, my results document that the six 5'- CCA-3' motifs (-215 to −213, -204 to −202, -196 to −194, -190 to −188, -183 to −181, and -171 to −169) that were required for the *mig2-5* promoter activity *in planta* were also crucial for the Mzr1 function under culture conditions.
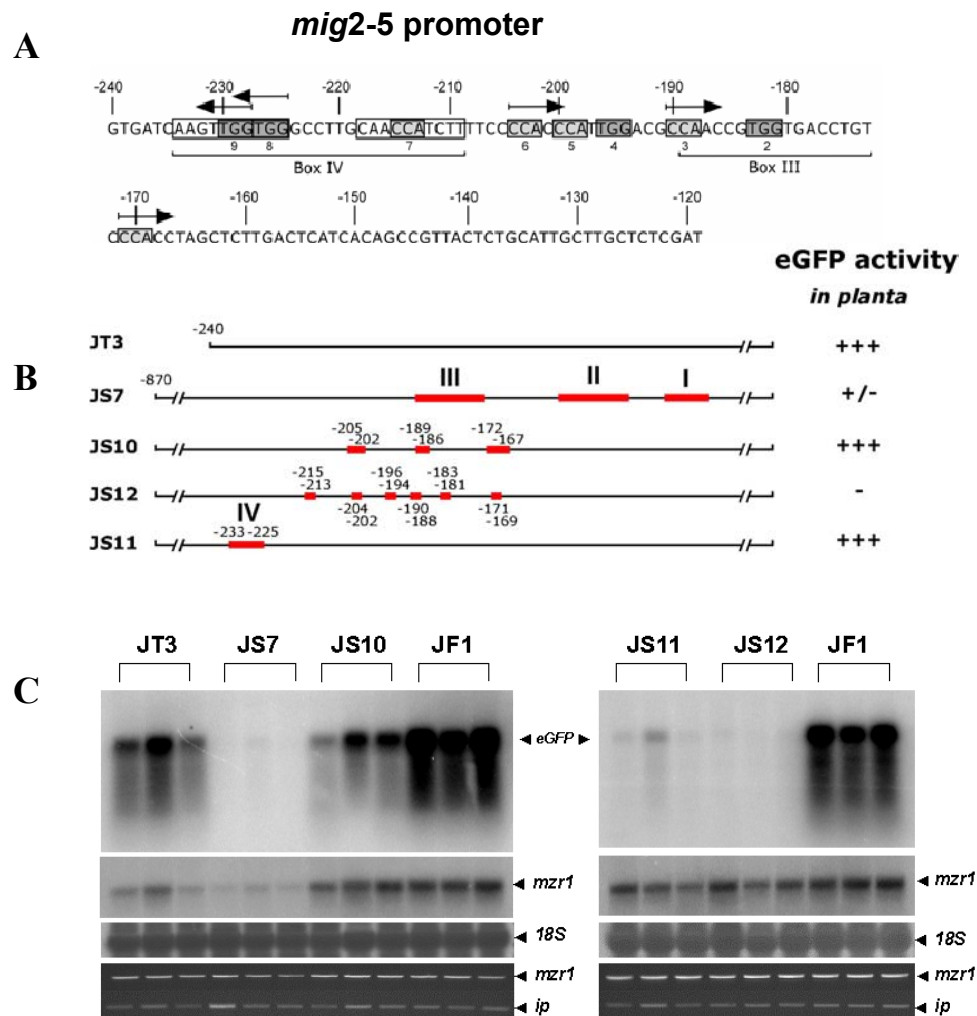
Figure 8. *mzr1* overexpression analysis.
A. Distribution of repetitive motifs in the *mig2-5* promoter from −240 to −119. Elements matching the consensus 5'- CCAMC-3' are denoted by arrows. CCA base triplets are boxed in light gray. The two inverted repeats of box IV are framed (depiction from Farfsing *et al*., 2005). **B**. Schematic representation of the various promoter substitution constructs and their activities in the respective transformant 4 days after inoculation. Relative green fluorescent protein (GFP) activities *in planta* were evaluated by microscopy and are indicated by + and − symbols, where - means no detectable GFP fluorescence and + to +++ = increasing fluorescence levels from faintly to brightly fluorescent (depiction from Farfsing *et al*., 2005).

C. *eGFP* transcript levels in culture were determined by Northern blot analysis using RNA from strains grown in liquid CM/Ara and a ^{32}P-labeled *eGFP* fragment. Staining with methylene blue reflects the amounts of total RNA loaded (10 μg). *mzr1* and *ip* specific primers were used in RT-PCR (28 cycles) for comparison of *mzr1* and *ip* gene expression levels between independent transformants for each construct. The primer pair YZ7/YZ20 was used for the *mzr1* expression confirmation; primer pair CBS1/CBS2 was used for the *ip* gene.

2.3.2 Mzr1 specificity for *mig* regulations

Based on the finding that Mzr1 can induce the *mig2-5* promoter activity, I addressed specificity of Mzr1. For this purpose, I screened the *U. maydis* genome for related zinc finger proteins. In addition, the C2H2 zinc finger gene *biz1* (Flor-Parra *et al*., 2006) was involved in this analysis. It has been shown in an independent study that *biz1* overexpression is able to induce expression of *mig2-4*, *mig2-5* and *mig2-6* (M. Vranes and J. Kämper, unpublished).

After comparison of C2H2 zinc-fingers of *U. maydis* Znf proteins, it was found that the C2H2 zinc-fingers of Znf7, Znf12 and Znf23 are very similar to Biz1 or Mzr1 (**Fig.9)**.

Figure 9. Comparison of zinc finger motifs.
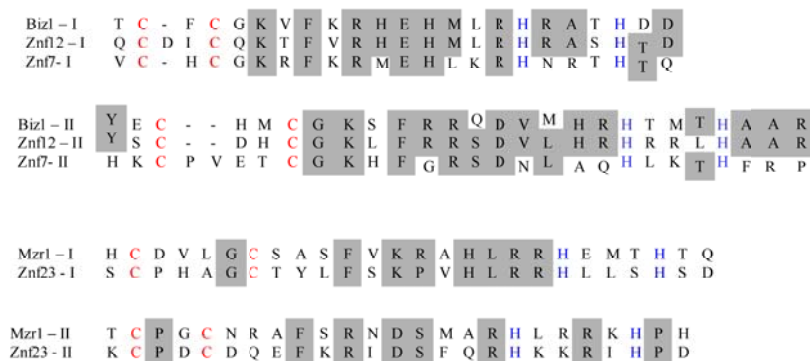Amino acid alignment of the zinc finger domain. Cys residues are marked with red color; His residues are marked with blue color.

To investigate the influences of *znf7*, *biz1*, *znf12* and *znf23* to *mig* gene expression, JF1/p*crg1-z7*, JF1/p*crg1-biz1*, JF1/p*crg1-z12* and JF1/p*crg1-z23 U. maydis* strains were constructed based on plasmid pCZ7, pCZ8, pCZ12 and pCZ23, in which

expression of *znf7, biz1, znf12* and *znf23* is controlled under the carbon source-regulated *crg1* promoter. PCR was performed to confirm the integration of the *crg1* promoter-*znf* constructs in *U. maydis* transformants using primers against the *crg1* promoter and the *znf* genes. Primer pairs PCRG/Z7b, PCRG/Z8b, PCRG/Z12b, PCRG/Z22b, and PCRG/Z23b were used for *znf7, biz1, znf12, mzr1,* and *znf23* genes individually. PCR products of the expected size could be obtained only for those transformants, in which the correct integration took place.

To determine the expression levels of these target genes in each independent transformant, each *U. maydis* transformant, together with the strain JF1/p*crg1-mzr1* described above, was grown in CM/Ara for about 15h until an OD_{600} of 0.5-0.8 was reached. RNA was isolated and used for Northern blot analysis using the ^{32}P-labeled *znf* gene specific probes. The Northern hybridization results showed that expression levels of each *znf* gene in the different transformants varied (**Fig.10**). From these transformants, JF1/p*crg1-z7* #1, #3, JF1/p*crg1-biz1* #2, #3, JF1/p*crg1-z12* #1, #2, JF1/p*crg1-mzr1* #1, #3, JF1/p*crg1-z23* #4, #6 strains showed the strongest gene expression levels. These strains were selected and grown under conditions as described above. RNA was prepared and used for the following Northern blot analysis to detect *mig* gene expression in these strains. RNA from strain JF1 as well as from six day-old plant tumours of plants infected with the FB1xFB2 mixture was used for Northern hybridizations as negative and positive controls respectively.

Northern blot analysis showed that both *biz1* and *mzr1* overexpression could induce expressions of *mig1*, *mig2-5,* and *mig2-6*. However, Biz1 and Mzr1 play different roles in *mig* gene regulation (**Fig.11)**. Mzr1 appeared more specific for *mig2-5* than for *mig1* or *mig2-6*. In contrast, Biz1 was more important for the *mig1* and *mig2-6* induction. For *mig2-1* and *mig2-2*, no signal could be detected in these *U. maydis* strains after either *mzr1* or *biz1* inductions. Very faint *mig2-5* and *mig2-6* signals were detected in the *znf7* overexpression strains. This illustrated that Znf7 could only weakly influence the *mig2-5* and *mig2-6* activities. In addition, *mig2-5* and *ip* expression levels in these strains were tested by RT-PCR

analysis. The RNA prepared for the Northern analysis was used as template after reverse transcription. Primers used for *mig2-5* and *ip* were the same as described above (see **Fig.10)**. This showed similar levels of *ip* expression, except for the lane showing *ip* level in infected plant tissue, as expected. Furthermore, the weak *mig2-5* signals in the *znf7* overexpression strains could be confirmed.
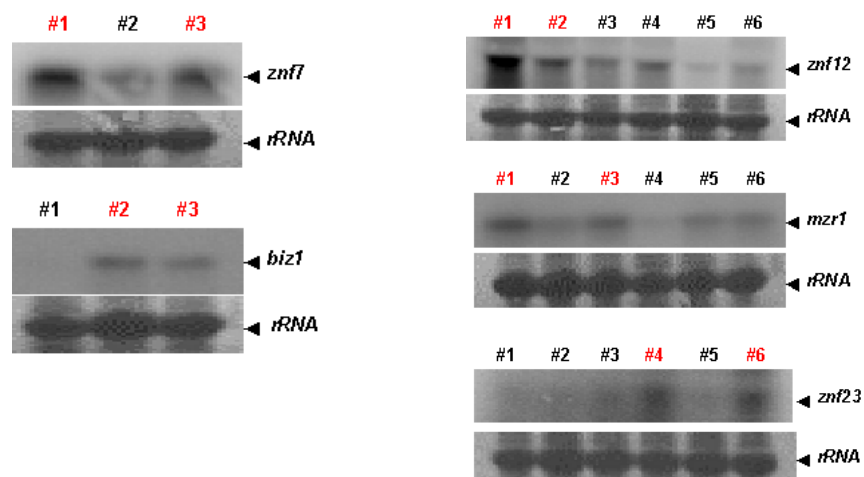
Figure 10. Expression analysis of *mzr1*, *biz1*, *znf7*, *znf12* and *znf23*.
Transcription levels of each *znf* gene in individual transformants were determined by Northern blot analysis using RNA from strains grown in liquid CM + 1% arabinose. Northern blots were probed with ^{32}P labeled *znf7, biz1, znf12, mzr1* and *znf23* fragments. Staining with methylene blue reflects the amounts of total RNA loaded (9 μg). The red marked strains were used for further analysis.

Taken together, overexpression of *mzr1* could induce *mig1*, *mig2-5* and *mig2-6* expression under culture conditions. Furthermore, Mzr1 was more specific for the *mig2-5* regulation. Biz1 could also induce transcriptional activation of *mig1*, *mig2-5* and *mig2-6* in culture. Znf7 could weakly induce *mig2-5* and *mig2-6* expression. In conclusion, together with expression in promoter mutant strains (see above), this underlines the specificity of Mzr1 in activating the *mig* gene promoters. However, regulators for *mig2-1* and *mig2-2* genes remain unknown.
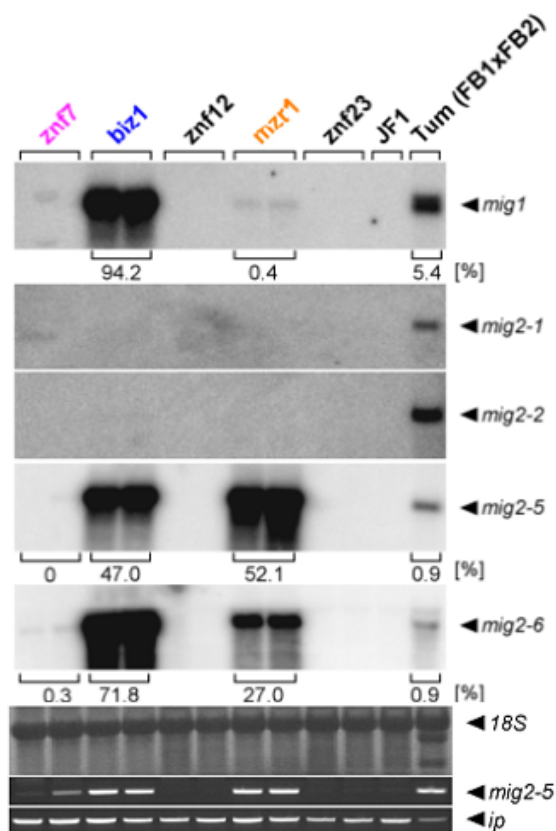
Figure 11. Overexpression analysis of zinc finger genes.
mig transcription levels in culture were determined by Northern blot analysis using RNA from strains grown in liquid CM/Ara. RNA was isolated from five day-old tumors infected with strains FB1xFB2. This served as positive control. RNA prepared from the wild type strain JF1 grown in liquid CM/Ara was used as negative control. Northern blots were probed with ^{32}P labeled *mig1, mig2-1, mig2-2, mig2-5* and *mig2-6* fragments. Staining with methylene blue reflects the amounts of total RNA loaded (9 μg). The *mig2-5* and *ip* specific primers were used in RT-PCR (32 cycles) for gene expression level determinations in independent transformants of each construct.

2.3.3 Relationship between Mzr1 and Biz1

The above results showed that expression of both *mzr1* and *biz1* could induce *mig* gene expression. To determine the relationship between Mzr1 and Biz1 for *mig* regulation, two overexpression strains JF1 △ *mzr1*/p*crg1-biz1* and SG200 △ *biz1*/p*crg1-mzr1* were constructed: the *crg1* promoter-*biz1* fusion was ectopically integrated into strain JF1△*mzr1* on the one side, and the *crg1-mzr1* fusion was integrated into the *cbx* locus of strain SG200△*biz1* on the other side. To confirm

26

the sequence insertions into the *U. maydis* genome, PCR analysis was performed using a primer against the *crg1* promoter and gene specific primers against the *mzr1* construct (PCRG/Z22b) and the *biz1* construct (PCRG/Z8b), respectively.

Each five individual strains, which showed the expected PCR products, were selected for subsequent Northern hybridization to demonstrate *mig2-5* expression. To induce expressions of *biz1* and *mzr1*, the selected *U. maydis* strains were grown in CM/Ara for 15h to an OD_{600} of 0.5-0.8. Wild type strains JF1 and SG200 were grown under the same conditions as controls. RNA was prepared and used for the following Northern hybridizations. For *biz1* overexpressing strains, a ^{32}P-labeled *eGFP* specific DNA fragment was used as probe. A ^{32}P-labeled *mig2-5* fragment was used as probe for *mzr1* expression strains. To verify expression of *mzr1* or *biz1* in all *U. maydis* transformants, RT-PCR was performed using *biz1* and *mzr1* specific primers and the same RNA utilized for the Northern analysis (as **Fig.12**).

The Northern blot analysis showed that in the *mzr1* deletion strains, the *mig2-5* promoter could be activated after *biz1* overexpression. Interestingly, for the *biz1* deletion strains, no *mig2-5* signal could be detected after *mzr1* overexpression. RT-PCR analysis confirmed comparable expression of *biz1* or *mzr1* in these strains (**Fig.11**).

In summary, Biz1 could induce *mig2-5* promoter activity in the absence of Mzr1, whereas *mzr1* expression in the *biz1* deletion mutant could no longer induce *mig2-5* promoter activity, demonstrating that Mzr1 requires Biz1 for *mig2-5* induction.
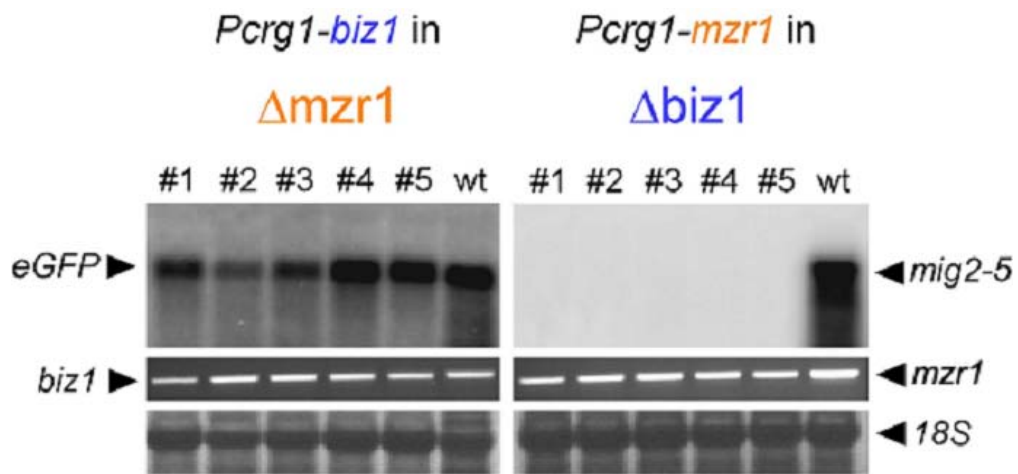
Figure 12. Overexpression analysis in *biz1* and *mzr1* deletion mutants.
mig2-5 and *eGFP* expression levels in culture were determined by Northern blot analysis using RNA from strains grown in liquid CM/Ara. RNA isolated from strains JF1/pcrg1-biz1 and JF1/pcrg1-mzr1 grown in liquid CM/Ara was used as positive control, denoted with wt, respectively. Northern blots were probed with ^{32}P-labeled *mig2-5* and *eGFP* fragments. Staining with methylene blue reflects the amounts of total RNA loaded (10 μg). *mzr1* and *biz1* specific primers were used in RT-PCR (28 cycles) for gene expression confirmation in independent transformants for each construct. Primer pair YZ22/YZ23 (see Table7) was used for *biz1* and YZ7/YZ20 (see Table7) was used for *mzr1*.

2.3.4 Phenotype of *mzr1* overexpression strains

Recently, it has been shown that *U. maydis biz1* deletion mutants have a severe penetration defect upon inoculation of maize plants. The few hyphae that had penetrated could not proliferate *in planta*. Thus, the sexual development was blocked (Flor-Parra *et al.*, 2006). My results indicated that Mzr1 requires Biz1 for *mig2-5* induction. Since both Mzr1 and Biz1 obviously regulate the same promoter, it was interesting to know whether *mzr1* overexpression could compensate, at least partially, the pathogenicity of *biz1* deletion strains. Furthermore, it was also confirmed that the *mig2-5* promoter activity was strongly reduced in *mzr1* deletion strains after plant inoculation. Therefore, another interesting question was whether *mzr1* overexpression in strain JF1△*mzr1* could

28

induce *mig2-5* promoter activity *in planta* to a high level.

To answer these questions, *U. maydis* strains JF1 $\triangle$ *mzr1*/p*otef-mzr1*, JF1/p*otef-mzr1* and SG200$\triangle$*biz1*/p*otef-mzr1* were generated, in which the *mzr1* ORF was linked to the constitutive *otef* promoter (Spellig *et al.*, 1996). For the generation of strain SG200$\triangle$*biz1*/p*otef-mzr1*, the *otef* promoter linked *mzr1* ORF was integrated into the *cbx* locus of strain SG200$\triangle$*biz1*. Integration of the construct was confirmed by Southern blot using a ^{32}P-labeled *cbx* DNA fragment. Those transformants, which produced two *cbx* linked fragments after BamHI digestion, were selected for further analysis (**Fig.13**). Integration of the constructs into the JF1$\triangle$*mzr1* and JF1 strains was confirmed by RT-PCR using primer pair JF255/Z22b. Next, the selected JF1$\triangle$*mzr1*/p*otef-mzr1* and JF1/p*otef-mzr1* strains, together with the wild type strain JF1, were cultivated in YEPS$_L$ medium for 15 hours for subsequent RNA isolation to confirm expression of the *mzr1* and *ip* genes by RT-PCR. Primer pairs YZ7/YZ20 and CBS1/CBS2 were used for *mzr1* and *ip* gene detection.

This showed that *mzr1* was strongly expressed in these transformants relative to strain JF1 (**Fig.14**). Next, the selected strains were incubated for plant inoculation. Astonishingly, the *mzr1* overexpression strains grew very slowly in YEPS$_L$ medium. To address growth in more detail, these strains were incubated in YEPS$_L$ medium for 25 hours to determine the growth rate in comparison to the wild type strain JF1. The OD$_{600}$ values of growing cultures were measured at multiple intervals during the incubation period. The growth curve illustration shows that the *mzr1* overexpression strains grew significantly slower than the wild type strain JF1 under culture conditions (**Fig.15**). As expected, the $\triangle$*mzr1* strain grew comparable to the parental strain.

In addition, the morphologies of these strains after a 12 h incubation period were compared. In these *mzr1* overexpression strains, filamentous cells appeared increased in number compared to the wild type strain JF1 or to the JF1 $\triangle$*mzr1* mutant strain (**Fig.16**). Additionally, the *mzr1* overexpression also formed aggregates.
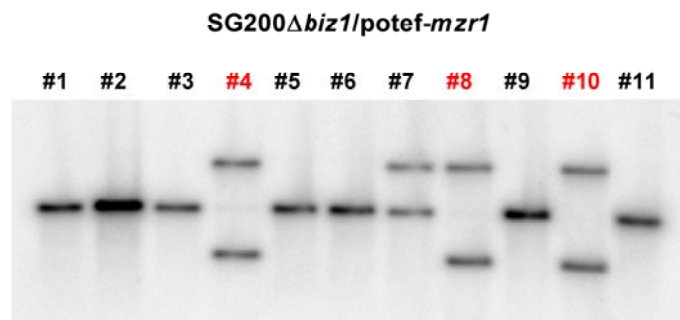
Figure 13. Southern blot analysis for the SG200△*biz1*/potef-*mzr1* constructs.
The Integration of the the *otef* promoter linked *mzr1* ORF into the *cbx* locus of strain SG200△ *biz1* was confirmed by Southern blot using a ^{32}P-labeled *cbx* DNA fragment and genomic DNA from strains grown in YEPS$_L$ medium for 15h. 10 μg of genomic DNA was loaded for each independent transformant after *Bam*HI digestion. The selected correct transformants (producing two fragments after digestion) are marked in red.
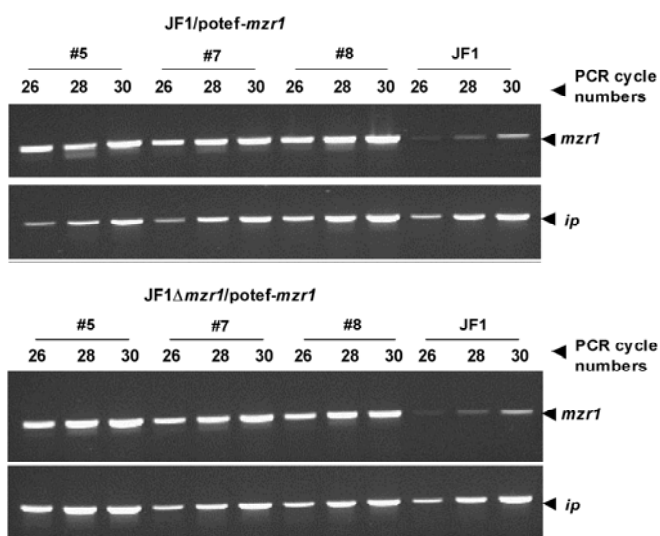
Figure 14. RT-PCR for the detection of *mzr1* expression levels.
mzr1 transcript levels in culture were determined by RT-PCR analysis using cDNA from *mzr1* overexpression strains and strain JF1. Total RNA was isolated from strains grown in YEPS$_L$. *mzr1* and *ip* specific primers were used in the RT-PCR analysis to determine the *mzr1* and *ip* gene expression during independent transformants for each construct. 26, 28, and 30 represent PCR cycle numbers.
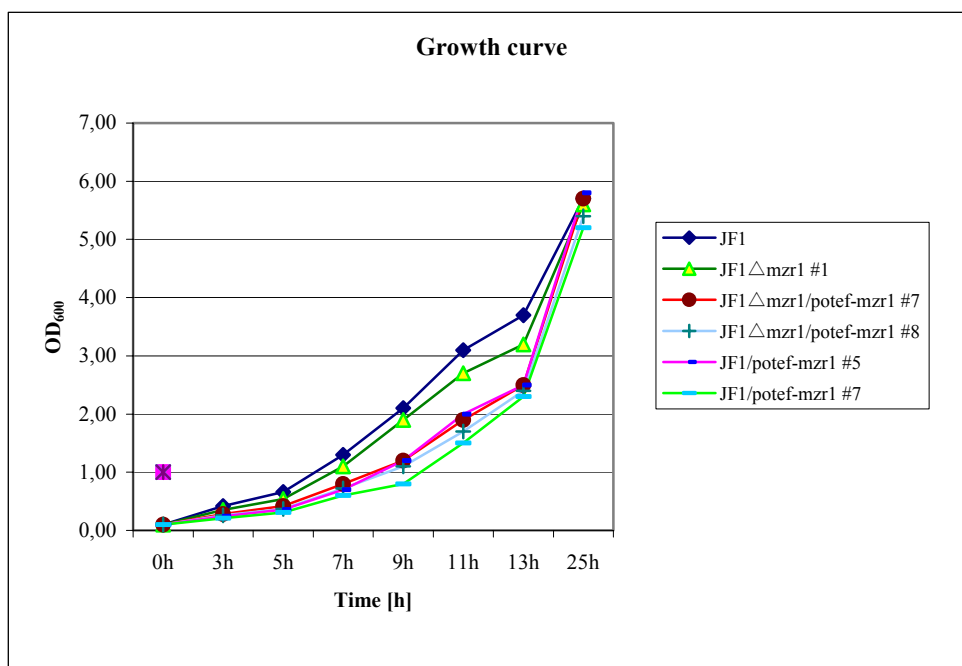
Figure 15. Growth comparison of *mzr1* overexpression strains with wt and *mzr1* deletion strains.

Growth comparison between the *mzr1* overexpression and JF1 strains. All *U. maydis* strains were grown in YEPS$_L$ medium for 15 hours. OD$_{600}$ values for each strain were determined at different time points: 0, 3, 5, 7, 9, 11, 13 and 25 hours after incubation. The starting OD$_{600}$ for each strain was 0.075 adjusted with precultures. Different *U. maydis* strains were marked with different colors in the figure.
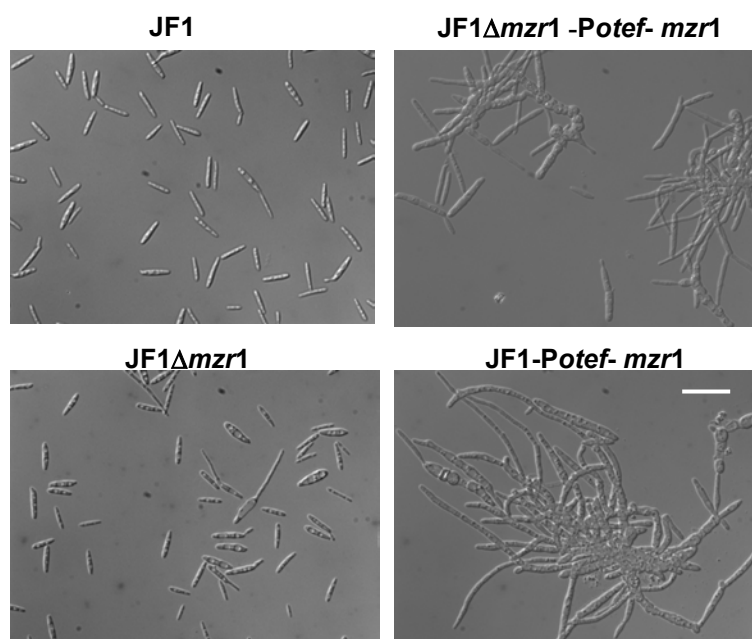
Figure 16. Morphology comparison in response to *mzr1* overexpression.
Morphology of different *U. maydis* cells was examined by DIC after a 12 hour incubation period. The starting OD$_{600}$ for each strain was 0.075 adjusted with precultures. Strain types are marked on the top of each figure. Bar= 10 μm for all panels.

31

Next, I investigated the behavior of *mzr1* overexpression strains in infected plant tissue. Here, it was particularly interesting to find out whether they were able to complement *biz1* deletion strains with respect to pathogenic development. For this purpose, plants were infected with JF1, JF1△*mzr1*, SG200△*biz1*/p*otef-mzr1*, JF1 △*mzr1*/p*otef-mzr1*, SG200△*biz1* and JF1/p*otef-mzr1* strains. In this experiment, JF1, JF1△*mzr1*, SG200△*biz1* strains were used as control. Three days after inoculation, the infected plant tissue was treated with Chlorazole Black E and examined by microscopy. This showed that the fungal penetration occurred for the JF1 and JF1△*mzr1* strains. For the SG200△*biz1*/p*otef-mzr1* strain, some *U. maydis* cells had penetrated into plant tissue, but most of them still resided on the plant leaf surface. As expected, fungal penetration was almost completely blocked for the SG200△*biz1* strain. Interestingly, most of the *U. maydis* JF1△ *mzr1*/p*otef-mzr1* and JF1/p*otef-mzr1* cells were floating on the leaf surface without forming penetration structures (**Fig.17**).

Plants were further inspected five days after inoculation to assess tumor formation. This revealed that no tumors could be found for the SG200△*biz1* and SG200△ *biz1*/p*otef-mzr1* strains. The number of tumors was also drastically diminished for the JF1△*mzr1*/p*otef-mzr1* and the JF1/p*otef-mzr1* strains compared to the strain JF1. On the other hand, no obvious difference could be detected for tumor formation in the JF1△*mzr1* strain compared to strain JF1 (**Table 3**).

Taken together, *mzr1* overexpression apparently influenced *U. maydis* morphology under culture conditions; more filamentous cells were observed. In addition, *mzr1* overexpression decreased the growth rate of *U. maydis* cells in culture, and could also interfere with the efficiency of plant infection as assessed from reduced penetration and tumor formation. This may explain why *mzr1* is hardly expressed in culture, but is strongly upregulated *in planta* (see **Fig.4**).

JF1

JF1Δ*mzr*1

10 μm

SG200Δ*biz*1

SG200Δ*biz*1/p*otef-mzr1*

JF1Δ*mzr*1/p*otef-mzr1*

JF1/p*otef-mzr1*
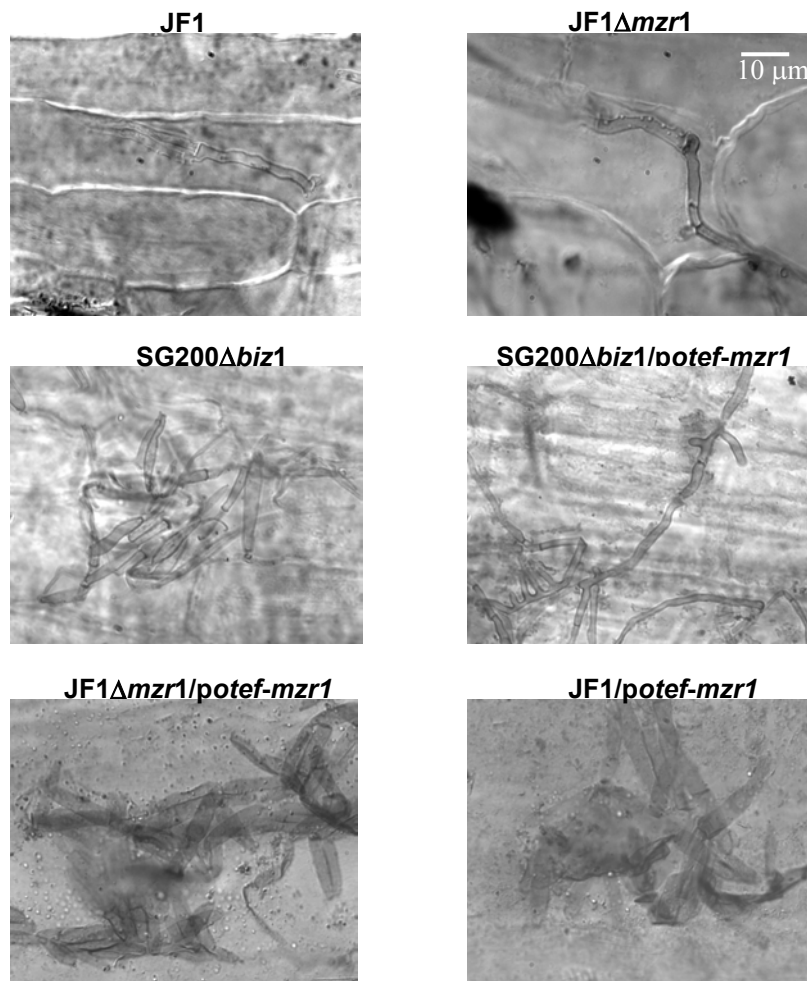
Figure 17. Microscopical examination for infected plant tissue three days after inoculation.
Infected plant tissue was examined by DIC microscopy three days after inoculation. Infected plant leaves were cut and stained with Chlorazole Black E (see Materials and Methods). Strains used are indicated on top of each panel. Bar= 10 μm for all panels.

Table 3. Examination of infected plants

Strains	Infected plants	Tumor formation	Percentage
JF1	18	8	44%
JF1Δ*mzr1*	19	6	32%
JF1Δ*mzr1/potef-mzr1*	45	6	13%
JF1*/potef-mzr1*	44	5	11%
SG200Δ*biz1*	21	0	0
SG200Δ*biz1/potef-mzr1*	23	0	0

Maize plants were inoculated with the *U. maydis* indicated on the left. Tumor formation is determined five days after inoculation.

2.4 DNA-protein interaction *in vitro*

All results obtained thus far had pointed out that Mzr1 was involved in *mig* gene regulation: *mzr1* overexpression could induce *mig* gene expression in culture, and *mig2-5* expression was drastically decreased in the *mzr1* deletion strain after plant infection. All these findings suggested that Mzr1 acts as a positive regulator for *mig* genes. However, the question remained whether the *mig* genes were directly regulated by Mzr1; alternatively Mzr1 could induce expression of regulator(s) of *mig* genes. In the latter case, Mzr1 would be an indirect regulator. To address whether Mzr1 is a direct regulator for *mig2-5*, I investigated the interaction between the Mzr1 protein and the *mig2-5* promoter using the electrophoretic mobility shift assay (EMSA) technique.

The EMSA technique is based on the fact that protein-DNA complexes migrate more slowly than free DNA molecules when subjected to non-denaturing polyacrylamide or agarose gel electrophoresis (Hendrickson *et al.*, 1985; Revzin*, 1989). Because the rate of DNA migration is shifted or retarded upon protein binding, this assay is also denoted as gel shift.

EMSA can be used qualitatively to identify sequence-specific DNA-binding proteins (such as transcription factors) and, in conjunction with mutagenesis, to identify the important protein binding sequences within a given gene's upstream regulatory region. EMSA can also be utilized quantitatively to measure thermodynamic and kinetic parameters (Fried *et al.*, 1981; Garner *et al.*, 1981; Fried *et al.*, 1984; Fried *,* 1989).

2.4.1 *U. maydis* cell extracts for DNA binding

One advantage to investigate DNA-protein interactions by EMSA is the ability to resolve complexes of different stoichiometry or conformation. Another major advantage is that the source of the protein used for DNA-binding may be a crude nuclear or whole cell extract rather than a purified preparation, which has been

utilized successfully for *U. maydis* research (Kotani *et al.*, 1993; An *et al.*, 1997).

I initially utilized *U. maydis* cell extracts as the DNA-binding protein source for EMSA. *mzr1* and *biz1* overexpression strains previously described (JF1/p*crg1-mzr1*, JF1/p*crg1-biz1*) were incubated in CM/Ara medium. The strain FB1 was incubated under the same conditions as a negative control. The protein preparation was performed according to a standard method described below (preparation of *U. maydis* cellular extracts followed the method described in Materials and Methods)

A 500-bp *mig2-5* promoter fragment isolated from plasmid pUMa13 was end-labeled with ^{33}P dCTP. The labeled 500-bp *mig2-5* promoter fragment was mixed with protein extracts from strains overexpressing either Mzr1, Biz1, or the Mzr1/Biz1 mixture individually. After gel running, no clearly shifted band was detectable on the gel (**Fig.18**). To enrich the DNA-binding fraction, the crude protein extract was purified by heparin affinity chromatography for subsequent EMSA under the same conditions. However, the same negative result was obtained even in the presence of 10 µg protein.
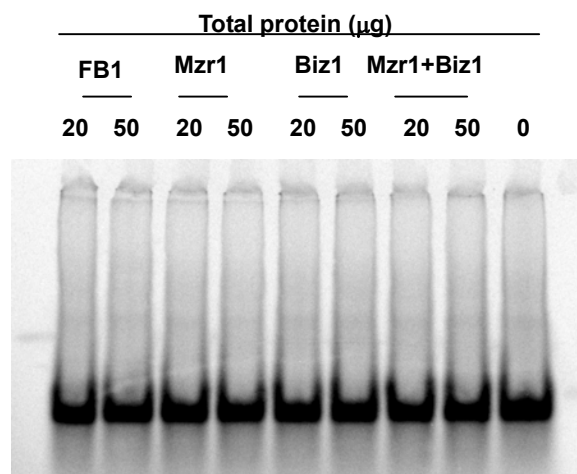
Figure 18. EMSA with crude extracts of *mzr1* and *biz1* overexpression strains
EMSA with crude protein extracts and a 500-bp *mig2-5* promoter fragment. Crude proteins extracts were prepared from FB1, JF1/p*crg1-mzr1* and JF1/p*crg1-biz1* strains grown in CM/Ara medium for 15 hours. The 500-bp *mig2-5* promoter fragment was end labeled with ^{33}P dCTP and then incubated with the crude protein extracts from strains FB1, JF1/p*crg1-mzr1*, JF1/p*crg1-biz1* and the JF1/p*crg1-mzr1*/JF1/p*crg1-biz1* mixture individually. 20 and 50 represent 20 µg and 50 µg protein mixed with DNA.

2.4.2 *mzr1* expression in *E. coli*

Based on the negative EMSA result obtained with crude or partially purified protein fractions, a strategy was designed to purify Mzr1. For this purpose, the plasmid pBAD102/D-TOPO was selected as cloning vector, which can be used directly for insertion of a blunt-ended PCR product possessing a 5'-CACC overhang. This vector contains coding sequences for a C-terminal His-tag (6xHis) and a N- terminal thioredoxin for increased translation efficiency and solubility of heterologous proteins. The His-tag fusion was used for detection of protein expression and for purification of the recombinant fusion protein. The arabinose-inducible *ara*BAD promoter initiates the gene expression in this plasmid.

In order to express the Mzr1 protein successfully in *E. coli*, I selected a truncated N-terminal portion containing the zinc-finger domains as cloning target (**Fig.19**). The zinc finger domain of C2H2 proteins has been shown to be sufficient for establishing specific DNA contacts (Pavletich and Pabo, 1991). The DNA fragment was amplified by PCR using the cDNA from strain JF1/*crg1-mzr1* previously prepared for RT-PCR analysis (**Fig.8**). A 1102 bp PCR product (sequence of truncated *mzr1* + CACC), in which the 80 bp intron of *mzr1* gene (positions from 559 to 639) had been deleted, was ligated into the pBAD102/D-TOPO vector. The resulting plasmid pTOPO-Z22 was transformed into *E. coli* TOPO10 cells. The generated *E. coli* strain TOPO10-Z22 was used as host strain for subsequent protein expression and purification assays.

To identify the proper expression conditions, the selected *E. coli* strain TOPO10-Z22 was grown under different arabinose concentrations (0, 0.0002%, 0.002%, 0.02% and 0.2%). After 14 hours of incubation, the *E. coli* cells were cracked using a French-Press. Both soluble and insoluble fractions were collected for Western blot analysis using an anti-His (C-terminal) antibody.

The result showed that a 0.0002% arabinose concentration (in the absence of glucose) was sufficient to induce expression of the fusion protein, which could be

obtained from the soluble fraction of cell extracts. However, most of the Mzr1 fusion protein was detected in the insoluble pellet fractions (**Fig.20**). This implied that the concentrated Mzr1 fusion protein formed inclusion bodies in *E. coli* cells. For further purifications, I selected the 0.0002% arabinose concentration.

zinc-finger I

MPAFRSHDPARK FHCDVLGCSASFVKRAHLRRHEMTH TQRRD FTC

zinc-finger II

PGCNRAFSRNDSMARHLRRKH PHLYRSPEAPSASSTTPAERLYTGAAP

GAASSNFVSTSSYSMLALRSPFESAFNSNNSAYQRRAHDPRTLPDPLART

ASFPDIYSRDGATHSPKGISSAHWRDSSRAPDAAFLPGAAPPEDGMRPYQ

NRTSYSIKEEPSCQPSYSTPSLFSNTSEPMDRVGPTRRASHDQSTSMYRSN

WMQASDFDHGASQAPLPSQFPWERQDGQTNYVHPSSHAGWSGAVGAM

GLASFPPSDHGRRGYIDPSFASSATPSGLPSFGELPHLADFPTQTEMLQSEF

FVGAMPSRHGDECWASLDPSML

Figure 19. The truncated N-terminal portion of Mzr1 used for cloning (obtained from http://www.broad.mit.edu).
The truncated N-terminal portion of Mzr1 expressed in *E. coli*. The zinc finger domains are denoted. Cys residues of the zinc fingers are marked with red color; His residues are marked with blue color.

To confirm these results, the *E. coli* strain TOPO10-Z22 was grown in LB medium containing 0.0002% arabinose for 14 hours and cracked using a French-Press. After centrifugation, the supernatant fraction was collected for the Western blot analysis to confirm the expression of the soluble fusion protein (~ 63 kD, **Fig.21**). The Western blot result showed that 0.0002% arabinose could be used successfully for the preparation of the soluble Mzr1 fusion protein in *E. coli*.
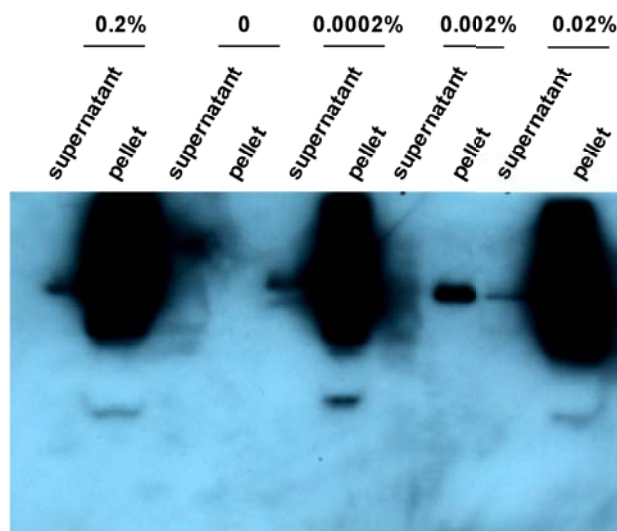
Figure 20. Determination of the concentration of arabinose for inducible protein expression.

Western blot analysis for the detection of the Mzr1-His fusion protein. Proteins used for the Western blot analysis were prepared from *E. coli* TOPO10-Z22 strains grown in LB medium, with different arabinose concentrations from 0 to 0.2%. Both soluble and insoluble fractions were collected for the Western blot analysis using an anti-His antibody. Arabinose concentrations are marked on top. 80 μg protein was loaded on each lane of the gel.
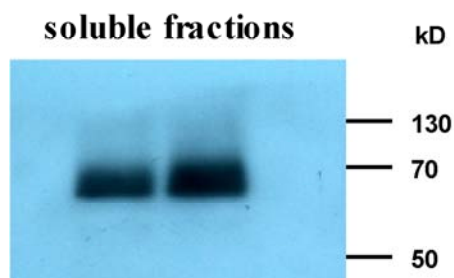
Figure 21. Western blot analysis for the determination of the Mzr1-His fusion protein.

Western blot analysis for the detection of crude Mzr1-His fusion protein. Proteins used for the Western blot were prepared from *E. coli* TOPO10-Z22 strains grown in LB medium containing 0.0002% arabinose. The soluble supernatant was collected after centrifugation for the Western detection by the anti-His antibody. Protein markers were used to determine the protein size of the fusion protein (~ 63 kD). The two lanes on the gel are from the same preparation (80 μg fusion protein).

To obtain the purified Mzr1 fusion protein based on the His-tag in the constructed plasmid pTOPO-Z22, the Ni-NTA Spin Kit was used. The high affinity of Ni-NTA resins for His-tagged proteins is due to the specificity of the interaction between histidine residues and immobilized nickel ions held to the NTA resin. After binding of His-tagged proteins to the NTA resin, the NTA resin was first washed and then eluted. Subsequently, the collected eluate was loaded on a PD-10 column (to desalt) to prepare the purified Mzr1 fusion protein used for EMSA studies.

To examine that the fusion protein is present in the eluate, the eluate was applied to SDS-PAGE gel for Western blot analysis using the anti-His antibody. The Mzr1 fusion protein of the expected size could be detected in the Western blot confirming the existence of the His-tagged fusion proteins after protein purification (**Fig.22**). The purified Mzr1 fusion protein was finally used for the EMSA studies.
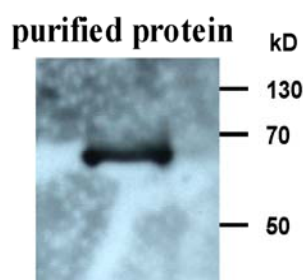
Figure 22. Western blot analysis for the Mzr1 fusion protein after purification.
Western blot analysis for the detection of the purified Mzr1-His fusion protein. Proteins used for the Western blot were prepared from *E. coli* strain TOPO10-Z22 grown in LB medium containing 0.0002% arabinose. The soluble supernatant (after centrifugation) was collected and purified by Ni-affinity chromatography. The collected protein was desalted using a PD-10 column and was then used for the Western detection using the anti-His antibody. Protein markers were used to determine the protein size (marked on right). 7 μg of fusion protein was loaded onto the gel.

2.4.3 DNA binding analysis with purified Mzr1 fusion protein

Previous work had demonstrated that 5'-CCA-3' motifs located in the *mig2-5* promoter are required for *mig2-5* promoter activity (Farfsing *et al*., 2005). It was thus presumed that CCA-containing sequences are crucial for binding by Mzr1. For EMSA, I initially used the 200-bp *mig2-5* promoter fragment from positions −120 to −320 (**Fig.23**). This promoter fragment contains 16 CCA/TTG motifs and was sufficient to induce full *mig2-5* promoter activity (Farfsing *et al*., 2005).

This 200-bp *mig2-5* promoter fragment prepared from pJM19 (see Materials and Methods) was end-labeled with ^{33}P dCTP for EMSA in the presence of the purified Mzr1 protein (see above). EMSA revealed several distinct bands (**Fig.24**). The intensity of shifted bands increased with increasing protein concentrations of the Mzr1 fusion protein and a second presumed DNA-protein complex could be detected when 1 µg of fusion protein was used (complex II in **Fig.24**).

Figure 23. The *mig2-5* promoter sequence position from −1 to −321.
A 200bp *mig2-5* promoter fragment positions from −120 to −320 was used for EMSA. CCA /TGG sequences are marked in orange.

To address specificity of the shifted bands, EMSA was performed in the presence of the unlabeled competitor fragment. For this purpose, the same 200-bp *mig2-5* promoter fragment prepared from pUMa13 using PCR was used as binding

competitor without labeling. Excess of unlabeled DNA competitor was mixed with the Mzr1 protein prior to addition of the labeled DNA fragment. If the DNA-protein binding is specific, the majority of the protein should be bound by the excess of unlabeled DNA and thus there should be only little protein left for binding to the radioactively labeled DNA fragment. To examine the DNA-protein binding specificity, I used 45, 150 and 300-fold molar excess of unlabeled DNA competitor for the binding assay. Along with increasing concentrations of the DNA competitor, the intensity of the shifted bands decreased. For the 300-fold molar excess of the unlabeled DNA fragment, almost no shifted band could be detected (**Fig.24**).
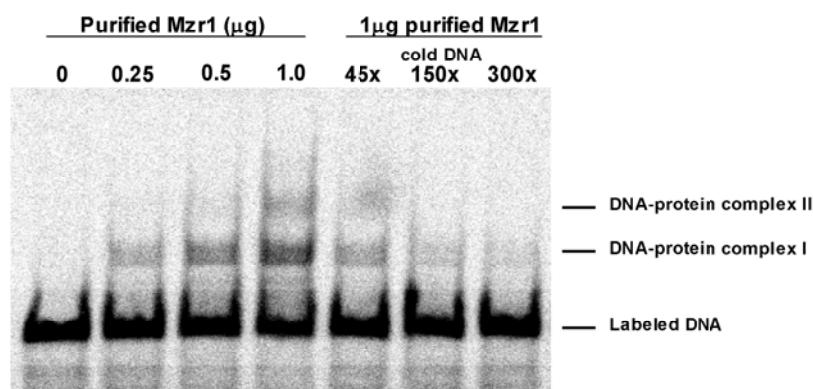
Figure 24. EMSA using the purified Mzr1 protein and a 200-bp *mig2-5* promoter fragment.
EMSA using the purified Mzr1 fusion protein and a 200-bp *mig2-5* promoter fragment (positions from -120 to –320). A 200-bp *mig2-5* promoter fragment was end labeled with ^{33}P dCTP and was then incubated with the purified Mzr1 fusion protein. 0, 0.25 μg, 0.5 μg and 1.0 μg of the Mzr1 protein preparation was added separately. For the competition analysis, excess of the unlabeled same *mig2-5* promoter fragment (45-fold, 150-fold and 300-fold) was mixed with 1 μg of Mzr1 protein before the radioactively labeled DNA fragment was added (see Materials and Methods).

This result provided evidence that the truncated Mzr1 fusion protein could specifically bind to the 200-bp *mig2-5* promoter fragment *in vitro*. The second shifted band, the presumed DNA-protein complex II, possibly comes from

multiple binding of Mzr1 to the *mig2-5* promoter region due to many potential CCA-containing sites. Based on the finding that the mutated *mig2-5* promoter construct, which is substituted in six CCA motifs, in strain JS12 could not be activated by *mzr1* overexpression (**Fig. 8**), it was interesting to know whether the Mzr1 fusion protein was able to bind to the 200-bp promoter fragment isolated from plasmid pJS12 containing the CCA substitutions (within positions –215 to –169, see **Fig. 25**).

```
                        -300                            -280
                          |                               |
   AGTGGTGCGTTCCAACCCACACCTTGAGGTCGAGATCCAGTAGCCACATATT
        -260                    -240                         -220
          |                       |                           |
   CCACGCATTTCTGGATTCGTTTCCAGTATGTGATCAAGTTGGTGGGCCTTGC
             -200                      -180
               |                         |
   AAGTCTCTTTTCCGTCCCCATGTCACGGTCACCGGTCTGACCTGTCGTCCCT
      -160                    -140                         -120
        |                       |                           |
   AGCTCTTGACTCATCACAGCCGTTACTCTGCATTGCTTGCTCTCGA
```
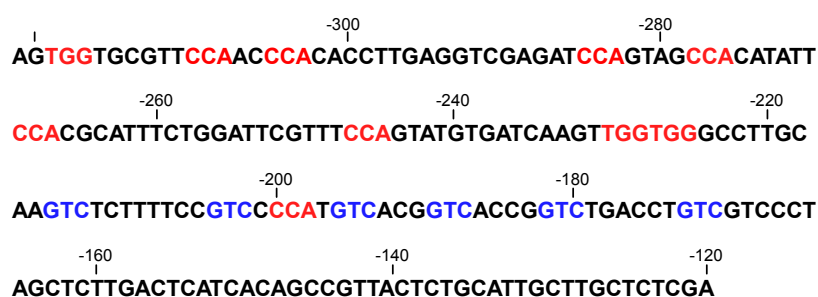
Figure 25. Mutated *mig2-5* promoter region in plasmid pJS12.
The 200bp mutant *mig2-5* promoter fragment (positions from –120 to –320) was used for EMSA. Six of CCA /TGG sequences were replaced by GTC (marked in blue).

Although, in plasmid pJS12 only six of the CCA motifs had been substituted within the 870 bp *mig2-5* promoter region, and thus many additional sites were left, it has been shown by J. Farfsing (Farfsing *et al.*, 2005) and in this study that this promoter could no longer be activated. Therefore, I used this fragment for the next EMSA study. For this purpose, 1 μg of the Mzr1 fusion protein was mixed with the ^{33}P end-labeled 200-bp mutant *mig2-5* promoter fragment. The ^{33}P end-labeled 200-bp wild-type *mig2-5* promoter fragment was used as control. The DNA competitor used for the 200-bp mutant *mig2-5* promoter fragment was prepared by PCR using the primer pair YZ70/YZ71 and pJS12 as template.

EMSA revealed that for the wild-type *mig2-5* promoter fragment, the same shifted bands (complex I and II) were obtained as expected**.** Furthermore, one additional shifted band (DNA-protein complex III) appeared in this experiment (**Fig.26**).

This possibly arose from multiple protein binding. In contrast, for the 200-bp mutant *mig2-5* promoter fragment, only one shifted band (DNA-protein complex I) could be clearly detected by EMSA. Interestingly, this band also decreased to a lower level after addition of a 300-fold molar excess of mutant competitor DNA. This provided evidence that the 200-bp mutant *mig2-5* promoter fragment could also be specifically bound by the Mzr1 fusion protein *in vitro*, however, higher molecular weight complexes appeared reduced.
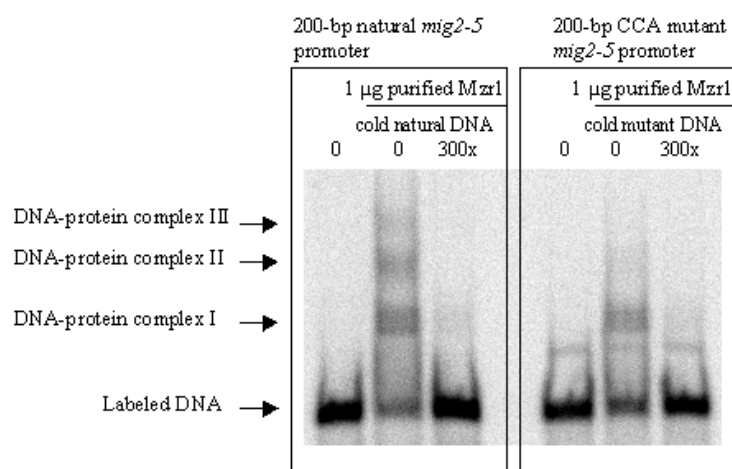
Figure 26. EMSA using the 200-bp natural and mutant *mig2-5* promoter fragments.
EMSA using the purified Mzr1 fusion protein and the 200 bp wild-type or mutant *mig2-5* promoter fragments (positions from -120 to –320). 200-bp wild-type and mutant *mig2-5* promoter fragments were end-labeled with ^{33}P dCTP and then incubated with 1 μg of the purified Mzr1 fusion protein. For the competition analysis, a 300-fold molar excess of the unlabeled 200-bp wild-type and mutant *mig2-5* promoter fragments (-120 to –320) were mixed with 1 μg of the Mzr1 protein preparation before the radioactively labeled 200-bp wild-type or mutant DNA fragments were added.

It has been shown that six of CCA/TGG motifs within the entire *mig2-5* promoter from positions –320 to –120 were required for *mig2-5* promoter activity (Farfsing *et al.*, 2005). However, the 200-bp mutant *mig2-5* promoter fragment from positions –320 to –120, in which six CCA/TGG motifs had been replaced, could still bind to the Mzr1 fusion protein (see above). This discrepancy might be explained as follows: the six CCA/TGG motifs within the *mig2-5* promoter

between positions –120 and –240 are crucial for *mig2-5* promoter activity but are not essential key positions for Mzr1 binding *in vitro*. In addition, there were still ten CCA/TGG motifs left in the 200-bp mutant *mig2-5* promoter at positions from –319 to –317, -310 to –308, -305 to –303, -285 to –283, -278 to –276, -269 to –267, -247 to –245, -230 to –228, -227 to –225 and -200 to –198 (**Fig.25**); these motifs might take part in protein binding *in vitro*, although they are not sufficient to confer inducible *mig2-5* promoter activity. There is still another possibility: the Mzr1 protein used in the EMSA study was truncated and analyzed *in vitro*; the binding conditions *in vivo* could be different and influenced by other proteins as suggested by the relationship with Biz1 (see Discussion).

The 200-bp wild-type and mutant *mig2-5* promoter fragments were shown to bind to the Mzr1 fusion protein. To further analyze this problem, I performed EMSA with the 120-bp *mig2-5* promoter fragment (from –120 to –240, **Fig. 23**). For control, I selected a 160-bp *mig2-5* promoter sequence from positions –1 to –161 (**Fig. 27B**). This promoter region could not confer high *mig2-5* promoter activity as detected *in planta* (Farfsing *et al*., 2005).

EMSA was performed using the ^{33}P end-labeled 160-bp (**Fig. 27B**), 120-bp wild-type and mutant (**Fig. 27A)** *mig2-5* promoter fragments in the presence of 1 μg of the truncated Mzr1 fusion protein as described above.

Again, several shifted signals were detected when the 120-bp fragment was used (**Fig. 28**). Explicitly, for the 120-bp natural fragment, two shifted signals (complex I and II) appeared. These two shifted signals disappeared when 300-fold molar excess of cold DNA competitor was added. For the 120-bp mutant *mig2-5* promoter fragment, only one shifted signal (complex I) could be detected, which also disappeared in the presence of a 300-fold molar excess of cold DNA. In contrast, no shifted band could be detected for the 160-bp control promoter fragment. This proved Jan Farfsing's result that this promoter region cannot confer inducible *mig2-5* promoter activity.

A

-240
GTGATCAAGT**TGGTGG**GCCTTGCAA**GTC**TCTTTTCC**GTC**C**CCA**TGT

-220

-200

-180
CACG**GTC**ACCG**GTC**TGACCT**GTC**GTCCCTAGCTCTTGACTCATCAC

-160

-140
AGCCGTTACTCTGCATTGCTTGCTCTCGA

-120

B

-160
CTTGACTCATCACAGCCGTTACTCTGCATTGCTTGCTCTCGATGCG**CCA**TTC

-140

-120

-100
TATCGC**CCA**TAAAAGCTCCTCGTTCATCCTCATCTACCTCTCATCTTTTC**CCA**

-80

-60

-40
CAACGACATCCT**CCA**TCTCCTCTTCCTTGTTTCTTCAGG**CCA**CGCTGCGAGA

-20

-1
AAAA

Figure 27. *mig2-5* promoter sequences used for EMSA.
A. The 120-bp mutant *mig2-5* promoter sequence from –120 to –240 was used for EMSA, in which six CCA /TGG motifs were replaced by GTC (marked in blue color). **B**. The 160-bp *mig2-5* promoter sequence from –1 to –161 was used for EMSA as negative control. There are five CCA motifs in this region (marked in red color)

These results provided evidence for specific binding of the truncated Mzr1 fusion protein to the 120-bp *mig2-5* promoter fragment *in vitro*. However, this also showed that upstream CCA motifs not present in the short 120-bp fragment might contribute to binding, although they are not sufficient for promoter activation. In consistence to the result of J. Farfsing (Farfsing *et al*., 2005), the 160-bp *mig2-5* promoter fragment, which cannot confer inducible *mig2-5* promoter activity, could also not be shifted by Mzr1.
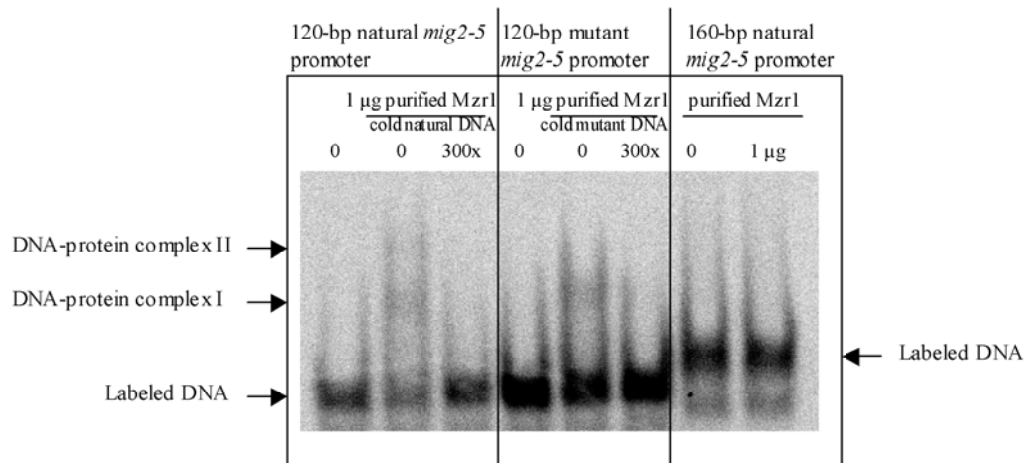
Figure 28. EMSA with the purified His-tagged Mzr1 protein and shorter *mig2-5* promoter fragments.
EMSA with the purified Mzr1 fusion protein. 160-bp (-1 to -161) and 120-bp natural/mutant *mig2-5* promoter (-120 to –240) fragments were end-labeled with ^{33}P dCTP and then incubated with 1 μg of the purified Mzr1 fusion protein. For competition analysis, 300-fold molar excess of unlabeled *mig2-5* promoter fragment (wild-type or mutant) were mixed with 1 μg of the Mzr1 protein preparation before addition of radioactively labeled DNA fragments.

In summary, the truncated Mzr1 fusion protein showed binding activity to the *mig2-5* promoter regions from –120 to –320 as well as from –120 to –240 *in vitro*. Furthermore, evidence could be provided that binding is influenced by the CCA/TGG motifs.

2.5 Mzr1 induced genes in *U.maydis*

2.5.1 Microarray analysis

Based on the finding that the Mzr1 protein was a positive regulator for *mig1*, *mig2-5,* and *mig2-6*, it was interesting to know whether there are additional genes that can be induced by Mzr1. Additional Mzr1 induced genes could be identified by DNA-microarray analysis (K. Auffarth and C. Basse, unpublished). For this purpose, the strain JF1/p*crg1-mzr1* was incubated in CM/Ara medium for an 8 h period upon transfer from CM/Glu. For comparison, strain JF1 was incubated in parallel. DNA-array analysis showed that *mig2-4*, as well as numerous additional genes were upregulated upon *mzr1* expression (**Table 4**). Among them, *um01820*, *um10055* and *um01240* were the most strongly upregulated genes besides *mig* genes after *mzr1* expression. Interestingly, many of the identified upregulated genes encode putative secreted proteins (**Table 4;** C. Basse). Thus, it is intriguing to note that Mzr1 regulates additional genes apart from the *mig* genes, but can induce only a subset of the *mig2* cluster genes, which show a very similar developmental expression pattern (Basse *et al*., 2002).

Table 4. Microarray analysis for *mzr1* expression (provided from Christoph Basse)

#	MUMDB um number	Factor	MUMBDB Homology http://mips.gsf.de/genre/proj/ustilago/	Predicted Localisation
1	um06180	402,74	MIG2-4	Secreted
2	um06181	319,47	MIG2-5	Secreted
3	um10055	159,98	related to gamma-glutamyltransferase	Secreted
4	**um01820**	82,72	hypothetical protein	Secreted
5	um01240	63,07	hypothetical protein	Secreted
6	um06126	55,42	MIG2-6	Secreted
7	um01297	43,97	hypothetical protein	Secreted
8	um05079	43,66	probable CTP1 - Mitochondrial citrate transporter - (MCF)	Transmembrane
9	um01239	41,62	hypothetical protein	Secreted
10	um05548	24,53	related to multicopper oxidase	Secreted

2.5.2 *um01820* is another major target regulated by Mzr1

To further analyse whether *um01820* is similarly regulated as *mig2-5*, Northern blot analysis was performed using the same membrane (see **Fig. 11**) as previously used to assess *mig* gene expression in response to Biz1, Mzr1 and related Znf proteins.
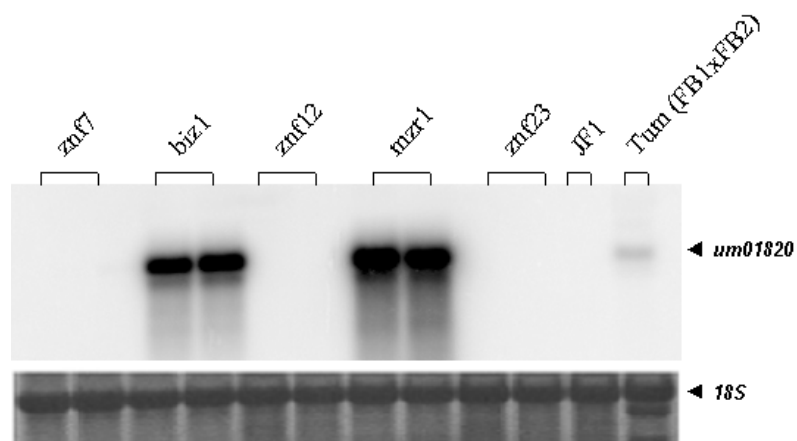
Figure 29. Overexpression analysis for *um01820*

um01820 expression levels induced in the various overexpression strains were determined by Northern blot analysis using RNA from these strains grown in liquid CM + 1% arabinose for 15 h. RNA isolated from five day-old tumors infected with strains FB1xFB2 was used as positive control. RNA prepared from the wild type strain JF1 grown in liquid CM/Ara was used as negative control. Northern blot analysis was probed with a ^{32}P labeled *um01820* fragment. Staining with methylene blue reflects the amounts of total RNA loaded (9 μg).

This analysis revealed that overexpression of both *mzr1* and *biz1* could induce *um01820* expression under culture conditions in a very similar way that observed for *mig2-5* (**Fig. 29**). As expected, neither Znf7, Znf12 nor Znf23 could confer *um01820* expression. In addition, the expression pattern of *um01820 in planta* was examined after plant inoculation. A similar expression profile was obtained for *um01820* compared to *mig2-5* (**Fig. 30**). This corroborates a similar mode of regulation of *mig2-5* and *um01820*, although they are not clustered.

FB1 x FB2

| 12h | 2d | 4d | 6d | 9d |

◄ *mig2-5*

◄ *um01820*

◄ *28S*
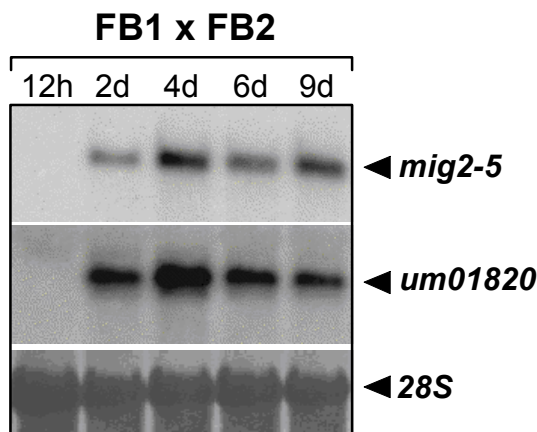
Figure 30. Expression analysis for *um01820* upon plant infection.
RNA gel blot analysis of *mig2-5* and *um01820* transcript levels during plant infection. Plants were inoculated with a mixture of FB1/FB2 strains and total RNA was extracted from infected parts. For the 12h and 2d-time points, material was collected 0.5-3 cm above ground and 0.5-3 cm below the injection site, respectively. For the 4d, 6d, and 9d-time points, chlorotic or early leaf tumor (4d) and leaf tumor (6d and 9d) tissue was collected between the ligule and >1 cm below the injection site. Filters were hybridised with the ^{32}P-labeled *mig2-5* and *um01820* probes. Methylene blue staining (28S) reflects the amounts of RNA loaded (7 μg).

2.5.3 The role of Mzr1 in host-dependent gene regulation

To verify if the *mzr1* deletion can also influence *um01820* expression *in planta*, maize plants were infected with the JF1, JF1Δ*mzr1*, and JF1Δ*znf23* strains. Strain JF1Δ*znf23* was selected based on the finding that expression of *mig2-5* and *mig2-6* were slightly increased in this strain in comparison to JF1 and other *znf* deletion strains (see **Fig. 7**). RNA was isolated from host tumor tissue six days after inoculation for Northern blot analysis using the ^{32}P-labeled *mig2-2*, *mig2-5*, and *um01820* probes. As expected from the above results (see **Fig. 7**), *mig2-2* expression in the three different *U. maydis* strains was comparable. In consistence with my previous investigation, the *mzr1* deletion strain showed a very weak *mig2-5* signal, corroborating the role of Mzr1 for *mig2-5* expression *in planta*. Interestingly, also a strongly decreased *um01820* signal was detected in the *mzr1*

deletion strain compared with the JF1 and JF1Δznf23 strains. This demonstrated that Mzr1 is also required for the transcription of *um01820 in planta*. Furthermore, the expression levels of *mig2-5* and *um01820* were clearly increased in the strain JF1Δ*znf23* compared to the wild type strain JF1 (**Fig. 31**). These results suggest that the additional Mzr1-induced genes identified by DNA-array analysis require Mzr1 for high-level gene expression *in planta*.
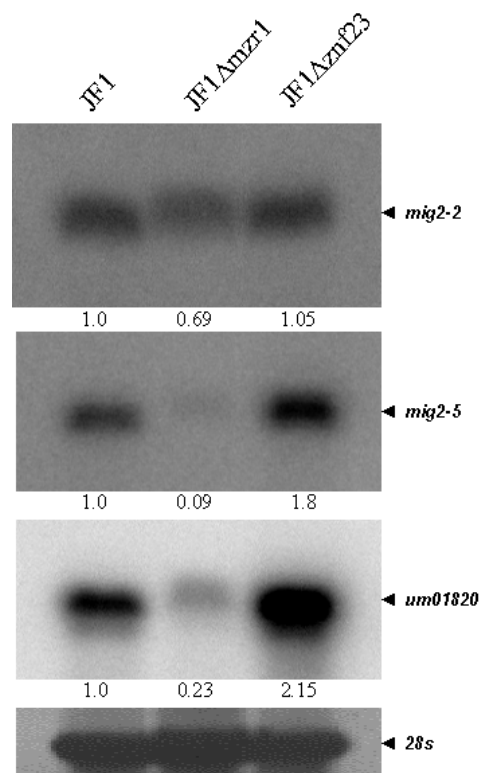
Figure 31. Expression analysis of *mig* and *um01820* genes in deletion mutants.
RNA was prepared from infected plant tissue six days after inoculation with the JF1Δ*mzr1,* JF1Δ*znf23* and wild type JF1 strains. Each gel was loaded with same amounts of the same RNA preparations (14 µg). The Northern blot was probed with ^{32}P-labeled *mig2*-2, *mig2-5* and *um01820* fragments. Staining with methylene blue (*28s*) reflects the amounts of total RNA loaded. The signals were quantified and are marked on the bottom of each lane.

3 Discussion

3.1 Summary and outlook

My results have demonstrated that Mzr1 (the C2H2-type zinc finger protein) is a positive regulator for a subset of the *mig* genes. In consistence with such a function, *mzr1* is strongly upregulated after plant penetration, whereas its expression was faintly detectable during axenic growth. Overexpression of *mzr1* could induce the transcriptional activation of the *mig* genes and several other genes (see **Table 4**). In addition, overexpression of *mzr1* was observed to favour formation of filamentous cells under culture conditions and compromised tumor formation. I could show that a truncated Mzr1 protein, which contains both zinc finger domains, could bind to the *mig2-5* promoter *in vitro*, and binding was influenced by CCA/TGG motifs, which are important for promoter activity *in vivo*. In addition, another C2H2-type zinc finger protein, Biz1, was found to be tightly connected to *mig* gene regulation. Overexpression of *biz1* strongly induced expression of the same subset of *mig* genes under culture conditions as induced in response to Mzr1. Moreover, evidence could be provided that the C2H2-type zinc finger protein Znf23, which is related in its zinc finger domains to Mzr1, negatively affects expression of the Mzr1-responsive genes *mig2-5* and *um01820*.

3.2 C2H2 zinc finger regulators

Accurate control of gene expression is important for understanding gene function and for developing therapeutics to treat diseases (Urnow *et al*., 2002). Transcriptional regulators bearing a C2H2 zinc finger are thought to be confined to eukaryotes; however, recent studies have confirmed their presence in prokaryotes (Bouhouhe *et al*., 2000). The zinc finger often interacts with specific

DNA sequences in the promoter or enhancer region. Basic and hydrophobic residues in the α-helix of the ββα structure appear to be the primary determinants of DNA binding, making specific contacts with 2-4 bases in the major groove of the DNA helix (Choo *et al.*, 1997).

Many C2H2 zinc fingers have been shown to interact with RNA and DNA/RNA heteroduplexes with high affinity. Wilms' tumour protein 1 (WT1), a KLF protein that can bind to both DNA and RNA, is thought to play an important role in the maturation of mRNA (Little *et al.*, 1999). In addition, it has been shown that the zinc fingers themselves can be involved in protein-protein contacts: they often interact with other transcription factors (Gregory *et al.*, 1996; Lee *et al.*, 1993; Merika *et al.*, 1995). However, relatively little is known about zinc finger-RNA interactions or about protein-protein interactions involving zinc fingers. What is the structural basis for such contacts? What are the biological roles for these interactions?

Some transcriptional regulators have been described in phytopathogenic fungi. The C2H2 zinc finger transcription factor PacC in *Fusarium oxysporum* is involved in pH sensing and required for virulence (Caracuel *et al.*, 2003). The CREB-like transcription factor CPTF1 in *Claviceps purpurea* is involved in oxidative stress response and virulence influence (Nathues *et al.*, 2004). A pathway–specific transcription factor ToxE is essential for the expression of HC-toxin required for pathogenicity of *Cochliobolus carbonum* (Pedley and Walton, 2001). However, only little has been known on Mzr1 function. In this work I could show that it is required for expression of the *mig* genes. No significant homologous protein could be found in the databases outside the zinc finger domain using blast search (http://www.ncbi.nih.gov/blast/).

3.3 Protein-DNA interaction *in vivo*

Protein-DNA binding assays have shown that the truncated Mzr1 fusion protein binds to the *mig2-5* promoter *in vitro* in dependence of the CCA/TGG triplet motifs that are essential for promoter activity. However, the truncated Mzr1 fusion protein could still bind to the CCA mutant promoter, although the mutant *mig2-5* promoter in JS12 was unable to confer inducible promoter activity *in planta* (see **Fig. 8**). This could be explained as follows: 1) the 5'-CCA-3' motifs are important for *mig2-5* promoter activity but are not crucial for protein binding; 2) the CCA motifs left in the mutant promoter sequence are sufficient for protein binding but not enough to activate *mig2-5* transcription; 3) EMSA revealed three shifted bands for the 120-bp and 200-bp *mig2-5* promoter fragments, whereas only one shifted signal could be detected for the mutant *mig2-5* promoter fragment from plasmid pJS12. This suggests that the two additional shifted bands (DNA-protein complex II, III; see **Fig. 26**) that were detected for the native promoter are relevant for the inducible *mig2-5* promoter activity.

This raises the question as to whether Mzr1-DNA interactions occur in the same way *in vivo*. The protein used for EMSA represents the truncated Mzr1 protein, which was expressed in *E. coli* and purified via affinity chromatography. Therefore, I cannot judge whether the entire Mzr1 protein expressed in *U. maydis* confers the same binding specificity.

To investigate the protein-DNA interactions *in vivo*, a new strategy based on chromatin immunoprecipitation was attempted to verify specific binding of Mzr1 to predicted target promoters *in vivo* and will be finished in future. For this purpose, an *U. maydis* strain has been constructed, in which the *crg1* promoter controlled *mzr1-strep-tag* sequence was introduced. The principle of this method is described in **Fig. 32**.
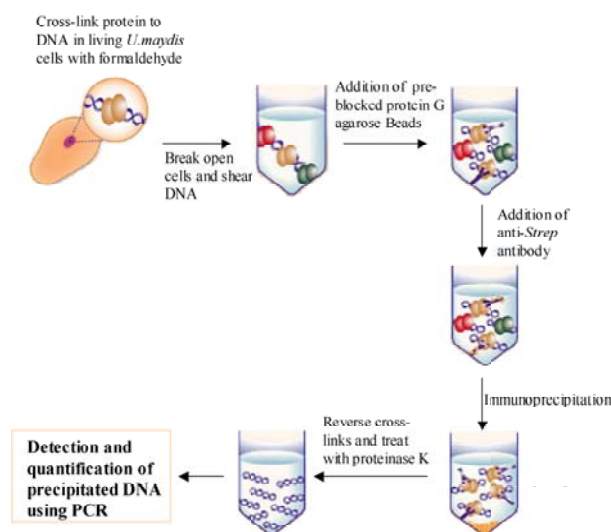
Figure 32. Chromatin immunoprecipitation strategy.

Chromatin immunoprecipitation is performed as follows. Formaldehyde is used for the cross-link of Mzr1-Strep fusion protein to the predicted target promoter in living *U. maydis* cells. Cells are broken open and the chromatin DNA is cut into small fragments. Mzr1-Strep protein binding DNA fragments is linked to pre-blocked protein G agarose beads. Next, immunoprecipitation is performed after addition of anti-*Strep* antibody. Enriched DNA-Mzr1-Strep complex is reverse cross-linked and treated with proteinase K. Finally, the precipitated DNA is used for sequence detection and quantification by PCR.

3.4 The relationship of Biz1-Mzr1 for *mig* gene regulation

Intriguingly, although the zinc finger motifs from Biz1 differ from those of Mzr1 (**Fig. 33**), both Biz1 and Mzr1 triggered induction of the same subset of *mig2* genes. How can this relationship be explained? Mzr1 needs a low level of Biz1 as existing in strain JF1 due to the presence of compatible *bE/bW* alleles for *mig2-5* regulation under culture conditions, whereas Biz1 can induce *mig2-5* expression in the absence of Mzr1. However, the *mig2-5* promoter activity was very weak in the *mzr1* deletion strain after plant inoculation as judged from Northern blot analysis and GFP fluorescence microscopy. These results implied that the function of Biz1 is different from that of Mzr1 *in planta*. Based on the requirement for

Biz1, it was expected that *mig2-5* could not be expressed in the *biz1* deletion strain after plant penetration. However, this question remains hypothetical because plant penetration is almost blocked completely for *biz1* deletion strains.

Furthermore, the overexpression analysis of *mzr1* and *biz1* has shown that Mzr1 and Biz1 play different roles in *mig* gene regulation (see **Fig. 11**). While Mzr1 is more specific for *mig2-5* than for *mig1* or *mig2-6*, Biz1 contributes more to *mig1* and *mig2-6* induction than Mzr1. This implicates the following question: How do Mzr1 and Biz1 individually contribute to *mig* gene expression?

The interaction between a zinc finger protein and its target DNA is dependent on its amino acid residues. Generally, each zinc finger binds a single zinc ion that is sandwiched between the two-stranded antiparallel β-sheet and the α-helix, producing a compact fold. In this fold, it has been revealed that positions –1, 2, 3, and 6 of the α-helix are important for the base-specific contacts of the zinc finger-DNA binding (Scot *et al.*, 1999). The zinc finger comparison showed that the zinc finger I of Mzr1 and Biz1 share the same amino acid residues at positions 3 and 6, and the zinc finger II possess the same amino acid residues at positions –1, 2, and 6. This suggests that Mzr1 and Biz1 bind to similar DNA sequences.

In fact, only little is known about the relationship between Mzr1 and Biz1 for *mig2-5* regulation. Under culture conditions, Mzr1 needs Biz1 for *mig2-5* induction. Actually, it has been shown that zinc-centered domains can be involved in protein-protein interaction (Matthews and Sunde, 2002). However, the Mzr1 zinc finger domain can bind to the *mig2-5* promoter independently. In addition, it could be shown that Mzr1 resides in the nucleus independently of *biz1* expression (E. Kaya and C. Basse, personal communication). Based on these results, the following possibility for *mig2-5* regulation exist: Biz1 and Mzr1 bind to the *mig2-5* promoter at different regions for the following activation. In this case, I give the following regulation model (**Fig. 34**). Overexpression of *biz1* can independently induce *mig2-5* expression in culture (**Fig. 34B**). Expression of *mzr1* cannot induce *mig2-5* expression in absence of Biz1 because the Mzr1 protein cannot bind to the core promoter of *mig2-5* (**Fig. 34C**). This has been proven by

EMSA analysis (see **Fig. 28**). Overexpression of *mzr1* changes the conformation and thus strongly enhances *mig2-5* expression in the presence of Biz1 (**Fig. 34D**). In addition, this model could also offer an explanation for the drastically diminished eGFP signal in the *mzr1* deletion strain (see **Fig. 6**): deletion of an enhancer-binding protein can decrease the level of transcription by 100-fold or more.

Figure 33. Comparison of zinc finger motifs of Mzr1 and Biz1.
Amino acid alignment of the zinc finger domains in Biz1 and Mzr1. Cys residues are marked with red color; His residues are marked with blue color.

Figure 34. Model of *mig2-5* regulation by interplay of Mzr1 and Biz1.
A. Binding sites of Mzr1 and Biz1. Mzr1 and Biz1 bind to the enhancer and the core promoter elements of the *mig2-5* promoter individually. **B**. In the *mzr1* deletion strain, expression of *mig2-5* is induced by *biz1* overexpression under culture conditions. **C**. Overexpression of *mzr1* can no longer induce the transcriptional activation of *mig2-5* in the *biz1* deletion strain under culture conditions. **D**. Overexpression of *mzr1* changes the conformation and thus strongly enhances *mig2-5* expression in the presence of Biz1.

59

3.5 Other possible candidates for *mig* gene regulators

In the deletion analysis of *znf* genes that were selected based on their expression levels *in planta* (see **Fig. 4**), the only gene whose deletion showed a significant decrease for the *mig2-5* expression was *mzr1*. However, for Δ*znf23* deletion, I could show that the expression of *mig2-5* and *um01820* was increased compared to the wild type strain JF1 in infected tissue (see **Fig. 7, Fig. 31**). The zinc fingers of Znf23 are very similar to that of Mzr1 (see **Fig. 9**). This suggests that Znf23 can also bind to the *mig2-5* promoter. Therefore I conclude that Znf23 acts as a negative regulator of *mig2-5* and *um01820*. In such a scenario, an interplay between Mzr1, Znf23 and Biz1 is conceivable as depicted in the following extension of the previous model (see **Fig. 34**): Znf23 acts as repressor by binding to specific promoter elements of *mig2-5* (enhancer or core promoter), blocking the assembly of Mzr1 or Biz1 required to initiate transcription. Thus, the pattern of transcription of *mig2-5* at a particular time may depend on the balance between Mzr1, Znf23 and Biz1. Both overexpression of *mzr1* and *biz1* may destroy this balance and thus initiate transcription of the *mig2-5* gene; deletion of *znf23* therefore promotes expression of *mig2-5 in planta*. For this model, it is interesting to verify the binding and the binding sites of Znf23 to the *mig2-5* promoter.

Znf7 was considered as another candidate regulator of the *mig2* genes. Comparison of the zinc fingers showed that Znf7 is the closest homolog of Biz1 besides Znf12 (see **Fig. 9**). The present overexpression analysis has shown that Znf7 can confer weak transcriptional activation of *mig2-5* (**Fig. 10**). However, the *znf7* deletion strain showed no significant difference in *mig2-5* activation *in planta*, thus its function might be related to activation of genes different from *mig* and similarly regulated genes.

3.6 The function of Mzr1 induced proteins

Mzr1 confers induction of numerous *mig* genes as well as of additional genes, and furthermore, contributes to expression of some of these genes *in planta* (see **Fig. 31**). This raises the question whether Mzr1-regulated genes have similar functions. Interestingly, the real-time PCR result showed that the expression of many Mzr1-induced genes is strongly upregulated early after plant inoculation (J. Kief, personal communication). This result illustrates that Mzr1-induced genes could have a function *in planta*. This is consistent with the finding that many of these genes encode predicted secreted proteins (see **Table 4**). Um1820 is predicted to be secreted and contains few cysteine residues just as the Mig1 protein. I could explicitly show that *um01820* exhibits an expression pattern very similar to that of *mig2-5*, and that *mzr1* is already ~30-fold upregulated two days after plant inoculation (**Fig. 35**). After plant penetration, expression of all *mig* genes and of *um01820* was kept at a high level until teliospore formation. This suggests that Mzr1-induced genes influence the host interaction until the sexual life cycle is completed. Since neither *mig* genes nor Mzr1 was required for pathogenesis, I assume that this originates from redundant protein functions and from residual gene expression in the Δ*mzr1* mutant.
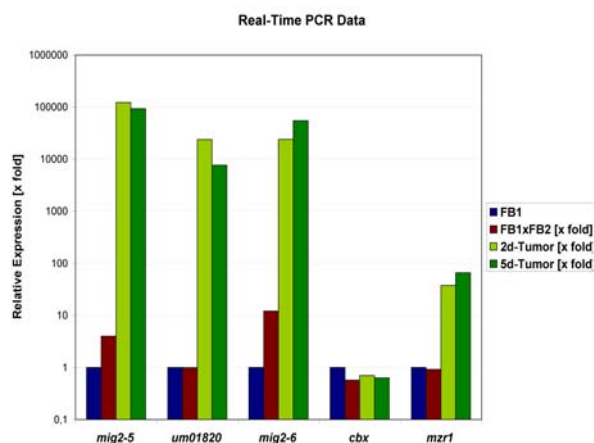
Figure 35. Real-time PCR analysis (provided from Jan Kief).

Expression levels of the *mig2-5, mig2-6, um01820, cbx* and *mzr1* were determined by real-time PCR analysis during different pathogenic development stages. RNA was isolated from four development stages: FB1, FB1xFB2, and plant tissue infected with FB1xFB2 two days and five days after inoculation. Different colors represent the four different stages and are marked on right.

I could show that overexpression of *mzr1* has an influence on the morphology of *U. maydis* cells in culture. Furthermore, pathogenicity of strains overexpressing *mzr1* under the *otef* promoter is reduced (see **Table 3**). *mzr1* is only weakly expressed in culture, but is strongly upregulated *in planta* (see **Fig. 35**). Additionally, I could show that in *mzr1* overexpression strains, plant penetration happened only rarely. Thus, Mzr1-induced genes might interfere with pathogenic development.

Overexpression of *biz1* induces expression of *mig1, mig2-5*, and *mig2-6*. In addition, it has been found that Biz1 is required for downregulation of the mitotic cyclin *clb1* (Flor-Parra *et al*., 2006). Clb1 forms a complex with Cdk1 and, together with the Clb2-Cdk1 complex, is required for the G2/M transition in *U. maydis* (Garcia-Muse *et al*., 2004). Therefore, overexpression of *biz1* arrests the cell cycle and confers elongated and polar growth phenotype. Furthermore, it has been confirmed that *biz1* is expressed at all stages during pathogenic development and required for pathogenic development of *U. maydis* beyond penetration. In particular, the *biz1* deletion mutant cells show a severe reduction in appressoria formation and plant penetration. Those hyphae that invade the plant arrest their pathogenic development after plant penetration (Flor-Parra *et al*., 2006).

These results showed that overexpression of both *biz1* and *mzr1* confer an elongated growth phenotype, therefore it would be interesting to address whether Mzr1 is involved in the control of *clb1* expression and thus plays a role in the cell cycle too.

3.7 Outlook

Based on the finding that Mzr1 needs Biz1 for *mig2-5* regulation, it would be interesting to identify the possible Mzr1-Biz1 interaction. Presently we are trying to verify the interaction between Mzr1 and Biz1 proteins using the yeast-two

hybrid system. This result may offer further insight into the regulation model for *mig2-5* and more clues to investigate the protein-protein interactions involving zinc fingers. In addition, it would also be an exciting effort to investigate the *mig2-5* regulation by the Mzr1-Biz1 complex, which can contribute more information about the biological roles for zinc finger protein-protein interactions.

Up to now, 11 *znf* gene deletion mutants have been constructed, and none of them could show obvious influence for expression of *mig2-1* and *mig2-2* (see **Fig. 7**). However, functions of many zinc finger proteins in *U. maydis* are still unknown (see **Table 1**). Further investigation for the remaining *znf* genes may uncover additional regulators required for *mig2-1* and *mig2-2*.

In addition, to prove the regulation model described above (see **Fig. 34**), it is necessary to investigate the protein-DNA binding and the binding sites between Biz1, Znf23 and the *mig2-5* promoter.

4 Materials and methods

4.1 Materials and their sources of supply

4.1.1 Chemicals, Buffer, Enzymes and Kits

All chemicals used for my experiments were ordered from Fluka, Invitrogen, Roth or Sigma.

Restriction enzymes, the ligase and the Phusion DNA Polymerase were obtained from New England Biolabs (NEB). Taq-Polymerase was obtained from Fermentas. The Klenow enzyme was ordered from Roche. The Anti-His antibody was obtained from Invitrogen. The Anti-Mouse IgG was obtained from Promega. The complete protease inhibitor cocktail was ordered from Roche. Poly [dI-dC] was obtained from Sigma. The Trizol reagent was ordered from Invitrogen. The Novozyme was obtained from other group (Kämper lab). The antarctic phosphatase was ordered from NEB. The protein marker peqGold protein-marker IV was ordered from peQlab. The RNAse, DTT, DNaseI and were ordered from Invitrogen. Specific buffers used for each experiment are listed within the corresponding method.

The concentrations of antibiotics used for normal plates in this work were described as follows:

PD/Cbx: 2 μg/ml of carboxin

PD/Nat: 150 μg/ml of nourseothricin

PD/Hyg: 200 μg/ml of hygromycin

The following kits were used following the protocol recommended by the supplier:

-TA Cloning Kit (Invitrogen)   for directly cloning of PCR products

-Jet Sorb Gel Extraction Kit (GENOMED)   for DNA extraction from gels

-QIAquick Gel Extraction Kit (QIAGEN)　for DNA extraction from gels

-QIAquick PCR Purification Kit (QIAGEN)　for PCR product and plasmid DNA
purification

-Ni-NTA Spin Kit (QIAGEN)　for His-tag fusion protein purification

-Western Blotting Detection Kit (GE Healthcare)

4.1.2 Plasmids used in this work

Table 5. Plasmids used for cloning in my work

Plasmid	Reference	Comments
pCR4.0 TOPO	Invitrogen	PCR product cloning vector
pBShhn	J. Kämper, 2004	For the isolation of the Hyg Sfil fragment
pHD-3	C. Basse *et al*., 2002	P*otef-eGFP-cbx*
pRU11	A. Brachmann, 2001	Plasmid vector for *mzr1* expression
p123	Christian Aichinger	P*otef-eGFP-cbx*
pSL1180	Amersham Pharmacia	Pharmacia cloning vector
pSLcbx	A. Brachmann, 2001	*cbx* fragment vector
pSLnat	A. Brachmann, 2001	*nat* fragment vector
pBAD 102/D-TOPO	Invitrogen	For *mzr1* expression
pCZ22v	Kathrin Auffarth	P*crg1-mzr1-nat*
pCZ7	Kathrin Auffarth	P*crg1-znf7-nat*
pCZ8	Kathrin Auffarth	P*crg1-biz1-nat*
pCZ12	Kathrin Auffarth	P*crg1-znf12-nat*
pCZ23	Kathrin Auffarth	P*crg1-znf23-nat*
pJS12	J. Farfsing *et al*., 2005	200-bp CCA mutant *mig2-5* promoter vector
pJM19	J. Farfsing *et al*., 2005	200-bp *mig2-5* promoter vector
pJM20	J. Farfsing *et al*., 2005	120-bp *mig2-5* promoter vector
pJM17	J. Farfsing *et al*., 2005	500-bp *mig2-5* promoter vector

crg1-promoter of *U. maydis*; *otef*- promoter of *U. maydis*; *nat*- nourseothricin resistence; *cbx*-carboxin resistence.

4.1.3 *U. maydis* strains used in this work

Table 6. *U. maydis* strains used in this work

Strains	Genotype	Resistance	Reference
FB1	a1b1		Banuett and Herskowitz, 1989
FB2	a2b2		Banuett and Herskowitz, 1989
521	a1b1		Kämper *et al.*, 2006
SG200	a1mfa2bE1bW2		Bölker and Genin, 1995
JF1	a1mfa2bE1bW2 pmig2-5-eGFP	C	Farfsing *et al.*, 2005
JF1Δznf3	Δznf3	H	This study
JF1Δznf4	Δznf4	H	This study
JF1Δznf5	Δznf5	H	This study
JF1Δznf7	Δznf7	H	This study
JF1Δznf14	Δznf14	H	This study
JF1Δznf20	Δznf20	H	This study
JF1Δznf21	Δznf21	H	This study
JF1Δznf22	Δznf22	H	This study
JF1Δznf23	Δznf23	H	This study
JF1Δznf25	Δznf25	H	This study
JF1Δmyb2	Δmyb2	H	This study
JF1Δmyb8	Δmyb8	H	This study
SG200Δbiz1	a1mfa2bE1bW2 Δbiz1	H	Flor-Parra *et al.*, 2006
SG200Δbiz1/pcrg1-mzr1	a1mfa2bE1bW2 Δbiz1 pcrg1-mzr1	N	This study
JF1Δznf22/pcrg1-biz1	JF1Δznf22- pcrg1-biz1	N	This study
JF1/pcrg1-biz1	JF1 pcrg1-biz1	N	This study
JF1/pcrg1-mzr1	JF1 pcrg1-mzr1	N	This study
JF1/pcrg1-znf7	JF1 pcrg1-znf7	N	This study
JF1/pcrg1-znf12	JF1 pcrg1-znf12	N	This study
JF1/pcrg1-znf23	JF1 pcrg1-znf23	N	This study
JF1-potef-mzr1	JF1 potef-mzr1	N	This study
JF1Δmzr1/potef-mzr1	JF1Δmzr1 pcrg1-mzr1	N	This study
SG200Δbiz1/potef-mzr1	SG200Δbiz1 potef-mzr1	C	This study

Resistence marker: C, carboxin; H, hygromycin; N, nourseothricin; *a*, *b*, mating type loci; *crg1*, arabinose-inducible *U. maydis* promoter; *otef*, constitutive promoter; *eGFP*, enhanced green fluorescent protein.

4.1.4 Plasmids constructed in this work

Vectors for the deletion of specific genes

For the construction of gene deletion vectors, PCR was performed to amplify an approximately 1 kb DNA fragment upstream of the respective ORF using the primer pairs given in **Table 7** and the genomic DNA of *U. maydis* strain 521 as template. Additionally, another approximately 1 kb DNA fragment downstream of the respective ORF was amplified using another primer pair (**Table 7).** The two PCR products were digested with SfiI and then ligated with the hyg-SfiI fragment, which was isolated from plasmid pBShnn (Kämper, 2004) by SfiI digestion. Subsequently, the ligation product was ligated into the pCR4.0 TOPO plasmid vector. For generation of gene deletions, the resulting vector was used as template to amplify an approximately 4 kb DNA fragment (upstream fragment + hyg-SfiI fragment + downstream fragment) using Taq-Polymerase. This PCR product was transformed into strain JF1 to generate *U. maydis* deletion mutants by homologous recombination.

Table 7. plasmid for gene deletion and primers used for their construction.

Plasmids	Primers*	Comments
pmyb1	M1-1/M1-2; M1-3/M1-4	For the *myb1* deletion
pmyb2	M2-1/M2-2; M2-3/M2-4	For the *myb2* deletion
pmyb3	M3-1/M3-2; M3-3/M3-4	For the *myb3* deletion
pmyb8	M8-1/M8-2; M8-3/M8-4	For the *myb8* deletion
pz3	JF209/JF210; JF211/JF212	For the *znf3* deletion
pz4	JF213/JF214; JF215/JF216	For the *znf4* deletion
pz5	Z5-1/Z5-2; Z5-3/Z5-4	For the *znf5* deletion
pz7	Z7-1/Z7-2; Z7-3/Z7-4	For the *znf7* deletion
pz9	Z9-1/Z9-2; Z9-3/Z9-4	For the *znf9* deletion
pz12	Z12-1/Z12-2; Z12-3/Z12-4	For the *znf12* deletion
pz14	Z14-1/Z14-2; Z14-3/Z14-4	For the *znf14* deletion
pz20	Z20-1/Z20-2; Z20-3/Z20-4	For the *znf20* deletion
pz21	Z21-1/Z21-2; Z21-3/Z21-4	For the *znf21* deletion
pz22	Z22-1/Z22-2; Z22-3/Z22-4	For the *znf22* deletion
pz23	Z23-1/Z23-2; Z23-3/Z23-4	For the *znf23* deletion
pz25	Z25-1/Z25-2; Z25-3/Z25-4	For the *znf25* deletion

* See Table 8 for sequence and details.

potef-Z22-cbx

The *otef* promoter was amplified by PCR using the primer pair YZ17/YZ18, Taq-Polymerase and the plasmid pHD3 as template. The PCR product was cleaved with NdeI/EcoRV and then inserted into the pCZ22v plasmid vector, in which the *crg1* promoter has been removed with NdeI and PmlI. The resulting plasmid was linearized with SpeI and then filled up with the Klenow enzyme. For the *cbx* cassette preparation, the plasmid pSL-cbx was cleaved with NotI and then filled up with Klenow enzyme. Finally, the blunt *cbx* fragment was inserted into the SpeI linearized plasmid vector to generate potef-Z22-cbx. This plasmid was confirmed by restriction enzyme control digestion and used for transformation of the *U. maydis* strain SG200 to generate the strains SG200/p*otef-mzr1* and SG200 △*biz1*/p*otef-mzr1*.

potef-Z22-nat

The *otef* promoter was amplified by PCR using the primer pair YZ17/YZ18, the Phusion DNA Polymerase and the plasmid pHD3 as template. The PCR product was cleaved with NdeI/EcoRV and then inserted into the pCZ22v plasmid vector, in which the *crg1* promoter has been removed with NdeI and PmlI. The resulting plasmid was linearized with NotI and was then dephosphorylated. The plasmid pSL-nat was cleaved with NotI to isolate the *nat*-resistance cassette. Finally the *nat*-resistance cassette was inserted into the NotI linearized plasmid vector described above to generate potef-Z22-nat. This plasmid was confirmed by restriction enzyme control digestion and used for *U. maydis* transformation to generate the strains JF1/p*otef-mzr1* and JF1△*mzr1*/p*otef-mzr1*.

pTOPO-Z22

The 1098 bp *mzr1* ORF was amplified by PCR using the primer pair TOPO1/TOPO2n, the Phusion DNA Polymerase and cDNA from JF1/*crg1-mzr1* as PCR template (prepared above, see **Fig.7** and 4.2.8 below). A 1102 bp PCR product was ligated with the pBAD102/D-TOPO vector. This plasmid vector

contains coding sequences for a C-terminal His-tag and an N-terminal thioredoxin for increased translation efficiency and solubility of heterologous proteins. The His-tag fusion was used for the detection of protein expression and for the purification of the recombinant fusion protein. The *ara*BAD promoter regulates gene expression in this plasmid. The resulting plasmid pTOPO-Z22 was confirmed by restriction enzyme control digestion and used for *E. coli* transformation to express the truncated Mzr1 fusion protein in *E. coli*.

pmig-200/M

A 200-bp 5'-CCA-3' mutant *mig2-5* promoter fragment was amplified by PCR using the primer pair YZ73/YZ74, the Phusion DNA Polymerase and the plasmid pJS12 (Farfsing *et al.*, 2005) as template. The PCR product was inserted into the pCR4.0 TOPO plasmid vector. The resulting plasmid pmig-200/M was confirmed by restriction enzyme control digestion and used to isolate a 200-bp 5'-CCA-3' mutant *mig2-5* promoter fragment by digestion with BamHI.

pmig-120/M

A 120-bp 5'-CCA-3' mutant *mig2-5* promoter fragment was amplified by PCR using the primer pair YZ77/YZ78, the Phusion DNA Polymerase and the plasmid pJS12 (Farfsing *et al.*, 2005) as template. The PCR product was inserted into the pCR4.0 TOPO plasmid vector. The generated plasmid pmig-120/M was confirmed by restriction enzyme control digestion and used to isolate a 120-bp 5'-CCA-3' mutant *mig2-5* promoter fragment by digestion with BamHI.

p160-C

A 160-bp *mig2-5* promoter fragment was amplified by PCR using the primer pair YZ75/YZ76, the Phusion DNA Polymerase and the genomic DNA of *U. maydis* strain 521 as template. The PCR product was inserted into the pCR4.0 TOPO plasmid vector. The resulting plasmid p160-C was used to isolate a 160-bp *mig2-5* promoter by digestion with BamHI, which served as negative control in EMSA.

4.1.5 *Escherichia coli* strain

Escherichia coli K12 strain TOP10 (Invitrogen) was used as host strain for plasmid amplifications. This strain allows stable replication of high-copy number plasmids.

4.1.6 PCR primers used in this work

All primers used in this work were ordered from MWG BIOTECH.

Table 8. Primers for PCR in my work

Primers	Sequence	T_m	Comments
JF209	5'-CGATCACCATCGTTCCCTTTAGCC	64.4°C	Amplification for upstream of *znf3* ORF
JF210	5'-CACGGCCTGAGTGGCCGGCTCTTTGGGTCGATAGAATG	75°C	Amplification for upstream of *znf3* ORF
JF211	5'-GTGGGCCATCTAGGCCTCGGTGCGGCCAACAAACCCTTT	75°C	Amplification for downstream of *znf3* ORF
JF212	5'-CGCTGAGGTTGTAGGAGACGTGG	66°C	Amplification for downstream of *znf3* ORF
JF213	5'-CCGTCTTTCGCATCGATCTTGGC	64.2°C	Amplification for upstream of *znf4* ORF
JF214	5'-CACGGCCTGAGTGGCCCTTGGTGAATACGA	75°C	Amplification for upstream of *znf4* ORF
JF215	5'-GTGGGCCATCTAGGCCACGACTCGCAGACGCTCGCTTCTC	75°C	Amplification for downstream of *znf4* ORF
JF216	5'-GTTGTCGAAGGTAGTCGATCTCG	62.4°C	Amplification for downstream of *znf4* ORF
Z3-0	5'-CTCGCTTGTTGGCTCGTTGGCTGG	67.8°C	Outer primer for upstream of *znf3* ORF
Z3-5	5'-GCCGATACGTGAGGGAGCAGACG	67.8°C	Outer primer for downstream of *znf3* ORF
Z4-0	5'-GTTCACGTCTCTACCACCATCTCC	64.4°C	Outer primer for upstream of *znf4* ORF
Z4-5	5'-CGACGTATCTGACCCGCTCGCATCC	69.5°C	Outer primer for downstream of *znf4* ORF
Z20-1	5'-GCAAAGGATGCACGTGCCGAGTCGAG	69.5°C	Amplification for upstream of *znf20* ORF
Z20-2	5'-CACGGCCTGAGTGGCCGCGTCGAACTGCTCACCAATGTACG	75°C	Amplification for upstream of *znf20* ORF
Z20-3	5'-GTGGGCCATCTAGGCCGGTATGATAGATGCCAGTGGCTCTC	75°C	Amplification for downstream of *znf20* ORF
Z20-4	5'-CTGTTCGCATAGACACAGAGATTGC	63.0°C	Amplification for downstream of *znf20* ORF
Z20-0	5'-CGGAGTTTTTGCTCCTGCCG	61.4°C	Outer primer for upstream of *znf20* ORF
Z20-5	5'-ATCCACCGAACCGACTCCGC	63.5°C	Outer primer for downstream of *znf20* ORF
Z7-1	5'-GCTCTCTTTCCGACTTGAACGCAG	64.4°C	Amplification for upstream of *znf7* ORF
Z7-2	5'-CACGGCCTGAGTGGCCGAGAAGCACGGCTCATGACTGAGTG	75°C	Amplification for upstream of *znf7* ORF
Z7-3	5'-GTGGGCCATCTAGGCCGCATGCAGCTTCCAGCCCACTTTGC	75°C	Amplification for downstream of *znf7* ORF
Z7-4	5'-GCGTGAGCAATCTAAGTTTCATCG	61.0°C	Amplification for downstream of *znf7* ORF
Z7-0	5'-TATCCAAGCTTCGACGACCC	59.4°C	Outer primer for upstream of *znf7* ORF
Z7-5	5'-CATCTCGGAGTTTGAATCGCC	59.8°C	Outer primer for downstream of *znf7* ORF
M3-1	5'-CAGACCGCTTCCGCCAACCGACC	69.6°C	Amplification for upstream of *myb3* ORF
M3-2	5'-CACGGCCTGAGTGGCCGTTGACAATGAGAAGCCTGACAGC	75°C	Amplification for upstream of *myb3* ORF
M3-3	5'-GTGGGCCATCTAGGCCCTGTCTGCCTAGTTGTGGCCAAG	75°C	Amplification for downstream of *myb3* ORF
M3-4	5'-CTGATAAACGGACAACACAGACC	60.6°C	Amplification for downstream of *myb3* ORF
M3-0	5'-GTACCTGGCAGCTGCCTCCC	65.5°C	Outer primer for upstream of *myb3* ORF
M3-5	5'-GCTAAAACCCAGAACCGCGC	61.4°C	Outer primer for downstream of *myb3* ORF

M1-1	5'-GCACATGTCGTGCTCGTAGCAG	64°C	Amplification for upstream of *myb1* ORF
M1-2	5'-CACGGCCTGAGTGGCCGATGACGGTGCTGGGTCAGCGCAG	75°C	Amplification for upstream of *myb1* ORF
M1-3	5'-GTGGGCCATCTAGGCCAGCGTCGCAAGCTTTGATCCACC	75°C	Amplification for downstream of *myb1* ORF
M1-4	5'-CCAGCGACCGAGGCCGAATCGC	69.6°C	Amplification for downstream of *myb1* ORF
M1-0	5'-GAGGAGCAACCGGGACCTCC	65.5°C	Outer primer for upstream of *myb1* ORF
M1-5	5'-TCGTGTACTGCAGCAAGCGG	61.4°C	Outer primer for downstream of *myb1* ORF
Z5-1	5'-CCGTGGATACCCTTTTGGCC	61.4°C	Amplification for upstream of *znf5* ORF
Z5-2	5'-CACGGCCTGAGTGGCCTGCGTTGATATTGGCAGACG	75°C	Amplification for upstream of *znf5* ORF
Z5-3	5'-GTGGGCCATCTAGGCCACCAAGGCGTCTGCCCATCC	75°C	Amplification for downstream of *znf5* ORF
Z5-4	5'-GGTGTGGAACCGTCACCTCC	63.5°C	Amplification for downstream of *znf5* ORF
Z5-0	5'-CGCCGTCAGCATTTCAAGGC	61.4°C	Outer primer for upstream of *znf5* ORF
Z5-5	5'-ATACAGAAGGAAGCGTGGCC	59.4°C	Outer primer for downstream of *znf5* ORF
M8-1	5'-GTCACGGGTGAACTTGAACC	59.4°C	Amplification for upstream of *myb8* ORF
M8-2	5'-CACGGCCTGAGTGGCCTGGAGGCGATCGTGAGAGGC	75°C	Amplification for upstream of *myb8* ORF
M8-3	5'-GTGGGCCATCTAGGCCCAGGCGCCTTCCGTCGAGTC	75°C	Amplification for downstream of *myb8* ORF
M8-4	5'-TAAGAGCTCTATCGCCAGGC	59.4°C	Amplification for downstream of *myb8* ORF
M8-0	5'-CCTTCGCCACACACAAGTCG	61.4°C	Outer primer for upstream of *myb8* ORF
M8-5	5'-CGGGCTGCAATGGATCGAGG	63.5°C	Outer primer for downstream of *myb8* ORF
M2-1	5'-CCTTCTTGGGCCGTCTTCGA	61.4°C	Amplification for upstream of *myb2* ORF
M2-2	5'-CACGGCCTGAGTGGCCGCGTTGAGCCAAGTAGCGAAC	75°C	Amplification for upstream of *myb2* ORF
M2-3	5'-GTGGGCCATCTAGGCCGCCAGCGCCACTAACACCGTG	75°C	Amplification for downstream of *myb2* ORF
M2-4	5'-GAGCGACGCCAAGAGCGCACTG	67.7°C	Amplification for downstream of *myb2* ORF
M2-0	5'-CGAGACGGCGCTCTCACTCA	63.5°C	Outer primer for upstream of *myb2* ORF
M2-5	5'-CATCCATCTCGCGTGCCAGC	63.5°C	Outer primer for downstream of *myb2* ORF
Z9-1	5'-GCTAAGTTAGTCACGATCGGC	59.8°C	Amplification for upstream of *znf9* ORF
Z9-2	5'-CACGGCCTGAGTGGCCCTCGGTGAAGAGGACAGCGC	75°C	Amplification for upstream of *znf9* ORF
Z9-3	5'-GTGGGCCATCTAGGCCAGGGCAGAGCCGACGAGAGG	75°C	Amplification for downstream of *znf9* ORF
Z9-4	5'-CGATCCACGATCCACGATCC	61.4°C	Amplification for downstream of *znf9* ORF
Z9-0	5'-TGCCATTCAAGCGTGTGCCG	61.4°C	Outer primer for upstream of *znf9* ORF
Z9-5	5'-CTCCCGATCCACGATCCACG	63.5°C	Outer primer for downstream of *znf9* ORF
Z12-1	5'-CAAGCTCTCGCACTGGGCCTG	65.7°C	Amplification for upstream of *znf12* ORF
Z12-2	5'-CACGGCCTGAGTGGCCCGTGAGTGGCATTCACAGATTC	75°C	Amplification for upstream of *znf12* ORF
Z12-3	5'-GTGGGCCATCTAGGCCCCAAAACAGGCTGGAGCTTG	75°C	Amplification for downstream of *znf12* ORF
Z12-4	5'-GAGCGGCACCATCTGGATCAA	64°C	Amplification for downstream of *znf12* ORF
Z12-0	5'-GTGCACACTCGCTGGTCTGAG	63.7°C	Outer primer for upstream of *znf12* ORF

Z12-5	5'-CTGCCGAGCGCATCGGTCGAC	67.6°C	Outer primer for downstream of *znf12* ORF
Z14-1	5'-CGTCCATCCAGTCGGAGTCG	63.5°C	Amplification for upstream of *znf14* ORF
Z14-2	5'-CACGGCCTGAGTGGCCCGCACGAGAGAGACCATCAACC	75°C	Amplification for upstream of *znf14* ORF
Z14-3	5'-GTGGGCCATCTAGGCCCAGGCCCCTCGAGCTTCTCG	75°C	Amplification for downstream of *znf14* ORF
Z14-4	5'-GTTGAACGAGCCGATGGGCG	63.5°C	Amplification for downstream of *znf14* ORF
Z14-0	5'-GATTTGCTCGCCCTGTCAAGG	61.8°C	Outer primer for upstream of *znf14* ORF
Z14-5	5'-TTACGGCCACCACACCGAGC	63.5°C	Outer primer for downstream of *znf14* ORF
Z21-1	5'-GGCTCGAATCGGCAACGCCC	65.5°C	Amplification for upstream of *znf21* ORF
Z21-2	5'-CACGGCCTGAGTGGCCGCTGGAACCTGGGACGCACC	75°C	Amplification for upstream of *znf21* ORF
Z21-3	5'-GTGGGCCATCTAGGCCCCAAGACCCGCAATTTAGGC	75°C	Amplification for downstream of *znf21* ORF
Z21-4	5'-CCCTCTGAAGCACATCTACG	59.4°C	Amplification for downstream of *znf21* ORF
Z21-0	5'-AGCAAGGATAGCAGGCGAGC	61.4°C	Outer primer for upstream of *znf21* ORF
Z21-5	5'-GTGTCGTAGCACTTGCAACG	59.4°C	Outer primer for downstream of *znf21* ORF
Z22-1	5'-CCCTGCACGCCGACAGTACC	65.5°C	Amplification for upstream of *znf22* ORF
Z22-2	5'-CACGGCCTGAGTGGCCAGCGAGTCAGAGACGGCCAC	75°C	Amplification for upstream of *znf22* ORF
Z22-3	5'-GTGGGCCATCTAGGCCAGCTTCTCCCTCTGCCGACG	75°C	Amplification for downstream of *znf22* ORF
Z22-4	5'-CCCCGATGCTTAAGGAGCCC	63.5°C	Amplification for downstream of *znf22* ORF
Z22-0	5'-CGTGGCCTGAACTGCCACCC	65.5°C	Outer primer for upstream of *znf22* ORF
Z22-5	5'-CGACAGCCGCCTTCTTCTCC	63.5°C	Outer primer for downstream of *znf22* ORF
Z23-1	5'-GTACAACACACGCCTCTGGC	61.4°C	Amplification for upstream of *znf23* ORF
Z23-2	5'-CACGGCCTGAGTGGCCAGCGGAAAGGATTGAGGCGGG	75°C	Amplification for upstream of *znf23* ORF
Z23-3	5'-GTGGGCCATCTAGGCCTTGATCAGTTGCGCAGTGCG	75°C	Amplification for downstream of *znf23* ORF
Z23-4	5'-GGATGGTCAGGGAATCCGGC	63.5°C	Amplification for downstream of *znf23* ORF
Z23-0	5'-CGGCTGTACGCGCTCGTCGC	67.6°C	Outer primer for upstream of *znf23* ORF
Z23-5	5'-ATCGTGCCGGCGTGTCCGGC	67.6°C	Outer primer for downstream of *znf23* ORF
Z25-1	5'-TGAACCAGCCATGACGCTCG	61.4°C	Amplification for upstream of *znf25* ORF
Z25-2	5'-CACGGCCTGAGTGGCCCAGCTTTCAGGACGAGTTCC	75°C	Amplification for upstream of *znf25* ORF
Z25-3	5'-GTGGGCCATCTAGGCCGGATCGGCGTGAGATTCACG	75°C	Amplification for downstream of *znf25* ORF
Z25-4	5'-CATCCAGCTCTGTCTCAACC	59.4°C	Amplification for downstream of *znf25* ORF
Z25-0	5'-GCTAGCAGACTTCTGGTCGC	61.4°C	Outer primer for upstream of *znf25* ORF
Z25-5	5'-GTGGTGCTGGGAGATGGAGG	63.5°C	Outer primer for downstream of *znf25* ORF
JF231	5'-CGCTACTGCCATCAGCAACG	61.4°C	*znf5* ORF specific primer
JF232	5'-CGCTTGGCCTTGGTGATAGG	61.4°C	*znf5* ORF specific primer

JF225	5'-CACCAGCGTTTTGGCACGGG	63.5°C	*myb8* ORF specific primer
JF226	5'-CGTCGGTGAGATTGCCCTGG	63.5°C	*myb8* ORF specific primer
JF241	5'-GTCTTGGCAGTAGCAGCACC	61.4°C	*znf12* ORF specific primer
JF242	5'-GCTTGGTGTGCTAGAAGCGC	61.4°C	*znf12* ORF specific primer z
JF245	5'-TCGCTTGAGCCGACTTGCAC	61.4°C	*znf14*ORF specific primer
JF246	5'-CATGGTTGTCGCAGCGCTCG	63.5°C	*nf14* ORF specific primer
JF253	5'-TCCCATGTCCATCTCAACCG	59.4°C	*znf21* ORF specific primer
JF254	5'-TGTGGTCGACAATGGGTGGC	61.4°C	*znf21* ORF specific primer
JF255	5'-AACAACAGCGCATACCAGCG	59.4°C	*znf22* ORF specific primer
JF256	5'-GCCTTCTCGCTAAGATTGCG	59.4°C	*znf22* ORF specific primer
JF257	5'-GAAGCGCATCCATCCTGACC	61.4°C	*znf23* ORF specific primer
JF258	5'-GTGGACATGGCTGTGGAGGC	63.5°C	*znf23* ORF specific primer
JF219	5'-GGCACCAGCTCAACTGCACC	63.5°C	*myb5* ORF specific primer
JF220	5'-CCTATCGTGTACGAGCCTGG	61.4°C	*myb5* ORF specific primer
JF221	5'-GTGCGCCATCCAACATCTCC	61.4°C	*myb6* ORF specific primer
JF222	5'-CGTCTGATAGGACACCTCCC	61.4°C	*myb6* ORF specific primer
JF223	5'-ACCGTAGCAGCTGAACGCCC	63.5°C	*myb7* ORF specific primer
JF224	5'-TGGAGGAGAGGAAGCTTGGG	61.4°C	*myb7* ORF specific primer
JF227	5'-ATCGATCCCAGCGCAATCCC	61.4°C	*myb9* ORF specific primer
JF228	5'-GATGCCAGTCTCGACGTCGG	63.5°C	*myb9* ORF specific primer
JF229	5'-ACTGTCCGCATACGATGCGC	61.4°C	*myb10* ORF specific primer
JF230	5'-CCCTCTTTGTCGTCTTCTGC	59.4°C	*myb10* ORF specific primer
JF233	5'-TGAGCAGTGGGTCGGATCGG	63.5°C	*znf6* ORF specific primer
JF234	5'-CACATGTCCGTTGCTTGGCG	61.4°C	*znf6* ORF specific primer
JF235	5'-TCCTCCGTTCGCCCATCAGG	63.5°C	*znf8* ORF specific primer
JF236	5'-CGAGCATATCCTGCATCGCC	61.4°C	*znf8* ORF specific primer
JF237	5'-CGCCATAAGCGACAATGCCG	61.4°C	*znf9* ORF specific primer
JF238	5'-GCTGTATACGGATCGTAGCC	59.4°C	znf9 ORF specific primer
JF243	5'-CACTTCCACCGAGTCGGACG	63.5°C	*znf13* ORF specific primer
JF244	5'-TATGCCTTGTCGCATCCGGG	61.4°C	*znf13* ORF specific primer
JF247	5'-CTGCCAATACTACCAGCGCC	61.4°C	*znf15* ORF specific primer
JF248	5'-CATATCCTTTGCCCATGCCC	59.4°C	*znf15* ORF specific primer
JF249	5'-CTGCCTCACTTGCAAGTGGG	61.4°C	*znf16* ORF specific primer
JF250	5'-TTGACCGAGGGGTTGCTAGG	61.4°C	*znf16* ORF specific primer
JF251	5'-AAGGCAATGCCATCGACAGG	59.4°C	*znf18* ORF specific primer
JF252	5'-GCGAACTGCTAGCTTCACCC	61.4°C	*znf18* ORF specific primer
JF261	5'-GTCGCAAAACGCTCATCGGG	61.4°C	*znf27* ORF specific primer
JF262	5'-GCAACACCAACTCGAGCTCC	61.4°C	*znf27* ORF specific primer
JF263	5'-TGCTCTCGACAACATCCCGG	61.4°C	*znf29* ORF specific primer
JF264	5'-TCATGGCACCATCCTCACCC	61.4°C	*znf29* ORF specific primer
JF265	5'-TTCACAAAGCATCGCTCGCC	59.4°C	*znf31* ORF specific primer
JF266	5'-CTCTGCGACATGAGTGGAGG	61.4°C	*znf31* ORF specific primer
JF267	5'-TGTCGCAAGCTCAAGCTCCC	61.4°C	*znf36* ORF specific primer

JF268	5'-CTTGTCCTGCAAACACTGGC	59.4°C	*znf36* ORF specific primer
JF269	5'-CGCGTTAAGGGTCCTTGGCG	63.5°C	*znf40* ORF specific primer
JF270	5'-ACCTTGTGAGTCTCTAGCCC	59.4°C	*znf40* ORF specific primer
YZ4n	5'-GCACCGATTGATCTGTTTCCTGTTCG	64.8°C	*znf22* ORF specific primer
YZ17	5'-GCAGGATATCACTAGTGGATCCCCCGTACCGAG	73.2°C	*otef* promoter amplification
YZ18	5'-GGAATTCCATATGGATCGAATTCCTGCAGCCC	69.5°C	*otef* promoter amplification
YZ7	5'-GAGAGCCGGAACGACACTGGTACG	67.8°C	*znf22* ORF specific primer
YZ20	5'-CTGTCTGGCACAGCACGTCAGCAC	67.8°C	*znf22* ORF specific primer
YZ22	5'-GTGTGGATCGCAGTCCTGCACAG	66°C	znf8 ORF specific primer
YZ23	5'-CATTGCCAGTAGCCTCGGTCAGTG	66.1°C	*znf8*ORF specific primer
YZ13	5'-CGGGATCCGATGCCTGCTTTTCGCAGCCATG	73.5°C	*znf22* ORF amplification
Not1-mzr1	5'-ATAGTTTAGCGGCCGCGACAACACACTCATGATTGTG	71.7°C	*znf22* ORF amplification
BamH-mzr1	5'-CGGGATCCTGCTTTTCGCAGCCATG	67.9°C	*znf22* ORF amplification
YZ1ad	5'-TCGCACGAACCGCCTCGTTTCC	65.8°C	pET-22b(+)-Z22 sequencing
YZ3ad	5'-CCGATTTATCATCCATTCATGCTCG	61.3°C	pET-22b(+)-Z22 sequencing
YZ5ad	5'-ACAGGCGCTCTACCCGAACAGC	65.8°C	pET-22b(+)-Z22 sequencing
YZT7	5'-CGACTCACTATAGGGGAATTGTGAG	63°C	pET-22b(+)-Z22(truncated) sequencing
YZ1	5'-GCGCCCTTATCAGAACAGGACGAG	66.1°C	pET-22b(+)-Z22(truncated) sequencing
YZ2	5'-CTCATGCTTGTCCTATACCTGCTGG	64.6°C	pET-22b(+)-Z22(truncated) sequencing
YZ60	5'-CACGAAGTGCAAGAAGGATTCGAG	62.7°C	pz22-strep sequencing
YZ61	5'-CCGTGTTGCGGTCGTGAACTCG	65.8°C	pz22-strep sequencing
TOPO1	5'-CACCATGCCTGCTTTTCGCAGC	64°C	Truncated *znf22* ORF amplification
TOPO2n	5'-GAGCATGGACGGATCGAGACTGG	66.0°C	Truncated *znf22* ORF amplification
strep1	5'-CGGTATCGGTAGGTGCTGGG	63.5°C	Strep specific primer
Strep2	5'-GTAACATAGATGACACCGCG	57.3°C	Strep specific primer
YZ71	5'-ATCGAGAGCAAGCAATGC	53.7°C	120-bp natural *mig2-5* promoter amplification
YZ72	5'-GTGATCAAGTTGGTGGGCCTTGC	64.2°C	120-bp *mig2-5* promoter amplification
YZ70	5'-AGTGGAGCGTTCCAACC	55.2°C	200-bp *mig2-5* promoter amplification
YZ73	5'-GCGGATCCAGTGGAGCGTTCCAACC	69.5°C	200-bp mutant *mig2-5* promoter amplification
YZ74	5'-GCGGATCCATCGAGAGCAAGCAATGCAGAG	70.9°C	200-bp mutant *mig2-5* promoter amplification
YZ75	5'-GCGGATCCCTTGACTCATCACAGCCGTTAC	70.9°C	160-bp *mig2-5* promoter (negative control) amplification
YZ76	5'-GCGGATCCTTTTTTCTCGCAGCGTG	66.1°C	160-bp *mig2-5* promoter (negative control) amplification
YZ77	5'-GCGGATCCGTGATCAAGTTGGTGGGCCTTG	73.5°C	120-bp mutant *mig2-5* promoter amplification
YZ78	5'-GCGGATCCATCGAGAGCAAGCAATGCAGAG	70.9°C	120-bp mutant *mig2-5* promoter amplification
YZ80	5'-ATAGTCATGATGAAGTTTGAATTTGGTGCCCTTGTCTGCG	70.5°C	*um01820* ORF amplification
YZ81	5'-GCAGGATATCCAAATAGCGATGGCCGGAAGTG	70.8°C	*um01820* ORF amplification

4.2 Genetic, microbiological and cell biological methods

4.2.1 Plasmid preparation from *E. coli*

The *E. coli* strain carrying the desired plasmid was grown in liquid dYT or LB medium (the concentration of Ampicillin used as selection marker was 100μg/ml) overnight under shaking at 37°C. Cells were harvested by centrifugation (30 sec, 13000 rpm), and the cell pellet was resuspended in 350 μl STET solution. 25 μl lysozyme solution was added. After mixing, the suspension was incubated at RT for 30 sec and then heated at 95°C for 50 sec. After centrifugation (10 min, 13000 rpm), the bacterial debris was removed using a toothpick. Then, 37 μl of Mini III solution and 420 μl of iospropanol were added. After mixing, the suspension was incubated at RT for 5 min. The supernatant was removed after centrifugation (5 min, 13000 rpm). The pellet was washed with 900 μl of 70% ethanol. Subsequently, the supernatant was removed as complete as possible after centrifugation (3 min, 13000 rpm). The pellet was dried at RT for 5 min. Finally, the DNA pellet was resuspended in 80 μl TE solution containing 20 μg/ml RNAse.

dYT
6% (w/v) Trypton
0% (w/v) Yeast-Extract
5% (w/v) NaCl
in H_2O

LB
1.0% (w/v) Trypton
0.5% (w/v) Yeast-Extract
0% (w/v) NaCl
in H_2O

Mini III
3.0 M Natriumacetat
in ddH_2O, pH4.8

STET
0.1 M NaCl
10 mM Tris-Cl, pH8.0
1 mM EDTA, pH8.0
5% (w/v) Triton x-100
in H_2O

TE
10 mM Tris-Base
1 mM Na_2-EDTA
in ddH_2O
pH 8.0

4.2.2 Transformation of *U. maydis*

U. maydis cells were grown overnight in YEPS$_{light}$ medium at 28°C until an OD$_{600}$ of 0.3–0.8 was reached. Cells were harvested by centrifugation (10 min, 13000 rpm). The cell pellet was washed with 20 ml SCS medium and was then resuspended in 4 ml SCS medium containing 5 mg/ml Novozyme. The sample was incubated at RT for 10 min at RT to digest the cell wall material (examined under the microscope). After rounding up of the elongated *U. maydis* cells, SCS solution was added to a volume of 40 ml. The sample was gently resuspended. After centrifugation (10 min, 2000 rpm), the cell pellet was washed two-times with 20 ml SCS buffer (8 min, 2000 rpm). Then, it was washed for an additional time with 20 ml STC buffer. Finally, the cell pellet was resuspended in 1 ml STC. The protoplasts were stored in aliquots at -80°C. 1-5 μg linearized DNA and 1 μl heparin solution were mixed and incubated on ice for 10 min. Then, 50 μl protoplasts were added and gently mixed. The mixture was incubated on ice for 10 min. After addition of 600 μl STC/PEG, the mixture was incubated on ice for further 15 min. The suspension was plated on a regeneration-agar plate and was then incubated at 28°C for ca. 5 days until colonies appeared.

SCS	**STC**
20 mM Na-citrate, pH5.	10 mM Tris-Cl, pH7.5
1 M Sorbitol	100 mM CaCl$_2$
in ddH$_2$O, filter sterilized	1 M Sorbitol
	in ddH$_2$O, filter sterilized
YEPS$_{light}$	**Regeneration-agar**
10 g Yeast Extract	1) Top agar
10 g Pepton	1.5% (w/v) Bacto Agar
10 g Saccharose	1 M Sorbitol
fill up to 1l with H$_2$O	in YEPS medium
	2) Bottom agar
STC/PEG	Top agar plus double concentrated antibiotic
15 ml STC	
10 g PEG4000	

4.2.3 Preparation of Glycerol cultures

For long time-storage of *U. maydis* strains, the cells were frozen at -80°C (glycerol cultures). *U. maydis* cells were grown in YEPS$_{light}$ medium at 28°C overnight under shaking until an OD$_{600}$ of 1 was reached. 1 ml of cell culture was mixed with 1 ml NSY Glycerol solution. Mixture was incubated at RT for 20 min and then stored frozen at -80°C.

NSY Glyceol
8 g Bacto nutrient broth
1 g Yeast extract
5 g Sucrose
800 ml 87% glycerol
fill up to 1l with H$_2$O

4.2.4 Genomic DNA isolation of *U. maydis*

U. maydis cells were grown in YEPS$_{light}$ medium at 28°C overnight under shaking. Cells from 2 ml of cell culture were harvested by centrifugation (2 min, 13000 rpm). The supernatant was removed. 0.3 g glass beads (acid-washed), 400 μl lysis buffer (see below) and 500 μl phenol/chloroform (1:1, v/v) were added. The sample was placed on a Vibrax-VXR shaker (IKA) running at ^{3}/4 speed for ~ 8 min. About 400 μl of the upper phase were collected in a 1.5 ml Eppendorf tube after centrifugation (15 min, 13000 rpm). Then, the 2.5-fold volume of 100% ethanol was added. The sample was mixed and incubated at RT for 5 min. The supernatant was removed after centrifugation (5 min, 13000 rpm). The pellet was washed with 1 ml 70% (v/v) ethanol. The residual liquid in the tube was removed as complete as possible after centrifugation (3 min, 13000 rpm). Finally, the dry DNA pellet was resuspended in 50 μl TE solution containing 20 μg/ml RNAse.

Lysis buffer
2% (w/v) Triton
1% (w/v) SDS
1 mM EDTA
100 mM NaCl
10 mM Tris-Cl, pH 8.0
in ddH$_2$O

4.2.5 Induction of inducible promoters

The use of the arabinose inducible *crg1* promoter allows the controlled regulation of gene expression by a change of the cultivation medium. The *crg1* promoter controlled genes are repressed in CM-glucose medium where glucose is the sole carbon source. Inducible conditions are given when arabinose is the sole carbon source in CM-arabinose medium. To induce the expression of *crg1* promoter controlled genes, *U. maydis* strains were grown in CM/Glu at 28°C for 12 hours. Cells were harvested by centrifugation (10 min, 3000 rpm) and were then washed two-times with ddH$_2$O. Cell pellets were resuspended in CM/Ara medium. Finally, cultures were incubated at 28°C for 15 hours (until an OD$_{600}$ of 0.8 was reached) under shaking, with a starting OD$_{600}$ of 0.1.

4.2.6 RNA isolation from *U. maydis*

U. maydis cells were grown in 15 ml CM medium (1% glucose or arabinose) at 28°C overnight under shaking until an OD$_{600}$ of 0.5-0.8 was reached. Cells were harvested by centrifugation (10 min, 13000 rpm). The supernant was discarded and the cells were resuspended in the remaining medium. The suspension was transfered to a 1.5 ml Eppendorf tube. The supernatant was removed after centrifugation (3 min, 13000 rpm). Cells were frozen in liquid nitrogen. Next, 440 µl aqua phenol, 400 µl AE buffer and 40 µl 10% (w/v) SDS were added into the tube. The sample was mixed for 20 sec and then incubated at 65°C for 4 min

under shaking (13000 rpm). Next, the sample was frozen at -80°C for 7 min until phenol crystals were formed. This mixture was thawed at RT for maximum 5 min. The upper phase was collected in a new 1.5 ml Eppendorf tube after centrifugation (10 min, 15000 rpm at 4°C). The 1-fold volume of aqua phenol/chloroform (1:1, v/v) was added. The upper phase was collected in a 1.5 ml Eppendorf tube after centrifugation (5 min, 13000 rpm at 4°C). The 0.1-fold volume of Mini III and 2.5-fold volume of 100% ethanol were added into the tube. The sample was mixed by reversion and then incubated at -20°C for 1 hour. The supernatant was removed after centrifugation (20 min, 20000 rpm at 4°C). The pellet was washed with 1 ml 80% (v/v) ethanol. The supernatant was removed after centrifugation (10 min, 20000 rpm at 4°C). Finally, the RNA pellet was dissolved in 30 µl RNAse free H_2O.

AE buffer
50 mM NaAc, pH 5.3
10 mM Na_2EDTA

Salt solution (Holliday, 1974)
16 g KH_2PO_4
4 g Na_2SO_4
8 g KCl
4 g $MgSO_4$x 7 H_2O
1.32 g $CaCl_2$ x 2 H_2O
8 ml trace elements solution
in 1l H_2O, filter sterilized

Trace elements solution
60 mg H_3BO_3
140 mg $MnCl_2$x $4H_2O$
400 mg $ZnCl_2$
40 mg $NaNoO_4$x $2H_2O$
100 mg $FeCl_3$x $6H_2O$
40 mg $CuSO_4$x $5H_2O$
in 1l H_2O, filter sterilized

CM (without glucose)
1.5 g NH_4NO_3
2.5 g casamino Acids
0.5 g DNA degree free acid
1 g Yeast extract
10 ml vitamin solution
62.5 ml salt solution
filled up to 1l with H_2O
pH 7.0

Vitamin solution
100 mg Thiamine
50 mg Riboflavin
50 mg Pyridoxine
200 mg Calcium pantothenate
500 mg p-Amino benzo acid
200 mg Nicotinic acid
200 mg Choline chloride
1 g myo-inositol
in 1l H_2O, filter sterilized

4.2.7 Total RNA isolation from plant tissue

1 g plant tissue was ground in liquid nitrogen. The resulting power was transferred to a 15 ml falcon tube containing 10 ml TRIZOL. The sample was mixed by vortexing until no clumps remained in the tube. The mixture was incubated at RT for 15 min. Next, 2 ml chloroform was added to the tube. After mixing by vortexing (10 sec), the mixture was incubated at RT for 3 min. The upper aqueous phase was collected in a new falcon tube after centrifugation (15 min, 3500 rpm at 4°C). The sample was mixed with 1-fold volume of phenol/chloroform (1:1, v/v, and equilibrated with TE to pH 8) for 10 seconds by vortexing. The aqueous upper phase was collected after centrifugation (10 min, 3500 rpm at 4°C). 5 ml isopropanol were added, and the sample was mixed by inversion. The mixture was incubated on ice for 10 min. The supernatant was removed after centrifugation (15 min, 9000 rpm at 4°C). Finally, the dry RNA pellet was dissolved in 80 μl RNAse free H_2O on ice. The sample was stored at -20°C or -80°C (for long time-storage).

4.2.8 Dnase treatment of RNA and reverse transcription

Following components were added in a 1.5 ml Eppendorf tube:

1. Dnase treatment:

1-15 μg total RNA
5 μl 10x DP buffer
1.5 μl 100 mM DTT (added before the RNase inhibitor)
0.3 μl human placental RNase inhibitor (40 u/μl; Roche)
2 μl DNaseI (RNase free; 10u/μl; Roche)
H_2O up to 50 μl

The mixture was incubated at 37°C for 30 min, and then 200 μl of TE buffer were added. The sample was extracted two times with the same volume of phenol/chloroform (vortexed and centrifuged at 15000 rpm, 4°C for 5 min). The upper phase was collected in a new Eppendorf tube. The 0.1-fold volume of

MiniIII and 3-fold volume of 100% ethanol were added into the tube. The mixture was incubated at -20°C for 15 min. After centrifugation (10 min, 22000 rpm at 4°C), the pellet was washed with 1 ml 70% (v/v) ethanol (10 min, 22000 rpm at 4°C). After removing of the supernatant, the pellet was dissolved in 20 μl ddH$_2$O. 0.5-2 μg of RNA were transferred into a 1.5 ml Eppendorf tube for subsequent reverse transcription.

2. Reverse transcription:

0.5-2 μg RNA (see above)
1.5 μl oligo dT primer CBAP5 (10 μM; 5'TTGTACAAGCT$_{30}$VN)
1 μl 10 mM dNTPs
H$_2$O to 12.5 μl

The mixture was incubated at 65°C for 5 min and was then transferred on ice for 2 min (to remove the secondary structures and anneal the primer). The following components were added:

4 μl 5x 1st Strand buffer (Gibco)
2 μl 100 mM DTT
0.5 μl Roche Rnase inhibitor (40 u/μl)
1 μl SuperScript III RT (200 u/μl, Gibco)

The mixture was incubated at 40°C for 5 min, and was then incubated at 42°C (up to 55°C) for 55 min. Finally, the sample was heated at 90°C for 5 min and was stored at -20°C.

10x DP buffer
100 mM Tris-HCl, pH 8.3
500 mM KCl
15 mM MgCl$_2$
in H$_2$O

4.2.9 Southern hybridization

A DNA sample was digested with appropriate restriction enzyme(s) and then was loaded onto a 1% (w/v) TBE agarose gel (10x12 cm). The gel was run at 110 V for 2 hours. Next, the gel was incubated in 0.25 M HCl solution for 15 min, and then in denaturation buffer for 25 min under gentle shaking. Finally, the gel was incubated in renaturation buffer for 15 min under gentle shaking. DNA was transferred to a Hybond-N+ membrane (Amersham Biosciences) in 20-fold SSC buffer overnight (**Fig. 36**). Then, the membrane was dried and stored at 4°C.
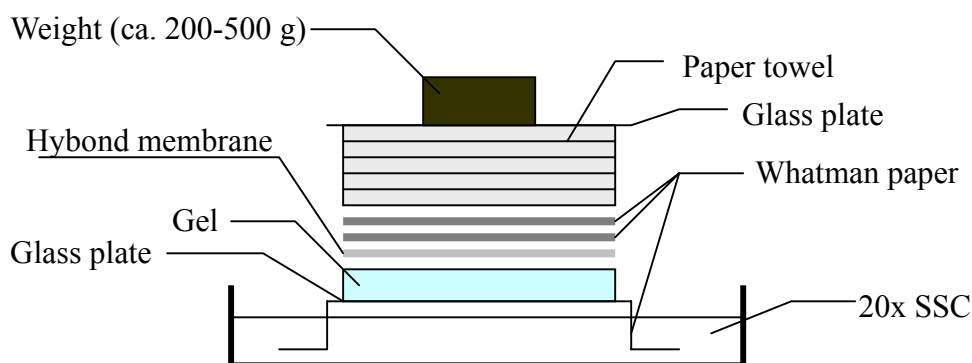

Figure 36. DNA transfer to hybond membrane.
DNA was transferred to a Hybond-N+ membrane in 20-fold SSC buffer overnight.

After bloting, the membrane prepared above was dried and UV cross-linked (Stratalinker, STRATA GENE), followed by incubation in Southern hybridization buffer at 65°C for 30 min under rotation. The Southern hybridization buffer was discarded and the radioactively labeled probe (see 'Probe labeling') was added. The membrane was incubated in the probe solution at 65°C overnight under rotation. After 12-24 h, the membrane was washed with S1 buffer for a short period (15-30 min). Then, the membrane was incubated in S2 and S3 buffer at 65°C for 30 min under rotation. Finally, the membrane was dried and exposed within a screen cassette for at least one day, followed by laser scanning (STORM Phosphorimager).

5x TBE	**Denaturation buffer**
440 mM Tris-Base	1.5 M NaCl
440 mM Boric acid	0.4 M NaOH
10 mM EDTA, pH 8.0	in H_2O
in H_2O	

Renaturation buffer	**20x SSC**
1.5 M NaCl	3 M NaCl
282 mM Tris-HCl	0.3 M Natriumcitrat
218 mM Tris-Base	in H_2O
in H_2O	pH 7.0

4.2.10 Northern hybridization

5-15 µg RNA sample was transferred into a 1.5 ml Eppendorf tube on ice. The following components were added into the tube:

2.4µl 10x MOPS
2.4 µl 8M Glyoxal
12 µl DMSO
dd H2O up to 24 µl

The mixture was incubated at 50°C for 1 hour, and was then transferred on ice.

6 µl RNA loading buffer were mixed with the RNA sample. A 1% (w/v) agarose gel (in 1-fold MOPS buffer) was prerun at 85V for 5-10 min, and then the RNA mixture was loaded. The gel was run at 85V for 2 hours in 1-fold MOPS buffer. The orientation of the gel in the chamber and the polarity of the chamber were inverted every 30 minutes to keep the pH value. Afterwards, the gel was equilibrated in 20-fold SSC buffer for 10-15 min under gentle rotation. The RNA sample in the gel was transferred to a Hybond-NX membrane (Amersham Biosciences) in 20-fold SSC buffer overnight (see **Fig. 36**). The dry membrane was UV cross-linked (Stratalinker, STRATA GENE). The membrane was stained in methylene blue solution for 5 min under gentle shaking. Next, the membrane was rinsed in ddH2O for 10 min under gentle rotation. Finally, the dry membrane

was stored at 4°C.

Next, the membrane prepared above was incubated in Northern hybridization buffer at 60°C for 30 min under rotation. The Northern hybridization buffer was discarded and the radioactively labeled probe (see 'Probe labeling') was added. The membrane was incubated in the probe solution at 60°C overnight under rotation. After 12-24 h, the membrane was washed with Northern wash buffer by shaking. Then, the membrane was incubated in Northern wash buffer at 60°C for 30 min under rotation. Finally, the membrane was dried and exposed to a cassette for at least one day, and then the cassette was scanned (STORM Phosphorimager).

10x MOPS
200 mM MOPS
80 mM Natriumacetate
10 mM Na_2-EDTA
in H_2O, pH 7.0

Gel loading buffer (for 10 ml)
1 ml 10x MOPS
5 g Glycerin
50 mg Bromphenol blue
50 mg Xylene blue
add H_2O to 10 ml

Methylene blue solution
300 mM Natriumacetate
0.02 (w/v) methylene blue
in H_2O

4.2.11 Isolation of the Mzr1 fusion protein from *E. coli*

E. coli strains carrying the plasmid pTOPO-Z22 were grown in 100 ml LB medium containing 100 μg/ml Amp at 37°C under shaking to an OD_{600} of 0.5. Arabinose stock solution was added to a final concentration of 0.0002% (w/v), and then the incubation was continued for 4 hours under shaking. Cells were harvested by centrifugation (3 min, 10000 rpm). The cell pellet was kept frozen at -80°C. Next, the cell pellet was thawed and resuspended in 3.5 ml lysis buffer. The sample was again frozen in liquid nitrogen. Next, the cell sample was thawed and lysed two-times at 10000-11000 psi using a French-Press (Minicell). The supernatant was collected after centrifugation (20 min, 10000 rpm at 4°C). Six

Ni-NTA spin columns (QIAGEN) were equilibrated with 600 µl lysis buffer each by centrifugation (2 min, 2000 rpm). 550 µl of supernatant prepared above were loaded on each column. After centrifugation (2000 rpm for 3 min), each column was washed three-times with 600 µl wash buffer (2000 rpm for 2 min). Next, each column was eluted twice with 230 µl elution buffer. The eluates were collected in 1.5 ml Eppendorf tubes. A PD-10 column was equilibrated with 5x5 ml protein buffer and then 2.5 ml of the protein eluate were loaded. PD-10 column was then eluted with 3.5 ml protein buffer and the eluate was collected. The prepared protein sample was stored frozen in aliquots at -80°C.

Lysis buffer
50 mM NaH$_2$PO$_4$
300 mM NaCl
8 mM imidazole
1-fold complete protease
inhibitor cocktail
in H$_2$O, pH 8.0

Elution buffer
50 Mm NaH$_2$PO$_4$
300 mM NaCl
250 mM imidazole
1-fold complete protease
inhibitor cocktail
in H$_2$O, pH 8.0

Wash buffer
50 mM NaH$_2$PO$_4$
300 mM NaCl
20 mM imidazole
in H$_2$O, pH 8.0

Protein buffer
20 mM HEPES, pH 7.9
50 mM KCl
2 mM MgCl$_2$
0.1 mM EDTA
0.2 mM ZnCl$_2$
1 mM DTT
0.3mg/ml BSA
in H$_2$O

4.2.12 Protein isolation from *U. maydis*

U. maydis cells were grown in 100 ml CM medium (containing 1% arabinose if gene expression was under the *crg1* promoter) at 28°C overnight under shaking. Cells were harvested by centrifugation (10 min, 3500rpm) and were then resuspended in 2.5 ml protein buffer. Sample was frozen in liquid nitrogen. Next, the cell sample was thawed and lysed two-times using a French-Press (Minicell). The supernatant was collected after centrifugation (20 min, 1000rpm at 4°C). The resulting protein sample was stored frozen in aliquots at -80°C.

Protein buffer
25 mM HEPES, pH 7.9
50 mM KCl
2.5 mM DTT
1-fold complete protease inhibitor cocktail
in H_2O

4.2.13 Preparation of DNA fragments

The 723 bp *eGFP* fragment used for Northern blot analysis was isolated from plasmid p123 by NcoI/NotI digestion (Basse *et al*., 2000). Gene-specific probes for *mig2-1, mig2-2, mig2-5* have been described (Basse *et al*., 2002) and were isolated as EcoRI fragments from pCR2.1-TOPO. The gene-specific probe for *mig1* has been described (Basse *et al*., 2000) and was isolated as EcoRI fragment from pCR2.1-TOPO. A *mzr1* ORF specific fragment was isolated from pZ22 by digestion with PstI/XbaI; a *biz1* ORF specific fragment was prepared from pZ8 by digestion with MfeI/NcoI; a *znf7* ORF specific fragment was isolated from pZ7 by digestion with XbaI/NcoI; a *znf12* ORF specific fragment was isolated from pZ12 by digestion with MluI; a *znf23* ORF specific fragment was isolated from pZ23 by digestion with HindIII/NcoI. A *mig2-6* ORF specific fragment has been described (Farfsing *et al*., 2005) and was isolated as EcoRI fragment. A 500-bp *mig2-5* promoter fragment was prepared from pJM17 (Farfsing *et al*., 2005) by digestion with XbaI/BamHI. A 200-bp *mig2-5* promoter fragment (from −320 to -120) was isolated from plasmid pJM19 (Farfsing *et al*., 2005) by digestion with XbaI/BamHI. The 120-bp *mig2-5* promoter fragment (from −240 to -120) was isolated from plasmid pJM20 (Farfsing *et al*., 2005) by digestion with XbaI/BamHI. The 200-bp CCA mutant *mig2-5* promoter fragment was isolated from pmig-200/M by BamHI digestion. A 120-bp CCA mutant *mig2-5* promoter fragment was isolated from pmig-120/M by BamHI digestion. The 160-bp *mig2-5* promoter fragment (from −161 to -1) used as control in EMSA was prepared from p170-C by BamHI digestion. Furthermore, the 200-bp *mig2-5* promoter fragment used as binding competitor was amplified by PCR using the primer pair

YZ70/YZ71, the Phusion DNA Polymerase and pJM19 as template; the 200-bp CCA mutant *mig2-5* promoter fragment used as binding competitor was amplified by PCR using the primer pair YZ70/YZ71, the Phusion DNA Polymerase and pJS12 as template; the 120-bp *mig2-5* promoter fragment used as binding competitor was amplified by PCR using the primer pair YZ71/YZ72, the Phusion DNA Polymerase and pJM19 as template; the 120-bp CCA mutant *mig2-5* promoter fragment used as binding competitor was amplified by PCR using the primer pair YZ71/YZ72, the Phusion DNA Polymerase and pJS12 as template.

The isolated DNA fragments described were either used for Northern blot analysis (see probe labeling, 4.2.16) or for the electrophoretic mobility shift analysis (see EMSA, 4.2.15).

4.2.14 Western blot

An appropriate protein sample was mixed with the loading buffer in an Eppendorf tube. The mixture was heated at 95°C for 5 min, and then was immediately transferred on ice. Next, the protein mixture was loaded onto a 12% (v/v) SDS-polyacrylamide gel (8x9 cm, BIO-RAD). The gel was run at 80 volt for 30 min in running buffer, then at 100 volt for 1 hour. Six sheets of thick Whatman and one sheet of Hybond-P membrane (Amersham Biosciences) were prepared at the appropriate size (6x9 cm). The Whatman papers and the Hybond-P membrane, together with the gel, were arranged in the following order:

a. two sheets of Whatman paper
   soaked with Anode I buffer
b. one sheet of Whatman paper
   soaked with Anode II buffer
c. Hybond-P membrane
1) soaked with methanol for 1 min
2) rinsed with ddH$_2$O
3) soaked with Anode II buffer for no more than 10 min
d. SDS gel

rinsed with ddH$_2$O
e. three sheets of Whatman paper
   soaked with Cathode buffer

The membrane was blotted at 0.8 mA/cm^2 for 1 hour. Next, the membrane was soaked at 4°C overnight (or at RT for 1 hour) in blocking buffer under gentle shaking, and was then soaked at RT for 15 min in fresh blocking buffer under gentle shaking. The antibody against the protein tag of interest was added in blocking buffer at an appropriate dilution. After one hour gentle shaking at RT, the membrane was washed three-times with blocking buffer (10 min for each wash under gentle shaking). The second IgG antibody was diluted in blocking buffer according to the recommendation of the supplier and added to the membrane. The reaction was incubated at RT for 30 min under gentle shaking. Next, the membrane was washed twice with PBS/0.1% (w/v) Tween solution (5 min for each wash under gentle shaking) and once with PBS buffer for 5 min. After removing of excess liquid, the membrane was soaked in detection mixture (Amersham ECL Plus Western Blotting Detection System, GE) for 5 min. Finally, the membrane was exposed to an X-ray film (medical X-Ray screen film, CEA) for 2 min and the film was developed.

12% SDS gel (for 2 gels)

1) lower gel	2) upper gel
5 ml H$_2$O	4.3 ml H$_2$O
3.75 ml 4x stacking gel buffer	1.875 ml 4x running gel buffer
150 µl 10% SDS	75 µl 10% SDS
6 ml Acrylamid (Acrylamid 30%, Mix 37.5:1, AppliChem)	1.2 ml Acrylamid (Acrylamid 30%, Mix 37.5:1, AppliChem)
75 µl 10% APS	37.5 µl 10% APS
7.5 µl Temed	3.75 µl Temed

4x stacking gel buffer	**4x running gel buffer**
15.39% (w/v) Tris-Base	0.67% (w/v) Tris-Base
3.69% (w/v) Tris-HCl	7.02% (w/v) Tris-HCl
in H$_2$O, pH 8.8	in H$_2$O, pH 6.8

10x Running buffer
1.92 M Glycin
0.25 M Tris-Base
1% (w/v) SDS
in H_2O

Blocking buffer
1x PBS
0.1% (w/v) Tween 20
5% (w/v) low fat powder milk
in H_2O

2x loading buffer
130 mM Tris-Cl, pH8.0
20% (v/v) Glycerol
4.6% (w/v) SDS
0.02% Bromophenol blue
2% DTT

10x PBS
80 g NaCl
2 g KCl
14.4 g Na_2HPO_4
2.4 g KH_2PO_4
in H_2O, pH 7.2

Cathode buffer
25 Mm Tris-Base
40 mM 6-amino.hexanoic acid
in H_2O, pH 9.4

Anode I buffer
0.3 M Tris-Base
in H_2O, pH 10.4

Anode II buffer
25 mM Tris-Base
in H_2O, pH 10.4

4.2.15 EMSA

A 4% acrylamide gel (20x20 cm, ~50 ml, BIO-RAD) was prerun at 12 mA for 1.5 h. The protein sample, 1 μg poly [dI-dC] (to inhibit unspecific binding, Sigma), 1-fold binding buffer, 10% (w/v) glycerol and a suitable volume of pure water for a total volume of 20 μl after the addition of DNA probe were mixed in a 1.5 ml Eppendorf tube. The mixture was incubated at RT for 15 min, and then an excess of cold DNA competitor was added if a binding competition assay was performed. In this case, a preincubation of 20 min was done. Then, 6 μg of the ^{33}P radioactively end-labeled DNA probe was added. The reaction was incubated at RT for additional 35 min. The mixture was loaded onto the gel, which then was run at 12 mA for 3.5 h. The gel was transferred to a Whatman paper and was dried at 85°C vacuum for 45 min. The vacuum was maintained for additional 15 min after heating was stopped. Finally, the gel was exposed within a screen cassette for 2 days and subsequently scanned (STORM Phosphorimager).

4% acrylamide gel	**5-fold binding buffer**
0.5-fold TBE buffer	100 mM HEPES, pH 7.9
4% acrylamide mix (37.5:1	250 mM KCl
acrylamide: bisacrylamide)	10 mM $MgCl_2$
1% (w/v) glycerol	1 mM $ZnCl_2$
0.07% APS (using freshly prepared	0.5 mM EDTA
10% APS stock solution)	5 mM DTT
35 μl TEMED (for 50 ml gel preparation)	1.5 mg/ml BSA
in H_2O	in H_2O

4.2.16 Probe labeling

50 ng of DNA fragment to be labeled were mixed with ddH_2O (total volume was 33 μl) and heated at 95°C for 5 min, and then the DNA sample was transferred on ice. After 2 min of incubation, 5 μl 10-fold labeling buffer (NEB) and 6 μl of 1 mM dNTPs (without dCTP, final concentration for dATP, dGTP and dTTP was 0.12 mM) were added. Next, 1 μl Klenow enzyme (NEB) and 50 μCi (5 μl) ^{32}P-labeled dCTP (HARTMANN ANALYTIC) were added. The reaction was incubated at 37°C for one hour and was then loaded on a MicroSpin S-300 HR column (centrifuged for 1 min at 2700 rpm before use, GE Healthcare). After centrifugation (2 min, 2700 rpm), the eluate was mixed with 13 ml hybridization buffer (Northern or Southern buffer) and then was heated at 97°C for 10 min. The labeled probe was used for Northern or Southern blot analysis (also could be stored at 4°C for a short period).

4.2.17 Cell density determination of *U. maydis*

U. maydis cell density in culture was determined by measuring the optical density with a Novosec II Photometer (Pharmacia Biotech) at a wavelength of 600 nm. The cell culture had to be diluted to a value below OD_{600} 0.8 before determination to ensure a linear range. A value of OD_{600} 1 correlates to $1-2x\ 10^7$ cells/ml.

4.2.18 Concentration determination of DNA, RNA and protein

The concentrations of DNA, RNA and protein samples were determined using a ND-1000 spectrophotometer (NanoDrop Technologies, Inc.).

4.2.19 Chlorazole Black E staining

This method is modified from (Brachmann *et al.*, 2003). Infected plant tissue was harvested and placed into 2 ml Eppendorf tubes containing 100% ethanol. This tube was then incubated at RT overnight until the chlorophyll was completely removed. The plant tissue was washed with H_2O, then soaked in 10% (w/v) KOH solution and heated at 90°C for 3 hours. Next, it was washed with H_2O after removal of KOH solution. Finally, the plant tissue was soaked in chlorazole solution for 1-2 days and was stored in 50% (w/v) glycerin.

Chlorazole solution
^{1}/3 100% glycerin
^{1}/3 lactic acid
^{1}/3 0.03% (w/v) chlorazole black E solution

4.2.20 Plant infection

U. maydis overnight cultures in $YEPS_L$ medium were adjusted in H_2O to an OD_{600} of 2.0. Cell suspensions were injected into the basal stem of six-day-old corn seedlings (Early Golden Bantam; Olds Seeds, Madison, WI) using a syringe and gauge needles (BD Drogheda).

4.2.21 Light Microscopy observation

Infected leaf tissue was excised from regions adjacent to chlorotic areas or from tumor tissue with a razor blade (Basse *et al.*, 2000). Cells in culture or plant tissue

were observed with differential interference contrast optics (DIC) or under fluorescence microscopy using a Zeiss Axioplan II microscope (Zeiss, Jena, Germany). All microscopical observations were done with a CoolSNAP-HQ CCD camera (Photometrics, Tucson, AZ, USA) controlled by the MetaMorph software (Universal Imaging, Downing Town, PA, USA).

4.2.22 Bioinformatic analysis

All DNA and protein sequences were retrieved from the public *Ustilago* database http://www.broad.mit.edu. DNA sequence analysis was done using the Clone Manager software. RT-PCR quantification was performed using Gel Doc2000: QuantifyOne 4.4.0 software (BIO-RAD). Northern results were quantified using the Image Quant software (Molecular Dynamics). Protein homologue searching was done using blast searching (http://www.ncbi.nih.gov/blast/).

5   References

An, Z.; Mei, B.; Yuan, W. M. and Leong, S.A. (1997). The distal GATA sequences   of the *sid1* promoter of *Ustilago maydis* mediate iron repression of siderophore production and interact directly with Urbs1, aGATA family transcription factor. EMBO J **16,** 1742-1750.

Anon. (1891). Fertilising clover and cow-grass. Agric Gaz N S W **2**, 636–637.

Barrett, J.A. (1985). The gene-for-gene hypothesis: parable or paradigm. In Ecology and Genetics of Host- Parasite Interactions, ed. D. Rollinson, R. M. Anderson, 215-225.

Basse, C.W., Stumpferl, S. and Kahmann, R. (2000)**.** Characterization of a *Ustilago maydis* gene specifically induced during the biotrophic phase: evidence for negative as well as positive regulation. Mol Cell Biol **20**, 321-329.

Basse, C.W., Kolb, S. and Kahmann, R. (2002). A maize-specifically expressed gene cluster in *Ustilago maydis*. Mol Microbiol **43**, 75-94.

Basse, C.W., and Steinberg, G. (2004). *Ustilago maydis*, model system for analysis of the molecular basis of fungal pathogenicity. Mol Plant Pathol **5,** 83–92.

Basse, C.W., and Farfsing, J. (2006). Promoters and their regulation in *Ustilago maydis* and other phytopathogenic fungi. FEMS Microbiol. Lett. **254**, 208-216.

Berg, J.M., and Godwin, H.A. (1997). Lessons from zinc-binding peptides. Annu Rev Biophys Biomol Struct **26,** 257–271.

Berg, J.M., and Shi, Y. (1996). The galvanization of biology: a growing appreciation for the roles of zinc. Science **271,** 1081–1085.

Biedenkapp, H., Borgmeyer, U., Sippel, A.E., and Klempnauer, K.H. (1988). Viral *myb* oncogene encodes a sequence-specific DNA-binding activity. Nature 335, 835-837.

Biffen, R.H. (1905). Mendel's laws of inheritance and wheat breeding. Journal of Agricultural Sciences **1**, 4- 48.

Black, A.R., Black, J.D., and Azizkhan-Clifford, J. (2001). Sp1 and krüppel-like factor family of transcription factors in cell growth regulation and cancer . J Cell Physiol **188**, 143-60.

Bohlmann, R. (1996). Isolierung und Charakterisierung von filaments pezifisch exprimierten Genen aus *Ustilago maydis*. Ph.D. thesis, Ludwig-Maximilians-Universität, Munich.

Bölker, M., Urban, M., and Kahmann, R. (1992). The *a* mating-type locus of *U. maydis* specifies cell signalling components. Cell **68**, 441–450.

Bölker, M., Böhnert, H.U., Braun, K.H., Görl, J., and Kahmann, R. (1995). Tagging pathogenicity genes in *Ustilago maydis* by restriction enzyme-mediated integration (REMI). Mol Gen Genet **248**, 547–552.

Bottin, A., Kämper, J., and Kahmann, R. (1996). Isolation of a carbon source-regulated gene from *Ustilago maydis*. Mol Gen Genet **253**, 342–352.

Bouhouche, N., Syvanen, M., and Kado, C.I. (2000). The origin of prokaryotic C2H2 zinc finger regulators. Teends in Microbiology **8**, 77-81.

Brachmann, A., Weinzierl, G., Kämper, J., and Kahmann, R. (2001). Identification of genes in the *bW/bE* regulatory cascade in *Ustilago maydis*. Mol Microbiol **42,** 1047-1063.

Brachmann, A., Schirawski, J., Müller, P., and Kahmann, R. (2003). An unusual MAP kinase is required for efficient penetration of the plant surface by *Ustilago maydis*. EMBO J **22**, 2199-2210.

Brefeld, O. (1883)**,** Botanische Untersuchungen über Hefenpilze. Untersuchungen aus dem Gesammtgebiete der Mykologie V Die Brandpilze I *Leipzig* 220.

Broomfield, P.L., Hargreaves, J.A. (1992). A single amino acid change in the iron-sulphur protein subunit of succinate dehydrogenase confers resistance to carboxin in *Ustilago maydis*. Curr Genet **22,** 117–121.

Brown, R.S., Sander, C., and Argos, P. (1985). The primary structure of transcription factor *TFIIIA* has 12 consecutive repeats. FEBS Lett **186**, 271–274.

Caracuel, Z., Roncero, M.I., Espeso, E.A., Gonzalez-Verdejo, C.I., Garcia-Maceira, F.I., and Di Pietro, A. (2003). The pH signaling transcription factor PacC controls virulence in the plant pathogen *Fusarium oxysporum*. Mol Microbiol **48**, 765–779.

Choo, Y., and Klug, A. (1997). Physical basis of a protein-DNA recognition code. Curr Opin Struct Biol **7**, 117-125.

Christensen, J.J. (1963). Corn smut caused by *Ustilago maydis*. Monogr No. 2, The Amer Phytopathol Soc.

Coleman, J.F. (1992). Zinc proteins: enzymes, storage proteins, transcription factors, and replication proteins. Annu Rev Biochem **61**, 897-946.

Coleman, M., Henricot, B., Arnau, J., and Oliver, R.P. (1997). Starvation-induced genes of the tomato pathogen *Cladosporium fulvum* are also induced during growth *in planta*. Mol Plant-Microbe Interact **10**, 1106-1109.

Crute, I.R. (1985). The genetic basis of relationships between microbial parasites and their hosts. In: R.S.S. Fraser (Ed.), Mechanism of resistance to plant disease, 80–142. Martinus Nijhoff Publishers, Dordrecht.

Dang, D.T., Pevsner, J., and Yang, V.W. (2000). The biology of the mammalian Kruppel-like family of transcription factors. Int J Biochem Cell Biol **32**,1103–1121.

Davis, G.N. (1936). Some factors influencing the infection and pathogenicity of *Ustilago zeae* on *Zea mays*. Iowa Agric. Exp. Sta. Res. Bull. **199**, 247.

Day, P.R. (1974). Genetics of host-parasite interaction. San Francisco: Freeman. 238.

Desjarlais, J.R., and Berg, J.M. (1992). Toward rules relating zinc finger protein sequences and DNA binding site preferences. Proc Natl Acad Sci USA **89**, 7345-7349.

De Wit, P.J.G.M. (1992). Molecular characterization of gene-for-gene systems in plant–fungus interactions and the application of avirulence genes in control of plant pathogens. Annu Rev Phytopathol **30**, 391 418.

Dynan, W.S., and Tjian, R. (1983). The promoter-specific transcription factor Sp1 binds to upstream sequences in the SV40 early promoter. Cell **32**, 669−680.

Ehrlich, H.G. (1958). Nuclear behavior in mycelium of a solopathogenic line and in a cross of two haploid lines of *Ustilago maydis* (DC.) Cda., Mycologia **50**, 622.

Engelke, D.R., Ng, S.Y., Shastry, B.S., and Roeder, R.G. (1980). Specific interaction of a purified transcription factor with an internal control region of 5S RNA genes. Cell **19**, 717–728.

Farfsing, J., Auffarth, K., and Basse, C.W. (2005). Identification of *cis*-active elements in *U. maydis mig2* promoters conferring high-level activity during pathogenic growth in maize. Mol Plant Microbe Interact **18**, 75-87.

Farrer, W. (1898). The making and improvement of wheats for Australian conditions. Agric Gaz NSW **9**, 131–168.

Flor, H.H. (1942) Inheritance of pathogenicity in*Melampsora lini*. Phytopathology **32**, 653–669.

Flor, H.H. (1946). Genetics of pathogenicity in *Melampsora lini.*. J Agric Res **73**, 335-357.

Flor, H.H. (1971) Current status of the gene-for-gene concept. Ann Rev Phytopathol **9**, 275–296.

Flor-Parra, I., Vranes, M., Kämper, J., and Perez-Martin, J. (2006). Biz1, a zinc finger protein required for plant invasion by *Ustilago maydis*, regulates the levels of a mitotic cyclin. Nucleic Plant Cell **18**, 2369–2387.

Fried, M., and Crothers, D.M. (1981). Equilibria and kinetics of lac repressor-operator interactions by polyacrylamide gel electrophoresis. Nucleic Acids Res **9**, 6505–6525.

Fried, M.G., and Crothers, D.M. (1984). Equilibrium studies of the cyclic AMP receptor protein-DNA interaction. J Mol Biol **172**, 241–262.

Fried, M.G., (1989). Measurement of protein-DNA interaction parameters by electrophoresis mobility shift assay. Electrophoresis **10**, 366–376.

Garcia-Muse, T., Steinberg, G., and Perez-Martin, J. (2003). Pheromone-induced G(2) arrest in the phytopathogenic fungus *Ustilago maydis*. Eukaryot Cell **2,** 494–500.

Garcia-Muse, T., Steinberg, G., and Perez-Martin, J. (2004). Characterization of B-type cyclins in the smut fungus *Ustilago maydis*: Roles in morphogenesis and pathogenicity. J. Cell Sci **117,** 487–506.

Garner, M.M., and Revzin, A. (1981). A gel electrophoresis method for quantifying the binding of proteins to specific DNA regions: application to components of the Escherichia coli lactose operon regulatory system. Nucleic Acids Res **9**, 3047-3059.

Gillissen, B., Bergemann, J., Sandmann, C., Schroeer, B., Bölker, M., and Kahmann, R. (1992). A two-component regulatory system for self/non-self recognition in *Ustilago maydis*. Cell **68**, 647–657.

Goff, S.A., Cone, K.C., and Chandler, V.L. (1992). Functional analysis of the transcriptional activator encoded by the maize B gene: evidence for a direct functional interaction between two classes of regulatory proteins. Genes Dev **6**, 864–875.

Grayer, R.J., and Kokubun, T. (2001). Plant-fungal interactions: the search for phytoalexins and other antifungal compounds from higher plants. Phytochemistry **56**, 253-263.

Gregory, R.C., Taxman, D.J., Seshasayee, D., Kensinger, M.H., Bieker, J.J., and Wojchowski, D.M. (1992). Functional interaction of GATA1 with erythroid Kruppel-like factor and Sp1 at defined erythroid promoters. Blood **87**, 1793–1801.

Hammond-Kosack, K.E., and Jones, J.D.G. (1997). Plant disease resistance genes. Plant Mol Biol **48**, 575-607.

Hanna, W.F. (1929). Studies in the physiology and cytology of *Ustilago zeae* and *Sorosporium reilianum*. Phytopathology **19**, 415-443.

Hanas, J.S., Hazuda, D.J., Bogenhagen, D.F., Wu, F.Y., and Wu, C.W. (1983). *Xenopus* transcription factor A requires zinc for binding to the 5S RNA gene. J Biol Chem **258**, 14120-14215.

Hendrickson, W. (1985). Protein-DNA Interactions Studied By The Gel Electrophoresis-DNA Binding Assay. BioTechniques **3**, 346-354.

Howe, K.M., and Watson, R.J. (1991) Nucleotide preference in sequence-specific recognition of DNA by c-*myb* protein. Nucleic Acids Res **19**, 3913-3919.

Islam, M.R., and Shepherd, K.W. (1991). Analysis of phenotypes of recombinants and revertants from testcross progenies involving genes at the *L* group, conferring resistance to rust in flax. Hereditas **114**, 125–129.

Kadonaga, J.T., Carner, K.R., Masiarz, F.R., and Tjian, R. (1987). Isolation of cDNA encoding transcription factor Sp1 and functional analysis of the DNA binding domain. Cell **51**, 1079–1090.

Kahmann, R., Basse, C., Feldbrügge, M., Kämper, J. (2000) *Ustilago maydis*, the causative agent of corn smut disease. In Fungal Pathology. Kronstad, J.W. (ed.). Dordrecht: Kluwer Academic Publishers, 347–371.

Kämper, J., Reichmann, M., Romeis, T., Bölker, M., Kahmann, R. (1995). Multiallelic recognition: nonself-dependent dimerization of the bE and bW homeodomain proteins in *Ustilago maydis*. Cell **81**, 73–83.

Kämper, J. (2004). A PCR-based system for highly efficient generation of gene replacement mutants in *Ustilago maydis*, Mol. Gen. Genomics **271,** 103–110.

Keen, N.T. (1982). Specific recognition in gene-for-gene hostparasite systems. Adv. Plant Pathol **1**, 35–82.

Kim, C.A., Berg, J.M. (1995). Serine at position 2 in the DNA recognition helix of a Cys_2-His_2 zinc finger peptide is not, in general, responsible for base recognition. J Mol Biol **252**, 1-5.

Klug, A., and Schwabe, J.W. (1995). Protein motifs5. Zinc fingers. FASEB J **9**, 597-604.

Knogge, W. (1996). Fungal Infection of Plants. Plant Cell **8**, 1711-1722.

Kotani, H., Kmiec, E.B., and Holloman, W.K. (1993). Purification and properties of a cruciform DNA binding protein from*Ustilago maydis*. Chromosoma **102**, 348-354.

Kronstad, J.W., and Leong, S.A. (1990). The *b* mating-type locus of *Ustilago maydis* contains constant and variable regions. Genes Dev **4**, 1384–1395.

Kronstad, J.W., and Staben, C. (1997). Mating type in filamentous fungi. Annu Rev Genet **31**, 245–276.

Little, M., Holmes, G., and Walsh, P. (1999). WT1: what has the last decade told us?. Bioessays **21**, 191–202.

Lee, J.S, Galvin, K.M., and Shi, Y. (1993). Evidence for physical interaction between the zinc-finger transcription factors YY1 and Sp1. Proc Natl Acad Sci USA **90**, 6145–6149.

Martin, G.B., Brommonschenkel, S.H., Chunwongse, J., Frary, A., and Ganal, M.W. (1993). Map-based cloning of a protein kinase gene conferring disease resistance in tomato. Science **262**, 1432-1436.

Matthews, J.M., and Sunde, M. (2002), Zincfingers-Folds for many occasions. IUBMB Life **54**, 351–355.

Merika, M, and Orkin, S.H. (1995). Functional synergy and physical interactions of the erythroid transcription factor GATA-1 with the Kruppel family proteins Sp1 and EKLF. Mol Cell Biol **15**, 2437–2447.

Michelmore, R.W., Ilott, T.; Hulbert, S.H. And Farrara, B. (1988). The downey mildews. Adv Plant Pathol **6**, 53-79.

Miller, J., McLachlan, A.D., and Klug, A. (1985), Repetitive zinc-binding domains in the protein transcription factor IIIA from *Xenopus* oocytes. EMBO J **4**, 1609–1614.

Müller, P., Aichinger, C., Feldbrügge, M., and Kahmann, R. (1999). The MAP kinase kpp2 regulates mating and pathogenic development in *Ustilago maydis*. Mol Microbiol **34**, 1007-1017.

Nardelli, J., Gibson, T.J., Vesque, C., And Charnay, P. (1991). Base sequence discrimination by zind-finger DNA-binding domains. Nature 349, 175-178.

Nardelli, J., Gibson, T.J., And Charnay, P. (1992). Zinc finger-DNA recognition: analysis of base specificity by site-directed mutagenesis. Nucleic Acids Res **20**, 4137-4144.

Nathues, E., Joshi, S., Tenberge, K.B., von der Driesch, M., Oeser, B., Baumer, N., Mihlan, M., And Tudzynski, P. (2004). CPTF1, a CREB-like transcription factor, is involved in the oxidative stress response in the phytopathogen *Claviceps purpurea* and modulates ROS level in its host *Secale cereale*. Mol Plant Microbe Interact **17**, 383-393.

Paredes-Lopez, O., Pataky, J.K., and Guevara-Lara, F. (1995). Huitlacoche (*Ustilago maydis*) as a food source—biology, composition, and production. CRC Crit Rev Food Sci Nut **35**.191-229.

Parlevliet, J.E. (1983). Race-specific resistance and cultivar-specific virulence in barley-leaf rust pathosystem and their consequences for the breeding of leaf rust resistant barley. Euphytia **32**, 367-375.

Pavletich, N.P., and Pabo, C.O. (1991**).** Zinc finger-DNA recognition: crystal structure of a Zif268-DNA complex at 2.1 A**.** Science **252,** 809-817.

Pedley, K.F., and Walton, J.D. (2001). Regulation of cyclic peptide biosynthesis in a plant pathogenic fungus by a novel transcription factor. Proc Natl Acad Sci USA **98**, 14174-14179**.**

Pieterse, C.M., Derksen, A.M., Folders, J., and Govers, F. (1994). Expression of the *Phytophthora infestans ipiB* and *ipiO* genes *in planta* and *in vitro*. Mol Gen Genet **244**, 269-277.

Revzin, A. (1989). Gel Electrophoresis Assays for DNA-Protein Interactions. BioTechniques **7**, 346-354.

Romeis, T., Brachmann, A., Kahmann, R., and Kämper, J. (2000). Identification of a target gene for the bE-bW homeodomain protein complex in *Ustilago maydis*. Mol Microbiol **37**, 1-14.

Schauwecker, F., Wanner, G., and Kahmann, R. (1995). Filament-specific expression of a cellulase gene in the dimorphic fungus *Ustilago maydis*. Biol Chem Hoppe-Seyler **376**, 617-625.

Snetselaar, K.M. (1993). Microscopic observation of *Ustilago maydis* mating interactions. Exp Mycol **17**, 345–355.

Snetselaar, K.M., Mims, C.W. (1994). Light and electron microscopy of *Ustilago maydis* hyphae in maize. Mycological Research **98**, 347-355.

Snetselaar, K.M., Bölker, M., and Kahmann, R. (1996). *Ustilago maydis* mating hyphae orient their growth toward pheromone sources. Fungal Genet Biol **20**, 299-312.

Song, W.Y., Wang, G.L., Chen, L.L., Kim, H.S., and Pi, L.Y. (1995), Areceptor kinase-like protein encoded by the rice disease resistance gene, *Xa21*. Science **270**, 1804–1806.

Stakman, E.C. (1917). Biologic forms of *Puccinia graminis* on cereals and grasses. J Agric Res **10**, 429-495.

Stakman, E.C., Parker, J.H., and Piemeisel, F.J. (1918). Can biologic forms of stemrust on wheat change rapidly enough to interfere with breeding for rust resistance? J Agric Res **14**, 111-123.

Suske, G.. (1999). The Sp-family of transcription factors. Gene **238**, 291-300.

Thomas, P. L. (1991). Genetics of small-grain smuts. Phytopathol **29**, 137-148.

Thukral, S. K., Morrison, M.L., and Young, E.T. (1992). Mutations in the zinc fingers of ADR1 that change the specificity of DNA binding and transactivation. Mol Cell Biol **12**, 2784-2792.

Turner, J., and Crossley, M. (1999). Mammalian Kruppel-like transcription factors; more than just a pretty finger. Teends in Biochemical Sciences **24**, 236-240.

Urban, M., Kahmann, R., and Bölker M. (1996). Identification of the pheromone response element in *Ustilago maydis*. Mol Gen Genet **251**, 31-37.

I. Urnow, F.D., and Rebar, E.J. (2002). Designed transcription factors as tools for therapeutics and functional genomics . Biochem. Pharmacol **64**, 919-923.

Van den Ackerveken, G.F., Dunn, R.M., Cozijnsen, A.J., Vossen, J.P., Van den Broek, H.W., and De Wit, P.J. (1994). Nitrogen limitation induces expression of the avirulence gene avr9 in the tomato pathogen Cladosporium fulvum. Mol Gen Genet **243**, 277-285.

Walton, J.D. (1996). Host-selective toxins: agents of compatibility. Plant Cell **8**, 1723–11733.

Wang, J., Holden, D.W., and Leong, S.A. (1988). Gene transfer system for the phytopathogenic fungus *Ustilago maydis*. Proc Natl Acad Sci USA **85**, 865-869.

Weinmann, P., Gossen, M., Hillen, W., Bujard, H., and Gatz, C. (1994). A chimeric transactivator allows tetracycline-responsive gene expression in whole plants. The Plant Journal **5**, 559–569.

Whitham, S., Dinesh-Kumar, S.P., Choi, D., Hehl, R., Corr, C., and Baker, B. (1994). The product of the tobacco mosaic virus resistance gene *N*: Similarity to Toll and the interleukin-1 receptor. Cell **78**, 1011–1015.

Wolfe, S.A., Nekludova, L., and Pabo, C.O. (1999). DNA recognition by Cys_2His_2 Zinc finger proteins. Biophys Biomol Struct **3**, 183-212.

Wösten, H.A., Bohlmann, R., Eckerskorn, C., Lottsspeich, F., Bölker, M., and Kahmann, R. (1996). A novel class of small amphipathic peptides affect aerial hyphal growth and surface hydrophobicity in *Ustilago maydis*. EMBO J **15**, 4274-4281.

Curriculum vitae

Personal information   Yan Zheng

born March 17, 1973 in Changchun, China

Education   1992-1996   Shanghai Railway University, Shanghai, China

2000-2003   College of Life Science, Jilin University, Changchun, China

2004-2007   PhD work at Max Planck Institute for Terrestrial Microbiology, Marburg, Germany

Dissertation   PhD thesis topic: Identification of transcriptional regulators for the *Ustilago maydis mig* genes.

Under the supervision of Dr. Christoph Basse

Acknowledgements